CELLULAR NAD STATUS AS A REGULATOR OF SKIN PHOTODAMAGE

by

Claudia Andrea Benavente Arias

A Dissertation Submitted to the Faculty of the

CANCER BIOLOGY GRADUATE INTERDISCIPLINARY PROGRAM

In Partial Fulfillment of the Requirements

For the Degree of

DOCTOR OF PHILOSOPHY

In the Graduate College

THE UNIVERSITY OF ARIZONA

2007

THE UNIVERSITY OF ARIZONA
GRADUATE COLLEGE

As members of the Dissertation Committee, we certify that we have read the dissertation

prepared by Claudia Andrea Benavente

entitled Cellular NAD Status as a Regulator of Skin Photodamage

and recommend that it be accepted as fulfilling the dissertation requirement for the Degree of Doctor of Philosophy

_____ Date: 11/09/2007
Elaine Jacobson, PhD

_____ Date: 11/09/2007
G. Tim Bowden, PhD

_____ Date: 11/09/2007
Margaret Briehl, PhD

_____ Date: 11/09/2007
Serrine Lau, PhD

_____ Date: 11/09/2007
Donato Romagnolo, PhD

Final approval and acceptance of this dissertation is contingent upon the candidate's submission of the final copies of the dissertation to the Graduate College.

I hereby certify that I have read this dissertation prepared under my direction and recommend that it be accepted as fulfilling the dissertation requirement.

_____ Date: 11/09/2007
Dissertation Director: Elaine Jacobson, PhD

STATEMENT BY AUTHOR

SIGNED: Claudia Andrea Benavente Arias

ACKNOWLEDGEMENTS

I would like to acknowledge the various people who have contributed to my success as a graduate student and my development as a scientist. First and foremost, I would like to thank my advisor, Dr. Elaine L. Jacobson for her mentoring, her commitment to developing my skills as a scientist and for being a source of encouragement and support. I would also like to give special thanks to the members of my graduate committee: Dr. G. Tim Bowden, Dr. Margaret Briehl, Dr. Serrine Lau, and Dr. Donato Romagnolo, for their support and constant advice. I would like to give special thanks to Stephanie Schnell for her assistance and friendship in the laboratory. Stephanie's dedication to science was essential to finishing my graduate career. I am also grateful to the members of the Cancer Biology Interdisciplinary Graduate Program and to the past and present members of Drs. Jacobson's laboratory for stimulating discussions, friendship, and for providing an enjoyable learning environment. Lastly, I would like to thank Anne Cione for her patience and assistance throughout my graduate career at the University of Arizona.

TABLE OF CONTENTS

TABLE OF CONTENTS – *Continued*

TABLE OF CONTENTS – *Continued*

TABLE OF CONTENTS – *Continued*

LIST OF TABLES

LIST OF FIGURES

LIST OF FIGURES - *Continued*

LIST OF FIGURES - *Continued*

ABSTRACT

The maintenance and regulation of cellular NAD(P)(H) content and its influence on cell function involves in many metabolic pathways which are poorly understood. Niacin deficiency in humans, which leads to low NAD status, causes sun sensitivity in skin, indicative of DNA repair deficiencies. Animal models of niacin deficiency demonstrate genomic instability and increased cancer development in sensitive tissues including skin. Therefore, we have developed a cell culture model that allows assessment of pathways regulated by NAD(P) content as a way to identify NAD-dependent signaling events that may be critical in early skin carcinogenesis. Using our model, we showed that niacin restriction, and consequent NAD depletion, reversibly alters NAD(P)(H) pools, increases apoptosis, induces G_2/M cell cycle arrest, and decreases DNA stability. These alterations are affected by increased expression and activity of NOX leading to an accumulation of ROS, which may provide a survival mechanism as has been shown in cancer cells. Our data also support the hypothesis that glutamine is a likely alternative energy source during niacin deficiency. Here, we also identified the expression of all seven NAD-dependent deacetylase (SIRT) family members in skin cells. We showed that in response to photodamage, the expression of several SIRTs is altered in keratinocytes. Furthermore, we showed that SIRTs responses to photodamage differ between normal and immortalized keratinocytes, which may be indicative of alterations potentially important in skin carcinogenesis. In addition, we have shown that NAD-depleted HaCaT

keratinocytes are more sensitive to photodamage. We observed that both poly(ADP-ribose) polymerases (PARPs) and SIRTs are inhibited by the unavailability of their substrate, NAD^+, leading to unrepaired DNA damage upon photodamage and subsequent increase in cell death. Our data demonstrate that both SIRTs and PARPs are critical following DNA damage and identify which SIRTs are essential. Finally, we identified for the first time the expression of the nicotinic acid receptor in human skin keratinocytes, mainly in the differentiating keratinocytes of the stratum corneum in the epidermis. This study identifies new roles for niacin as a potential skin cancer prevention agent and demonstrates that niacin status is a critical resistance factor for UV damaged skin cells.

CHAPTER I

INTRODUCTION

Non-melanoma Skin Cancer

Non-melanoma skin cancers (NMSC), which include basal cell carcinoma (BCC) and squamous cell carcinoma (SCC), are keratinocytes-derived tumors. SCCs have been described as malignancies of epidermal cells that retain characteristics of the normal suprabasal epidermis [1]. On the other hand, BCCs are low-grade, indolent, epidermal neoplasms recapitulating the normal basal layer of the epidermis [1]. Combined, NMSCs are the most common form of human neoplasia in the United States with more than one million cases documented every year and accounting for nearly 40% of all reported cancers [2]. The vast majority of NMSC are BCCs, comprising 75% of all NMSC cases, while SCCs account for 20% of NMSC cases. NMSC represents a serious disease given that approximately 10% of SCCs progress to metastatic disease and 40 to 50% of NMSC patients develop a second NMSC within five years of initial treatment [3-6]. Management of multiple primary neoplasms, along with their adjacent premalignant lesions, requires extended follow-up, repeated surgical intervention, and, at times, postoperative radiotherapy [7,8]. Therefore, although the absolute mortality caused by NMSC is relatively low, 20% of Americans will develop this type of cancer during their lifetime, a substantial

degree of morbidity is associated with treatment of the disease and high medical costs translate in expenditures of $426 million for Medicare alone [9-11].

Etiology

Although many environmental and genetic factors contribute to the development of skin cancers, the most important etiological factor in NMSCs is chronic exposure to UV radiation in sunlight. Solar radiation has been regarded as a major risk factor for non-melanoma skin cancer in humans since 1896, when Unna described the skin changes which ended in skin cancer among sailors exposed to the sun [12,13]. From a comprehensive review linking clinical, experimental, and epidemiologic evidence, Blum concluded in 1948, "we now have a number of lines of evidence, all of which converge to indict sunlight as the major cause of cancer of the skin in man [12]." Since then, various scientists have repeated and elaborated this conclusion [13-16].

Even though the ozone layer blocks UVC radiation (200-280 nm) and part of the UVB radiation (280-290 nm) from reaching the surface of the earth, UVB (290-315 nm) and UVA (315-400 nm) do reach the surface of the earth, and cause DNA damage, inflammation and erythema, sunburn, gene mutations, post-inflammatory immunosuppression, and eventually, skin cancer [17]. UV radiation plays two major roles in the development of NMSCs: (i) UV radiation causes mutations in cellular DNA. Failure to repair these genetic alterations ultimately leads to unrestrained growth and tumor formation. (ii) UV radiation affects the

cutaneous immune system, inducing a state of relative immunosuppression that prevents tumor rejection.

The process of skin-tumor formation is divided into three stages: tumor initiation, tumor promotion and tumor progression [18]. Both UVA and UVB irradiation play a variety of roles in the induction of skin cancers as they can serve as a complete carcinogen or as promoters of carcinogenesis. The typical UVB-induced DNA damage is the generation of dimeric photoproducts between adjacent pyrimidine bases. These unique lesions in the DNA give rise to unique mutations, predominantly C → T and CC → TT transitions. These UV-signature mutations have been detected in the tumor suppressor gene p53 in chronically sun-damaged skin, actinic keratoses (AKs – precancerous skin lesions) and SCCs, indicating that p53 gene mutations are a very early event in the process of skin carcinogenesis [19-21]. This p53 gene mutation confers the cells with a proliferative advantage over normal keratinocytes that results in neoplastic transformation. In contrast, UVA radiation and visible light are known to cause DNA damage mostly by the indirect production of reactive oxygen species (ROS) such as superoxide anion, singlet oxygen, and hydrogen peroxide via endogenous photosensitizers [22]. These highly-reactive, short-lived molecules produce single-strand breaks, DNA-protein crosslinks, and altered bases in the DNA. Recently, evidence for direct DNA damage by UVA, similar to UVB, has also emerged [23].

The skin has various protective mechanisms by which it reduces DNA damage and/or mutation formation. Melanin formation surrounds the nucleus of basal keratinocytes, reducing the exposure of the skin to UV and therefore the formation of DNA damage [24]. However, when DNA damage occurs, most of it is repaired and does not give rise to mutations. The G_1/S cell cycle arrest is another way to avoid mutations as it prevents cells from replicating damaged DNA [25]. UV-induced activation of p53 downregulates DNA polymerase η, a DNA polymerase specialized to bypass DNA photoproducts, leading to maintainance of a low mutagenic activity by blockage of the damage bypass [26]. High levels of DNA damage activates damage response signaling pathways that often results in death of UV-irradiated cells, preventing propagation of cells with mutations. Finally, even if mutations are established, most of these cells will be recognized and removed by the immune system. However, even though immune surveillance plays an important role in the prevention of cancer formation, as we mentioned before, sun exposure is known to induce immune-suppression in the skin.

Prevention

NMSC primary prevention has focused on educating people about the harmful effects of UV radiation present in the sunlight, the need to avoid its excessive exposure by wearing protective clothing, and the use of sunscreen. However, these primary prevention measures have not been successful. The use of sunscreens have grown widely, but their ability to protect across a broad

spectrum of solar radiation combined with poor public knowledge of appropriate selection and use, has not resulted in the decrease of skin cancer incidence [27]. Some studies have even indicated that sunscreen use is associated with an increase in the incidence of malignant melanoma due to increased exposure time [28,29]. Others, have raised the question as to whether the UVA portion of the spectrum may actually be protective against UVB damage [30], however these issues remain controversial [24]. Therefore, agents with the ability to reverse early signs of skin cancers (actinic keratoses) or prevent their progression to malignancy are urgently needed and are more likely to be effective due to increased motivation by subjects at risk.

Niacin

Niacin, also known as vitamin B_3 or vitamin PP, is a water-soluble vitamin that occurs in two chemical forms: nicotinic acid and nicotinamide (also known as niacinamide). Niacin can be obtained directly from the diet or synthesized from dietary tryptophan in the liver in some species. However, the synthesis of niacin from tryptophan is extremely inefficient, where the dogma suggests that approximately 60 mg of dietary tryptophan produces 1 mg of niacin in the presence of vitamins B_2 and B_6. However, metabolic studies suggest this is highly unlikely in humans under moderate niacin deficiency situations [31]. The most important dietary sources of niacin in industrilized countries are animal products such as red meats and fishes, cereals, legumes, seeds, milk and green leaf vegetables [32].

Functions

Both nicotinic acid and nicotinamide are dietary precursors for the synthesis of important coenzymes involved in hydride ion transfer: nicotinamide adenine dinucleotide [NAD(H)] and nicotinamide adenine dinucleotide phosphate [NADP(H)]. NAD and NADP are the coenzymes of hundreds of enzymes [33]. NAD-dependent dehydrogenases are found mainly in the mitochondria. The roles of NAD as a co-enzyme in oxidative metabolism, specifically in the citric acid cycle, fatty acid oxidation, and glycolysis are well understood. The transfer of electrons from NADH formed in these processes to oxygen is the major source of adenosine triphosphate (ATP) in aerobic metabolism. NAD also serves as a

substrate for nicotinamide adenine dinucleotide phosphate [NADP(H)] biosynthesis. NADP-dependent dehydrogenases are mainly localized to the cytosol. This coenzyme serves an analogous role for transfer of electrons in biosynthetic reactions, functioning as hydride ion donor for reductive biosyntheses including fatty acid synthesis, cholesterol synthesis and hydroxylations.

Besides its role as a coenzyme, back in 1963 NAD^+ was found to have the potential to serve as substrate for covalent protein modifications [34]. Since then, considerable progress has been made towards understanding the multiple roles of NAD^+ as a substrate for mono-ADP ribosylation, poly(ADP-ribosyl)ation and NAD-dependent protein deacetylation. Furthermore, besides protein modification, NAD^+ may also be used for the synthesis of a signaling molecule, cyclic ADP-ribose (cADPR) [35,36], important in Ca_2^+ signaling.

Niacin and skin

The first indication of the beneficial effects of niacin to human skin was the observation that it could reverse the dermatitis associated with pellagra. Pellagra (from “pelle agra” meaning rough skin) is caused by severe niacin deficiency and was first described by Casal in 1735 as “mal de la rosa”, with symptoms of dermatitis, diarrhea, dementia and death [37]. Dermatitis occurred especially in areas exposed to sunlight, and was characterized by skin thickening, scaling and hyperkeratinization [38]. The observation that the dermatitis observed in pellagra patients, along with other symptoms of pellagra, could be reversed by oral niacin

supplementation lead to establishing niacin deficiency as the major etiological component of pellagra.

A deficiency of either niacin or tryptophan can result in pellagra in a nutritionally weak person. However, even when there is sufficient dietary intake, it is possible for niacin deficiency to occur. An excess of dietary leucine can interfere with niacin utilization and result in pellagra [32]. Pellagra-like dermatitis (secondary pellagra) occurs when adequate quantities of niacin are present in the diet, but other diseases or conditions interfere with its intake, absorption and/or processing, such as prolonged diarrhea, anorexia nervosa, chronic alcoholism, chronic colitis, severe ulcerative colitis, regional ileitis, hepatic cirrhosis, carcinoid tumor, Hartnup's syndrome, and tuberculosis of the gastrointestinal tract [39-43]. In patients with carcinoid syndrome, tumor cells convert tryptophan into serotonin, depressing endogenous niacin production. As the antituberculosis medication isoniazid is an analog of niacin, it may also suppress endogenous niacin production and produce pellagra [40]. In Hartnup's disease dietary amino acids including tryptophan are poorly absorbed. Long-term administration of 5-fluorouracil is known to cause symptoms of pellagra, as 5-flurouracil inhibits the conversion of tryptophan to nicotinic acid. Other drugs may also produce pellagra by interfering with the tryptophan-niacin pathway, including pyrazinamide, 6-mercaptopurine, hydantoins, ethionamide, phenobarbital, azathioprine, and chloramphenicol. In addition, one of the many disfunctions

occurring in HIV disease is a massive plasma tryptophan and niacin deficiency, sometimes leading to a pellagra-like state [44,45].

NAD and poly(ADP-ribose) polymerases

As mentioned previously, in addition to its role as a co-factor in redox reactions and as a regulator of the redox state (NAD^+/NADH), NAD functions as a substrate for numerous classes of ADP-ribosyl transferases, enzymes involved in cellular processes including transcription, calcium homeostasis, DNA repair, cell death, neoplastic transformation, etc [46,47]. Considerable evidence now indicates that the relative NAD content of cells can influence cellular responses to genomic damage by multiple mechanisms. For example, NAD^+ is a substrate for the poly(ADP-ribose) polymerase (PARP) family of enzymes, which are important in DNA damage responses, including repair, maintenance of genomic stability, signaling following stress responses that influences apoptosis, telomere function, transcription regulation, and numerous other cellular functions [48-51]. Interestingly, PARP-1 functions both as a structural component of chromatin and a modulator of chromatin structure through its intrinsic enzymatic activity, promoting the formation of compact, transcriptionally repressed chromatin structures [52].

The beneficial effects of niacin have been attributed to the involvement of PARP-1 as a target for cancer prevention based on studies from many laboratories, including our own, that have demonstrated the involvement of PARP-1 in the maintenance of genomic integrity following genotoxic stress

[48,53]. PARP-1 functions in the synthesis of chromatin-associated ADP-ribose polymers (PAR) that function in cellular recovery from DNA damage and maintenance of genomic stability. The activation of PARP-1 by DNA strand breaks leads to complex signaling pathways that can enhance cell survival, result in cell death by apoptosis, or cause energy loss that leads to necrosis (Figure 1.1). In cases where the amount of damage is relatively small, PARP-1 activation enhances cellular recovery by interaction with other proteins such as p53 and the nuclear proteosome to stimulate both DNA repair and histone degradation such that the cell can fully recover from the genotoxic stress. When the damage is relatively higher, PARP-1 plays a key role in effecting cell death by apoptosis through its transcriptional activation role involving the NF-κB pathway and by preventing ATP depletion and DNA repair through PARP-1 cleavage [53]. Finally, when the damage is very high, PARP-1 overactivation can lead to cellular necrosis through depletion of first NAD and then ATP with a resulting loss of all energy dependent functions. A more recent study has suggested that a drop in NAD levels itself can trigger the mitochondria to initiate cellular apoptosis [54]. Inhibitors of PAR metabolism alter the repair of DNA strand breaks [55,56] and increase the cytotoxic effects of DNA alkylating agents [55-58]. These inhibitors also increase the frequency of malignant transformation by these agents [59]. Blocking ADP-ribose polymer metabolism using a molecular genetic approach that involved overexpression of the DNA binding domain of PARP-1 has also shown inhibition of DNA repair and increased cytotoxicity [60]. Furthermore, mice

with homozygous disruption of the PARP-1 gene show increased sensitivity to cytotoxic agents and increased susceptibility to chemical carcinogens [61].

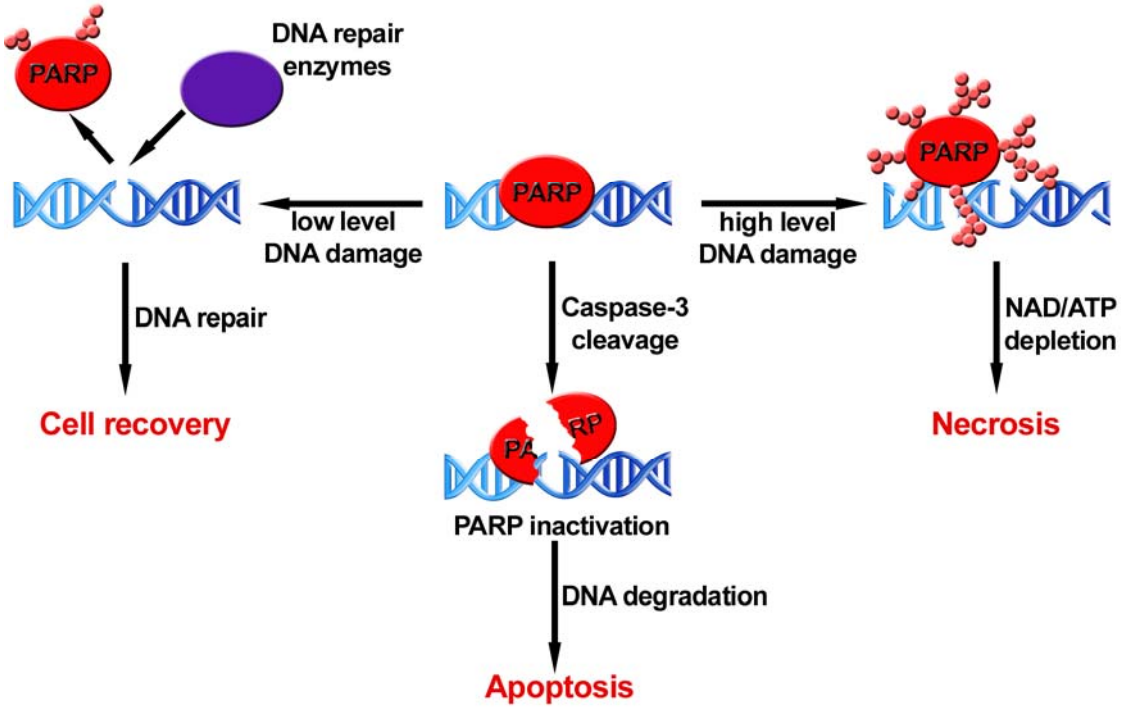

Figure 1.1. Outcomes upon PARP activation. PARP-1/2 activity is regulated by many factors, such as DNA damage, caspases, and the intracellular NAD^+ concentration. Inactivation of PARP-1 by caspase-3 cleavage is one of the key events of apoptosis, while over-activation of PARP-1 leads to ATP-depletion and subsequently to necrosis.

Among other members of the PARP family, PARP-2 is activated by DNA strand breaks, similarly to PARP-1. In fact, in the absence of PARP-1, PARP-2 is required for repair of single strand breaks and maintenance of genomic stability [62,63]. PARP-3 associates with the daughter centriole within centrosomes and

interferes with G_1/S cell cycle progression [64]. PARP-4 acts as a catalytic component of vault particles which are thought to function in intracellular transport and are involved in multidrug resistance in human tumors [65]. PARP-5 (also referred as tankyrase-1) and PARP-6 (tankyrase-2) regulate telomere homeostasis by diminishing the ability of the negative regulator of telomere length, TRF-1, to bind telomeric DNA and therefore, promoting telomere elongation [66,67].

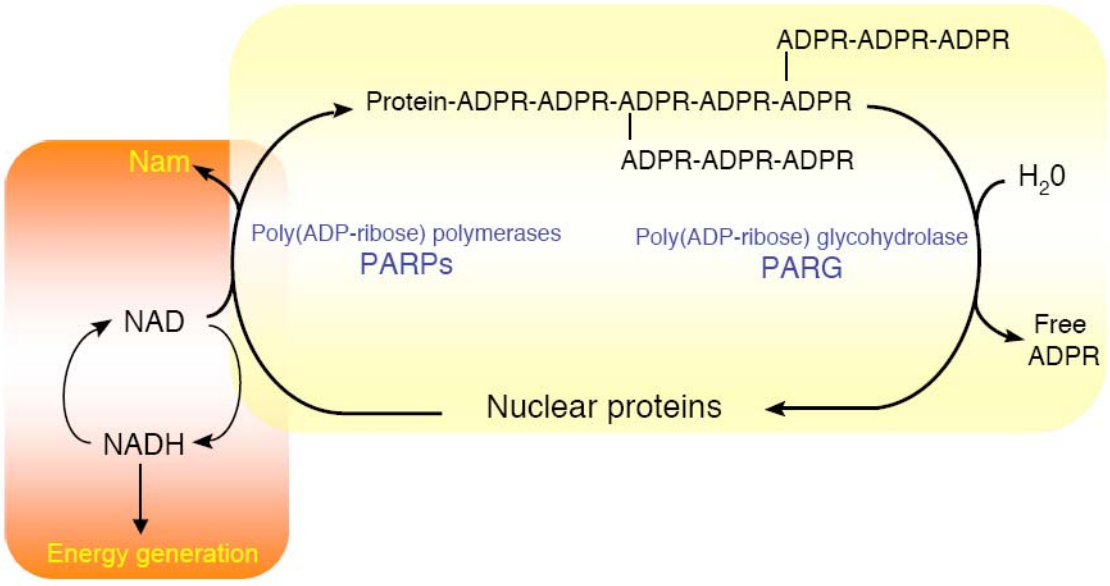

Figure 1.2. Metabolism of poly(ADP-ribose). Poly(ADP-ribose) polymerases (PARPs) hydrolyze NAD^+, releasing nicotinamide (Nam) and catalyzing the transfer of the ADP-ribose moiety to protein acceptors that might be transiently inactivated. Poly(ADP-ribose) glycohydrolase (PARG) reverses PARP action by cleaving glycosidic bonds between ADP-ribose units

NAD and sirtuins

In addition to NAD^+ serving as a substrate for ADP-ribosylation reactions, NAD^+ is a substrate for NAD^+-dependent protein deacetylases (sirtuins). Sirtuins (SIRTs) have been reported to function in stress responses, apoptosis, transcriptional regulation, metabolism, differentiation, and aging [68-71], and will be discussed in more detail later in the introduction.

Niacin as a chemoprotectant agent

In vitro as well as animal studies show that modulation of NAD^+ by nutritional control results in altered cellular processes and sensitivity to DNA damage. Cells cultured under conditions of nutritional depletion of NAD are more sensitive to the cytotoxic effects of DNA-damaging agents [49]. This sensitivity is thought to be due to reduced availability of NAD, resulting in impaired PARP-1 function and DNA repair mechanisms. In human cells, niacin deficiency has been shown to alter the expression of p53, induce inherent genomic instability, and reduce survival following exposure to solar simulated light [72,73]. Conversely, increased NAD^+ or more active NAD biosynthesis allows cells to recover more efficiently after DNA damage [72].

In animal studies, UV exposure in niacin deficiency leads to sensitized skin [74], while niacin supplementation protects mouse skin from UV irradiation [75]. Also in animals, niacin deficiency has been shown to cause changes in NAD^+ and poly(ADP-ribose) metabolism altering p53 expression, increasing

genomic instability, impairing cellular responses to DNA damage, and increasing cancer incidence [76-80].

In human subjects, pilot data has demonstrated that the NAD content of skin varies widely and that NAD content inversely correlates with malignant phenotype [72,81]. NAD content of normal skin in subjects diagnosed with squamous cell carcinoma is significantly lower than that of individuals showing pre-cancerous lesions [72]. Preliminary data also suggest that niacin supplementation may have protective effects against DNA damaging agents in a dose-dependent manner [75,82-84]. Thus, niacin supplementation may limit skin damage and consequently skin cancer by targeting multiple mechanisms including reduction of DNA damage and optimizing responses to DNA damage. These findings along with the evidence that the NAD content of human tissues, including skin, is deficient in a significant portion of the population raise the question as to whether niacin status (NAD content) is an important protective factor for genotoxic stresses resulting directly and indirectly from exposure to sunlight. Further, niacin deficiency allows one to model cellular conditions following DNA damage stress in order to investigate the NAD dependent signaling that occur under these conditions.

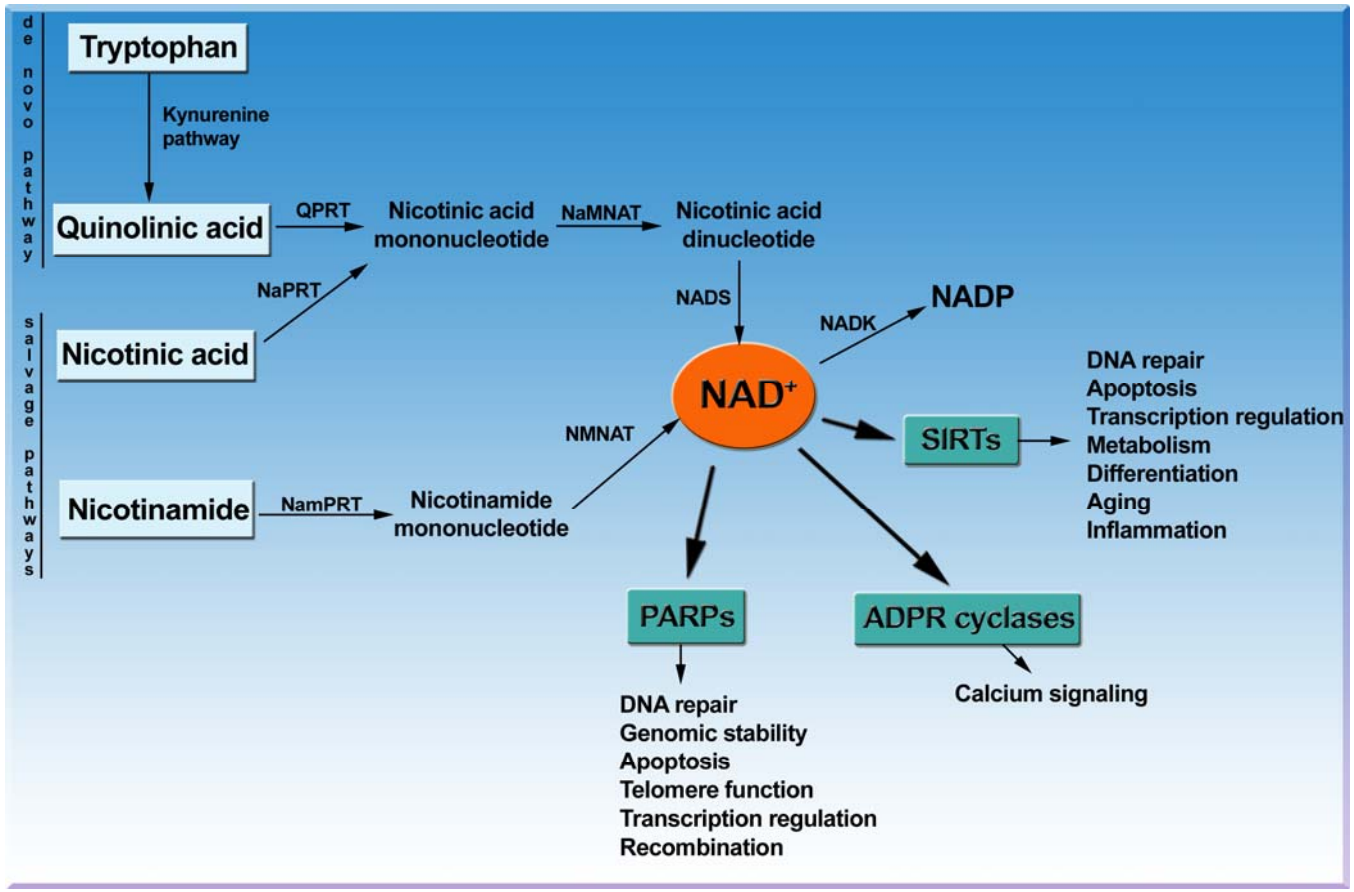

Figure 1.3. Mammalian NAD$^+$ metabolic pathways. Nicotinamide adenine dinucleotide (NAD), nicotinamide phosphoribosyltransferase (NamPRT), nicotinamide mononucleotide adenylyl transferase (NMNAT), nicotinic acid phosphoribosyltransferase (NaPRT), nicotinic acid mononucleotide adenylyl transferase (NaMNAT), NAD synthetase (NADS), quinolinic acid phosphoribosyl transferase (QPRT).

Sirtuins

Sirtuins (SIRTs) are members of a family of NAD^+-dependent enzymes that deacetylate histones and other proteins [85]. SIRTs belong to the Silent information regulator 2 (Sir2) family of histone deacetylases (HDACs), which play a central role in epigenetic gene silencing, DNA repair and recombination, cell-cycle regulation, microtubule organization, and in the regulation of aging.

All SIRTs share a conserved catalytic domain which is reported to function either as a NAD^+-dependent protein deacetylase and as a mono-ADP-ribosyltransferase (Figure 1.4) [86-89]. During the deacetylation reaction, SIRTs consume one NAD^+ molecule to generate acetyl-ADP-ribose and nicotinamide [88]. On the other hand, during mono-ADP-ribosylation, SIRTs consume one NAD^+ molecule to generate the ADP-ribosylated product and nicotinamide [86,90,91]. A conserved histidine residue in the catalytic core of the SIRTs is important for their deacetylase and mono-ADP-ribosyltransferase activities [86].

SIRT1

SIRT1, which is localized in the nucleus, is the most extensively studied member of the SIRT family. SIRT1 plays an important role in the regulation of cell fate and stress response in mammalian cells and has therefore been described as a guardian against cellular oxidative stress and DNA damage. SIRT1 promotes cell survival by inhibiting apoptosis or cellular senescence induced by stresses including DNA damage and oxidative stress. An increasing number of proteins have been identified as substrates of SIRT1 including p53 [70,92,93],

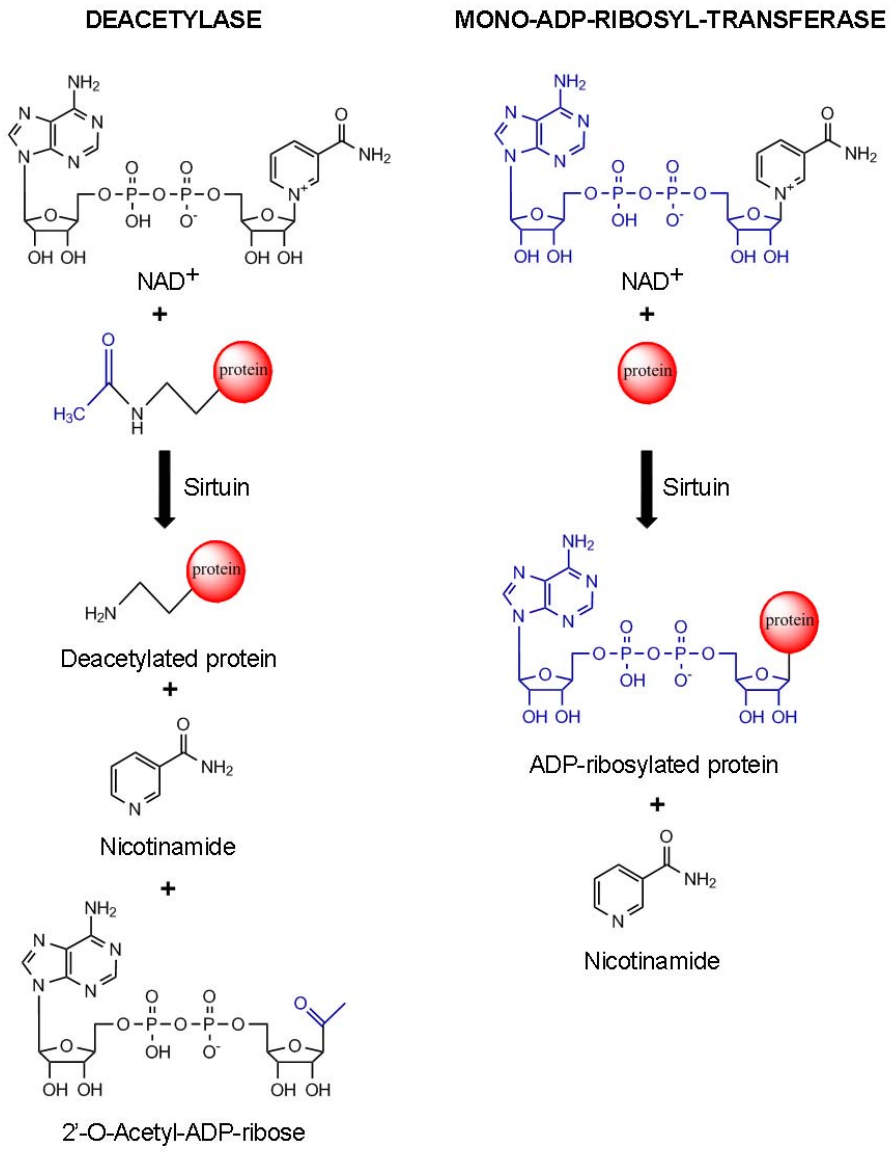

Figure 1.4. Enzymatic functions of sirtuins. Sirtuins deacetylation and ADP-ribosylation reactions. During the deacetylation reaction (left), NAD^+ is hydrolysed to generate nicotinamide, 2′-*O*-acetyl-ADP-ribose and the deacetylated target protein. During the ADP-ribosylation reaction (right), ADP-ribose is attached to the target protein and nicotinamide is released.

forkhead transcription factors (FOXO) [71,94-96], peroxisome proliferator-activated receptor-γ (PPARγ) [97] and Ku70 [98], which may relate to the observed stress resistance conferred by caloric restriction. SIRT1 also plays a role in muscle cell differentiation, adipogenesis, fat storage in white adipose tissue, and metabolism in the liver via regulation of the activity of the nuclear receptor PPARγ and PGC-α [97,99,100].

SIRT2

SIRT2 is a cytoplasmic protein which colocalizes both with chromatin during mitosis and microtubules in the cytoplasm. SIRT2 deacetylates tubulin [101] while in the cytoplasm and histone H4-K16 in the nucleus [102]. SIRT2 plays an important role in the control of mitotic exit in the cell cycle where increased SIRT2 activity severely delays cell cycle progression through mitosis [103]. SIRT2 also acts as a mitotic checkpoint protein that prevents chromosomal instability and the formation of hyperploid cells in the early metaphase [104].

SIRT3

SIRT3 is a nuclear SIRT that translocates to the mitochondria upon cellular stress [105]. In the nucleus, SIRT3 targets histone H4-K16 for deacetylation when recruited to a gene [105]. In the mitochondria, SIRT3's deacetylase activity has been linked with adaptative thermogenesis. SIRT3 expression is induced in mice in both white and brown adipose tissue by caloric restriction and in brown adipose tissue upon cold exposure. SIRT3 activates known mitochondrial genes such as PGC-1α and UCP-1 suggesting an important

role of SIRT3 in thermogenesis [106]. SIRT3 also has been linked to longevity [107,108].

SIRT4

SIRT4 is located to the mitochondria and contains the conserved SIRT domain, but it seems not to possess *in vitro* deacetylase activity [91]. SIRT4 has been shown to mono-ADP-ribosylate and inhibit glutamate dehydrogenase (GDH), a mitochondrial enzyme that converts glutamate to α-ketoglutarate [91]. GDH controls amino acid-stimulated insulin secretion by regulation of glutamine and glutamate oxidative metabolism. Inhibition of GDH activity by SIRT4 decreases insulin secretion in mouse pancreatic β-cells in response to amino acids [91].

SIRT5

SIRT 5 is the least characterized member of the SIRT family and little is known about its activity. SIRT5 has been described as a mitochondrial protein [109] with weak deacetylase [101] and no ADP-ribosyltransferase activity [91]. SIRT5 is most predominantly expressed in heart muscle cells and in lymphoblasts [110].

SIRT6

SIRT6 is a nuclear protein associated with heterochromatin that promotes resistance to DNA damage and suppresses genomic instability in mouse cells, in association with a role in base excision repair (BER) [109,111]. SIRT6 deficient mice display multiple pathologies that resemble human ageing including

lymphopenia, loss of subcutaneous fat, decreased bone density, hypoglycemia, decreased IGF-1 levels, and premature death [111]. SIRT6 was initially described as an ADP-ribosyl-transferase [90], but was later shown, *in vitro*, to deacetylate histones and DNA polymerase β, a DNA repair enzyme [111]. It is suggested that SIRT6 may play an essential role in maintaining organ integrity as animals age.

SIRT7

SIRT7 is a widely expressed protein localized in the nucleolus and associates with condensed chromosomes during mitosis [109,112]. SIRT7 expression is abundant in tissues with high proliferation and low in non-proliferating tissues [112]. SIRT7 has been suggested to play a role as a positive regulator of RNA polymerase I transcription and may be required for cell viability in mammals [112]. SIRT7 interacts with RNA polymerase I and histones, and positively regulates the transcription of active rRNA genes (rDNA). Depletion of SIRT7 stops cell proliferation and triggers apoptosis [112]. Like the rest of the SIRT family, the NAD^+ binding core domain is conserved in SIRT7, but no deacetylase or ADP-ribosyltransferase activity has been demonstrated to date [112]. It has been suggested that SIRT7 regulates rDNA transcription in a NAD^+ dependent manner, such that NAD^+/NADH ratio might modulate SIRT7 to link the cellular energy status with rRNA synthesis and ribosome production [113].

HaCaT keratinocytes

In this study, we utilize nicotinamide restriction mainly in cultured HaCaT keratinocytes to identify NAD-dependent signaling events that may be critical in early skin carcinogenesis. This cell line is derived from normal human abdominal skin and has been shown to exhibit a differentiation profile comparable with normal human keratinocytes [114]. Despite the altered and unlimited growth potential, these cells have been reported to form an orderly structured and differentiated epidermal tissue after transplantation on to athymic nude mice [114]. However, HaCaT cells exhibit UV-B type-specific mutations on the p53 tumor suppressor gene [115], and aberrant NF-kB signaling and altered responses to UVB [116], thus they represent an early stage of precancerous skin cells. We have used this model to test the hypothesis that restricted nicotinamide and NAD^+ status, under conditions where cells continue to proliferate indefinitely, allow identification of NAD-dependent signaling pathways involved in the early responses to UV damage important in limiting skin carcinogenesis.

Central Hypothesis

NAD status modulates human skin cell metabolism and the responses to photo-damage, acting through PARPs, SIRTs, and/or alterations in energy metabolism.

Specific Aims

- To establish *in vitro* skin models where cellular NAD can be modulated.
- To characterize the biological consequences of NAD modulation and pathways involved/altered under this condition to understand regulation of non-malignant cells.
- To identify the effects of modulating NAD on cellular responses to photo-damage and determine the mechanisms by which NAD regulates these responses.

CHAPTER II

NIACIN RESTRICTION UPREGULATES NADPH OXIDASE AND ROS IN HUMAN KERATINOCYTES

Abstract

NAD^+ and its reduced and phosphorylated forms play central roles in cellular metabolism, energy production processes, DNA damage response, and cell death among others. Because these molecular processes are important early in cancer development, we developed a model to identify critical NAD-dependent pathways potentially important in early skin carcinogenesis. Removal of niacin from the cell culture medium allowed control of intracellular NAD. Unlike many non-immortalized human cells, HaCaT keratinocytes, which are immortalized and have a mutant p53 and aberrant NF-kB activity, become severely NAD depleted but divide indefinitely under these conditions. Niacin deficient HaCaTs develop a decreased growth rate due to an increase in apoptotic cells and an arrest in the G_2/M phase of the cell cycle. Long- term survival mechanisms in niacin deficient HaCats involve accumulation of reactive oxygen species and increased DNA damage. These alterations result, at least in part, from increased expression and activity of NADPH oxidase, whose downstream effects can be reversed by nicotinamide or NADPH oxidase inhibitors. Our data support the hypothesis that glutamine is a likely alternative energy source during niacin deficiency and we suggest a model for NADPH generation important in ROS production.

Introduction

Niacin (Vitamin B_3) is a water-soluble vitamin that occurs in two forms: nicotinic acid and nicotinamide. Both nicotinic acid and nicotinamide are dietary precursors for the synthesis of nicotinamide adenine dinucleotide, NAD(H), and related coenzymes, NADP(H). In addition to its role as a co-factor in redox reactions and as a regulator of the redox state (NAD^+/NADH), NAD^+ functions as substrate for numerous classes of ADP-ribosyl transferases involved in cellular processes including transcription, calcium homeostasis, DNA repair, cell death, neoplastic transformation, etc. [46,47]. Considerable evidence now indicates that the relative NAD^+ content of cells can influence cellular responses to genomic damage by multiple mechanisms. For example, NAD^+ is a substrate for the nuclear enzymes poly(ADP-ribose) polymerases (PARPs), which are important in DNA damage responses, including repair, maintenance of genomic stability, signaling following stress responses that influences apoptosis, telomere function, transcription regulation, and numerous other cellular functions [48-51]. Interestingly, PARP-1 functions both as a structural component of chromatin and a modulator of chromatin structure through its intrinsic enzymatic activity, promoting the formation of compact, transcriptionally repressed chromatin structures [52]. Furthermore, NAD^+ is a substrate for NAD^+-dependent protein deacetylases (SIRTs), which have been reported to function in stress responses, apoptosis, transcriptional regulation, metabolism, differentiation, and aging [68-71]. As a specific example, the action of SIRTs in histone deacetylation leads to

a more compact chromatin structure and gene silencing. These enzymes also appear to protect sensitive areas of chromatin, such as telomeres, against translocation events and to play a role in extended life span associated with caloric restriction [117].

In vitro as well as animal studies indicate that modulation of NAD^+ by nutritional control results in altered cellular processes and sensitivity to DNA damage. In human cells, niacin deficiency has been shown to alter the expression of p53, induce inherent genomic instability, and reduce survival following exposure to solar simulated light [72,73]. Conversely, increased NAD^+ or more active NAD biosynthesis allows cells to recover more efficiently after DNA damage [72]. In animal studies, niacin deficiency has been shown to cause changes in NAD^+ and poly(ADP-ribose) metabolism altering p53 expression, increasing genomic instability, impairing cellular responses to DNA damage, and increasing cancer incidence [76-80]. In human subjects, NAD content has been inversely correlated with malignant phenotype [72,81]. Preliminary data also suggest that niacin may have protective effects against DNA damaging agents [75,82]. Thus, niacin may limit skin damage and consequently skin cancer by targeting multiple mechanisms including reduction of DNA damage and optimizing responses to DNA damage.

The turnover of NAD as a substrate by numerous classes of enzymes suggests that the flux of niacin through cellular pyridine nucleotides may be much greater than previously thought and may influence cellular regulation in a highly

complex manner. Since the maintenance and regulation of cellular NAD(P)(H) content and its influence on cell functions are poorly understood, we have developed a cell culture model that allows assessment of pathways regulated by NAD(P) content. In this study, we utilize nicotinamide restriction in cultured HaCaT keratinocytes to identify NAD dependent signaling events that may be critical in early skin carcinogenesis. This cell line is derived from normal human skin and has been shown to exhibit a differentiation profile comparable with normal human keratinocytes [114]. Despite the altered and unlimited growth potential, these cells have been reported to form an orderly structured and differentiated epidermal tissue after transplantation on to athymic nude mice [114]. However, HaCaT cells exhibit UV-B type-specific mutations on the p53 tumor suppressor gene [115], and aberrant NF-kB signaling and altered responses to UVB [116], thus they represent an early stage of precancerous skin cells. We have used this model to test the hypothesis that restricted nicotinamide and NAD^+ status, under conditions where cells continue to proliferate indefinitely, allow identification of NAD dependent signaling pathways involved in the early responses to DNA damage and early events in skin carcinogenesis.

Materials and Methods

Cell Culture and Growth Measurements

Normal human keratinocytes (NHEK cells, ATCC), were routinely cultured in Keratinocyte Medium 2 (KGM-2, Lonza) containing SingleQuots (Lonza). Normal human dermal fibroblasts (CF3, ATCC) and the established cell line of human epidermal keratinocytes (HaCaT cells), a gift from Dr. Norbert Fusenig (German Cancer Research Center, Heidelberg, Germany), were routinely cultured in Dulbecco's Modified Eagle Medium (DMEM) containing 10% bovine calf serum and kept in a humidified atmosphere containing 5% CO_2 at 37°C. For NAD(P) modulation, HaCaT and CF3 cells were grown in a specially formulated DMEM (Gibco BRL) without nicotinamide, 10% dialyzed fetal bovine serum (Gibco BRL) and with addition of 33 μM nicotinamide (33 μM Nam) or without added nicotinamide (0 μM Nam). Cell number was measured by counting in a Z1 Coulter Counter (Beckman Coulter Corporation). Sensitivity to glutaminase inhibition was performed using 0.1 μM 6-diazo-5-oxo-L-norleucine (DON) on cells grown in 33 μM Nam or 0 μM Nam for 7 days.

Extraction and Assay of NAD(H) and NADP(H*)*

NAD^+, $NADP^+$, NADH and NADPH were extracted from cultured cells by homogenization in 1.0 M NaOH. For total NAD and NADP determination, half of each sample was immediately neutralized with 2.0 M H_3PO_4 and the reduced pyridine nucleotides were then oxidized by adding a 1/10 volume of 2.0 mM phenazine ethosulfate (Sigma Biochemical Co.). The sample was then brought to

1.0 M $HClO_4$, incubated 10 min on ice, and the extract was centrifuged at 850 *g* for 10 min. The pellet was reserved for DNA quantification. The supernatant was neutralized with 1.0 M KOH, and the insoluble $KClO_4$ was removed by centrifugation. The resulting supernatant was assayed as described previously [118,119] to yield total NAD and NADP. NADH and NADPH were extracted using the other half of each cell extract, which was heated to 60°C for 10 min to destroy oxidized pyridine nucleotides. The extract was neutralized with 2.0 M H_3PO_4, chilled and processed as described above to provide NADH and NADPH. NAD^+ and $NADP^+$ were calculated as the difference between total and reduced pyridine nucleotides. The pellet precipitated by $HClO_4$ was dissolved in 0.5 M NaOH, and the DNA concentration was determined using the Quant-iT OliGreen Assay (Invitrogen). NAD(P)(H) values were normalized to DNA in each sample extracted.

Cell cycle analysis

Cell cycle analysis was performed using the method described by Krishan [120]. Cells were harvested, washed and resuspended in phosphate buffer saline (PBS) at a final concentration of $1\text{-}2\cdot10^6$ cells/ml. Cells were permeabilized and fixed using 3 volumes of cold absolute ethanol and incubated for 1 h at 4°C. Cells were washed twice with PBS and stained with propidium iodide at a final concentration of 50 µg/ml. Rnase A was added to a final concentration of 500 ng/ml and incubated for 1 h at 4°C. Samples were kept at 4°C until flow cytometry analysis.

Cell death analysis

Cell death was determined by Annexin-V-fluorescein isothiocyanate/ propidium iodide dual staining of cells followed by flow cytometric analysis, as first described by Vermes et al [121]. HaCaT keratinocytes (100,000) were seeded on 35 mm dishes and 24 h later the medium was changed. Cells were harvested 24 h later, and cell staining was performed using an apoptosis detection kit according to the manufacturer's specifications (APO-AF; Sigma-Aldrich). In the figures shown, lower left quadrant ($AnnexinV^-$, PI^-) represents viable cells, lower right ($AnnexinV^+$, PI^-) is early apoptosis and upper right ($AnnexinV^+$, PI^+) is late apoptosis and necrosis.

Detection of intracellular oxidative stress by flow cytometry analysis

Intracellular reactive oxygen species (ROS) were analyzed by flow cytometry using dichlorofluorescein diacetate (DCF-DA; Sigma) as a specific dye probe which fluoresces upon oxidation by ROS. HaCaT keratinocytes were seeded at $1 \cdot 10^5$ cells per 35 mm dish. Cells loaded with DCF-DA (50 µg/ml) with light exclusion for 60 min were washed three times with PBS. Intracellular accumulation of fluorescent DCF-DA was measured (10,000 cells each) using a FACScan flow cytometer (Becton-Dickinson, San Jose, California). Histograms were analyzed with the software program Cell Quest (Becton-Dickinson).

Comet assay

HaCaT keratinocytes were seeded at $1 \cdot 10^5$ per dish on 35 mm culture dishes (Sarstedt, Newton, NC) and left overnight to attach. Cells were removed by trypsinization and analyzed by alkaline single cell gel electrophoresis (comet assay) based on the method of Singh et al. [122]. Briefly, 100 µL of cells (100,000 cells/ml) suspended in PBS were mixed with 100 µL of 0.5% low melting point agarose (Sigma) and layered on CometSlides (Trevigen, Gaithersburg, MD). The mixture was allowed to solidify at 4ºC for 15 min on a metal plate. Cells were then exposed for 1 h at 4ºC to freshly prepared lysis buffer (2.5 M NaCl, 100 mM EDTA, 1% Triton, and 10 mM Tris, adjusted to pH 10 with NaOH). Following cell lysis, the slides were incubated with freshly prepared alkali buffer (300 mM NaOH, 1 mM EDTA, pH >13) at room temperature for 40 min to allow DNA denaturation and unwinding. Then, the slides were placed in a horizontal electrophoresis box and filled with chilled, freshly prepared alkali buffer at 4ºC and electrophoresis was carried out by a constant electric current of 300 mA for 23 min. After electrophoresis, the slides were neutralized with three 5 min washes in 0.4 mol/L Tris-HCl (pH 7.4). Finally, the slides were fixed in 100% ethanol for 5 min and stored in the dark at room temperature.

Quantification of DNA Damage

Immediately prior to imaging, comet slides were hydrated and stained by exposure to 1 mg/mL ethidium bromide for 15 min. Comets were analyzed using

fluorescence based digital imaging system. Tail moments were calculated using Comet Assay Software Project (Casp) imaging software.

Immunofluorescent detection of phosphorylated histone H2AX

Cells washed in PBS and fixed in 5% formaldehyde in PBS for 30 min at RT. Cells were then permeabilized with 0.4% Triton X-100 in PBS for 3 min at RT, washed with PBS and blocked with 3% BSA-PBS for 30 min at RT. Cells were then incubated for 1 hr at 37ºC in the presence of a γ-H2AX antibody (Upstate), followed by 3 washes in PBS and incubation with a suitable secondary antibody conjugated with FITC for 1 hr at 37ºC. Nuclear DNA was counterstained with DAPI and cells were examined at 60X magnification in an Olympus IX70 fluorescence microscope.

Measurement of reduced and oxidized glutathione

Reduced (GSH) and oxidized (GSSG) glutathione were measured using the Bioxytech GSH/GSSG-412 Assay Kit (OxisResearch, Portland, OR). $3 \cdot 10^6$ cells were detached using trypsin and centrifuged at 1300 *g* for 10 min at 4ºC. The cells were resuspended in 300 µL PBS. From this point the samples were treated and assayed following the manufacturer's protocol for whole blood assay.

RNA preparation and CodeLink microarray analyses

Total RNA was prepared from cultured HaCaT keratinocytes using the Rneasy purification system (Qiagen) according to the manufacturer's instructions. The RNA concentration was determined using an Eppendorf BioPhotometer (Eppendorf North America, Westbury, NY, USA). To test the

quality of the RNA, 1 µL (25-500 ng/µl) of the sample was analyzed on the Agilent 2100 Bioanalyzer (Agilent Technologies, Waldbronn, Germany) following the RNA 6000 Nano Chip Series II Assay protocol. For the CodeLink Bioarray system, 2 µg of total RNA were processed according to the protocol established by the CodeLink Gene Expression System manual. Total RNA was processed through first-strand and second-strand cDNA synthesis followed by purification using the QIAquick PCR Purification Kit (Qiagen, Inc., Valencia, CA, USA). The cDNA was used for an In Vitro Transcription and biotin labeling and the resulting cRNA was cleaned using the Rneasy Mini Kit (Qiagen, Inc., Valencia, CA, USA). The cRNA was quantified using the Eppendorf BioPhotometer and Agilent 2100 Bioanalyzer and then 10 µg were fragmented and subsequently hybridized on CodeLink Bioarray: UniSet Human 20K I slides overnight for 18-24 h at 37°C with agitation (300 rpm). The bioarray was removed and the subsequent staining and washing was performed according to the CodeLink Gene Expression System: Single-Assay Bioarray Hybridization and Detection protocol (GE Healthcare Bio-Sciences, Piscataway, NJ, USA). Fluorescence images were acquired using the GenePix 4000B Microarray Scanner (Axon Instruments, Foster City, CA, USA) along with the GenePix Pro 5.1 Software. The scans were performed following the specifications established by GE for their CodeLink bioarrays. Briefly, the GenePix software settings were as follows, 635 nm wavelength, with a PMT voltage of 600 V and a laser power set at 100%. The pixel size was set at 10 µm, and the focus position at 0 µm. The tiff images created were then imported

into the CodeLink Expression Analysis v4.0 Software (GE Healthcare Bio-Sciences, Piscataway, NJ, USA) where Bioarray QC readings were establish to test for hybridization efficiency and success. We used Loess normalization of the data using all the housekeeping genes present in the CodeLink bioarray as reference.

qPCR

Total RNA was prepared from cultured HaCaT keratinocytes using the Rneasy purification system (Qiagen) according to the manufacturer's instructions. cDNA synthesis was performed with the TaqMan Reverse Transcription kit (Applied Biosystems) according to manufacturer's instructions using random hexamers and 1 μg of total RNA. For TaqMan-based qPCR expression profiling, 25 ng of each cDNA were added to the TaqMan Universal PCR Master Mix along with the TaqMan MGB probes according to the manufacturer's instructions (Applied Biosystems).

qPCR was performed essentially as described [123]. Primers and probes designed to specifically detect the human NOX5 (TaqMan Gene Expression Assay Hs00225846_m1) and NCF-2 (TaqMan Gene Expression Assay Hs00166416_m1) transcripts were purchased from Applied Biosystems. Real-time fluorescence monitoring was performed with the ABI Prism 7900 (Applied Biosystems). Relative expression levels of the various transcripts were determined by comparison against the housekeeping genes GAPD and 18S rRNA. GAPD expression was verified to be unaltered upon niacin deficiency by

comparison against 18S rRNA. All expression measurements were performed in triplicate using three independently generated cDNA samples.

Results

NAD-modulation in skin cells

To study the role of NAD-dependent pathways in skin and ultimately identify their role(s) in responses to DNA damage and skin carcinogenesis, we developed an *in vitro* model in which intracellular NAD can be modulated by altering the availability of the NAD precursors in the medium [119]. Nicotinamide is commonly the form of niacin found in cell culture media. For our model, we omitted nicotinamide and used exhaustively dialyzed fetal bovine serum in the culture medium. We observed that HaCaT keratinocytes grown in this medium develop significantly reduced cellular NAD(H) concentrations as shown in Figure 2.1 and Table 2.1. Nicotinamide restriction reduced total intracellular NAD by >90% after 7 days and >99% after 14 days. The NADH/total NAD ratio (% NADH) increased at 7 days of restriction, but could not be measured at day 14 due to the fact that NADH fell below limits of detection. Thus, in this cell line, NAD can be nutritionally modulated over a large concentration range by controlling nicotinamide concentration in the culture medium and it appears that the NAD pool may become more reduced, at least early in the restriction phase.

When we measured NADP(H) in control and nicotinamide-restricted cells at 14 days, we found that the total NADP pools are relatively preserved compared to NAD, decreasing to about 35% of controls, as shown in Table 2.1. Interestingly, the percentage of reduced NADPH relative to the total NADP pool was maintained or slightly increased (60.4 ± 8.9 versus 65.7 ± 7.6) in restricted cells.

These alterations in pyridine nucleotides were sustained as long as cells were grown in medium with no added nicotinamide. The depletion in all pyridine nucleotide pools is reversed by addition of nicotinamide to the culture medium (Figure 2.1).

This depletion model was also used in normal human keratinocytes (NHEK) and normal human diploid fibroblasts (CF3). Interestingly, the NAD pool in NHEKs drop below limits of detection rapidly after niacin deprivation, while CF3 cells significantly reduce their NAD content, but are able to scavenge pyrimidine nucleotides to maintain their NAD levels to about 15% of controls (data not shown).

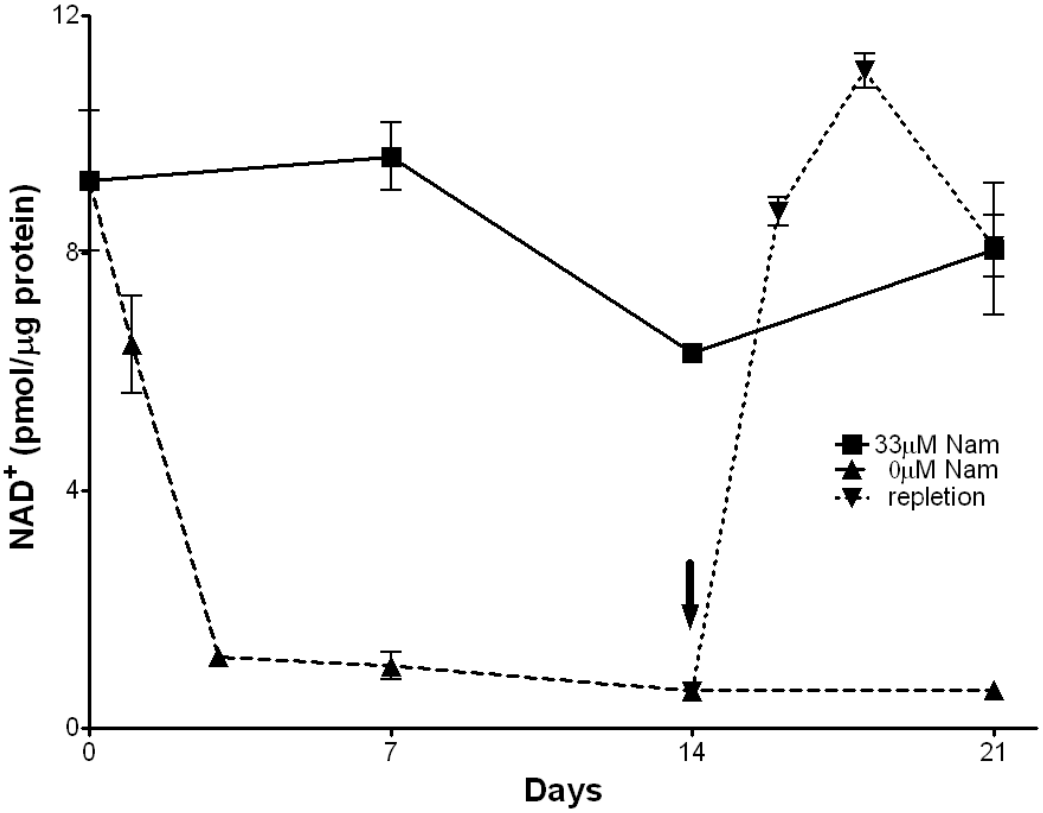

Figure 2.1. Effect of nicotinamide status on HaCaT keratinocytes NAD^+ levels. HaCaT keratinocytes were cultured on nicotinamide supplemented (33 µM Nam, squares), or nicotinamide restricted (0 µM Nam, triangles) conditions. HaCaT intracellular NAD^+ concentrations. Arrow shows the point at which nicotinamide was added back (repletion, inverted triangles).

Table 2.1. NAD(H), NADP(H) quantification and redox ratio in HaCaT cells grown with or without added nicotinamide

	Day 7		Day 14	
	33 µM Nam (fmol/ng DNA)	**0 µM Nam** (fmol/ng DNA)	**33 µM Nam** (fmol/ng DNA)	**0 µM Nam** (fmol/ng DNA)
Total NAD	3968 ± 385	337 ± 77***	3657 ± 322	7 ± 3***
NADH	97 ± 19	45 ± 15*	88 ± 23	ND
NAD^+	3871 ± 385	295 ± 83***	3567 ± 307	7 ± 3***
% reduced NADH/Total NAD	2.5 ± 0.5	13.2 ± 5.1*	2.4 ± 0.6	ND
Total NADP	199 ± 12	80 ± 12***	320 ± 25	109 ± 14***
NADPH	113 ± 14	50 ± 10**	181 ± 18	63 ± 4**
$NADP^+$	86 ± 18	30 ± 16*	141 ± 10	46 ± 15**
% reduced NADPH/Total NADP	61.5 ± 10.1	55.8 ± 10.9	60.4 ± 8.9	65.7 ± 7.6

Shown are the mean ± SEM of 6 replicates from 2 independent experiments. ND, not detectable. * $p < 0.05$, ** $p < 0.005$, *** $p < 0.0001$. p values were calculated comparing 0 µM Nam to the respective 33 µM Nam condition.

Nicotinamide-restricted HaCaTs divide indefinitely after establishing an altered growth rate

Under nicotinamide-restricted conditions, which lead to NAD depletion, HaCaT keratinocytes proliferate at the same rate as controls for approximately 7 days then develop a slower population doubling rate (77 h versus 48.8 h for control cells) that is constant and sustained indefinitely as shown in Figure 2.2. Addition of nicotinamide at any time during the study in Figure 2.2 restored the original doubling rate (data not shown). Surprisingly, growth was sustained indefinitely even though NAD was < 1% of that in control cells, unlike NHEK cells that are unable to sustain proliferation once they have become depleted (Figure 2.3). On the other hand, proliferation of CF3 cells is not affected by nicotinamide restriction, as we observe that depleted CF3s maintain a proliferation comparable to cells grown under control conditions (Figure 2.3). The inability of NHEKs to proliferate under nicotinamide-restricted conditions makes it an unfit model for comparison with nicotinamide-restricted HaCaTs. Therefore, we have chosen CF3s as an alternative reference for a normal dermal cell.

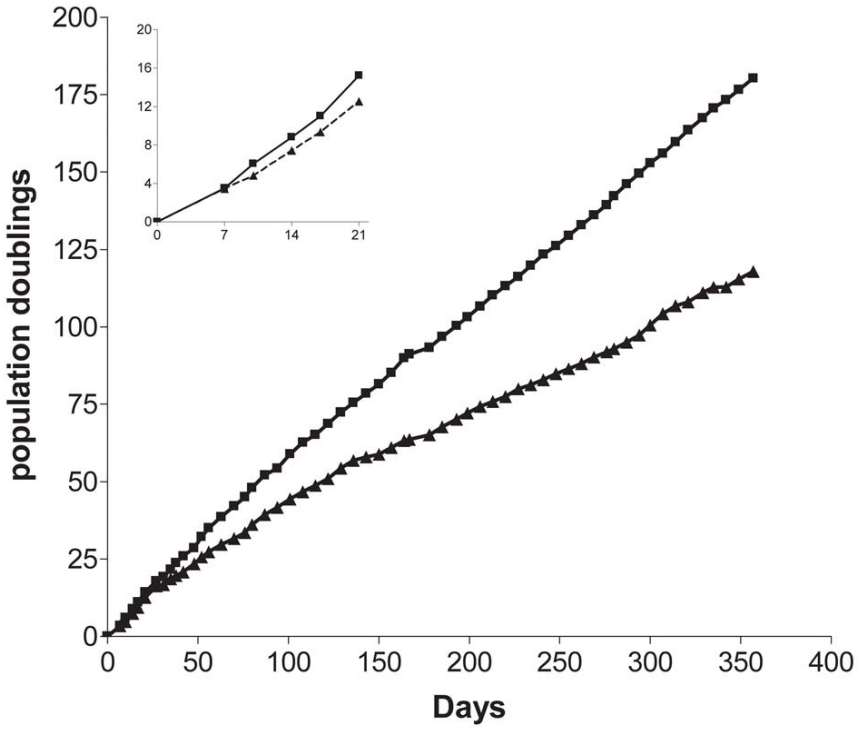

Figure 2.2. Effects of nicotinamide restriction on HaCaT keratinocytes proliferation. Growth rates of HaCaT cells grown under control (33 μM Nam, squares), or restricted (0 μM Nam, triangles) conditions. Inset shows details of growth for days 0 to 21. Values correspond to duplicate samples (Mean ± SEM).

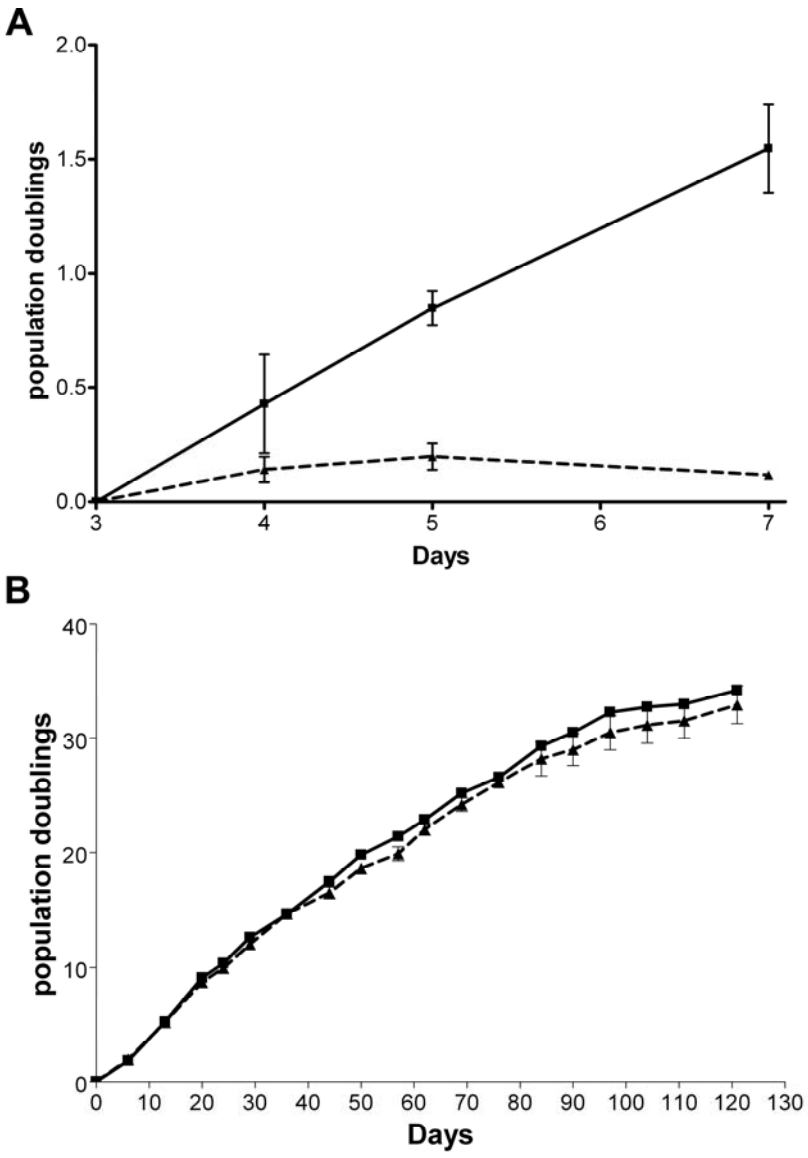

Figure 2.3. Effects of nicotinamide restriction on NHEK and CF3 proliferation. Growth rates of cells grown under control (33 μM Nam, squares), or restricted (0 μM Nam, triangles) conditions. (A) NHEKs; (B) CF3s. Values correspond to duplicate samples (Mean ± SEM).

Nicotinamide-restriction decreases cell viability and alters the cell cycle distribution in HaCaT keratinocytes

To study the mechanism(s) by which HaCaT cells with reduced NAD establish an altered population doubling time, we hypothesized that cell death rates increase in restricted cells and/or that cell cycle check points are altered affecting cell cycle progression. Thus, cell death rates and cell cycle distribution were assessed after 7 days, the time at which no change in population doubling rate is yet detectable, and after 14 days of restriction, when the slower proliferation rate is established. As can be seen in Figure 2.4, the viability of the control cell population is 91-94% at 7 and 14 days as assessed by Annexin V/PI staining and flow cytometry; however, cell death rates increased when cells were restricted for 14 days, dropping to approximately 85% viability ($p < 0.0001$). Addition of nicotinamide (repletion, Figure 2.4) completely reversed this effect. CF3s showed no change in proliferation rates upon nicotinamide restriction and consistent with this observation, we observe no changes in the viability of these cells, with normal cells displaying a 94.8 ± 0.4% viability and restricted cells a 94.9 ± 1.4% viability.

In order to account for the observed changes in population doubling times by loss of cell viability alone, a decrease in viability of approximately 15% would be required, assuming no change in cell cycle progression. In averaging five repeated experiments, we observed an average reduction in viability of 8.9 ± 4.2%. These data suggest that NAD depletion may affect cell proliferation by an

additional mechanism other than increased cell death. We examined the possibility that cell cycle progression may be altered by measuring the cell cycle distribution. The results are shown in Figure 2.5. We observe a small but significant increase, from 11.7 ± 1.6 to 17.4 ± 2.1 ($p = 0.0004$), in the percentage of cells in G_2/M-phase at day 7, despite the fact that no change in population doubling is observable yet at this time. An equivalent decrease in the percentage of cells in S-phase accompanied the G_2/M alteration. The observed alterations in cell cycle distribution at day 7 may be an early indication of changes in keratinocytes undergoing nicotinamide restriction. After 14 days of depletion, the increase in percentage of cells in G_2/M is elevated to 20.3 ± 1.1 ($p < 0.0001$), and is associated with a significant decrease of cells in both G_1 and S phases. Thus both a delay at G_2/M and a decrease in viability contribute to the increased doubling time observed in nicotinamide-restricted HaCaTs.

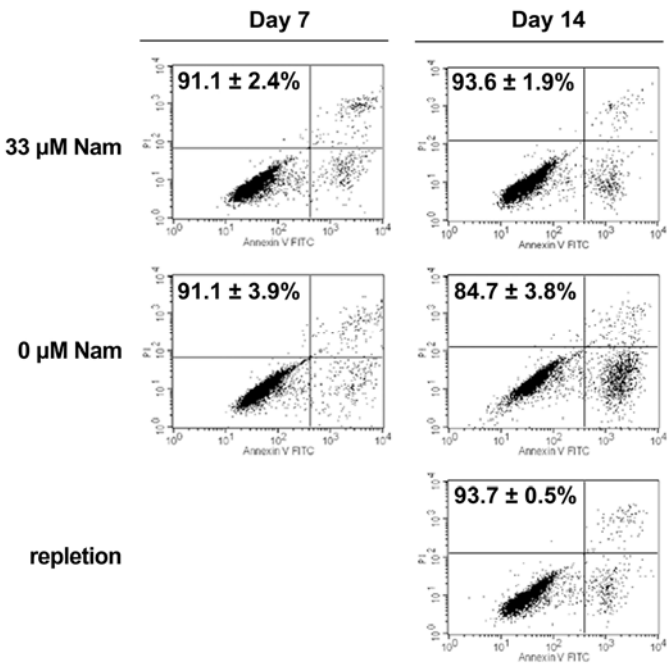

Figure 2.4. Effects of nicotinamide restriction on HaCaT keratinocytes viability. Cell viability was assessed for 33 µM Nam, 0 µM Nam and repleted cells using Annexin V/PI flow cytometry. Values represent percentage of viable cells from triplicate samples (Mean ± SEM).

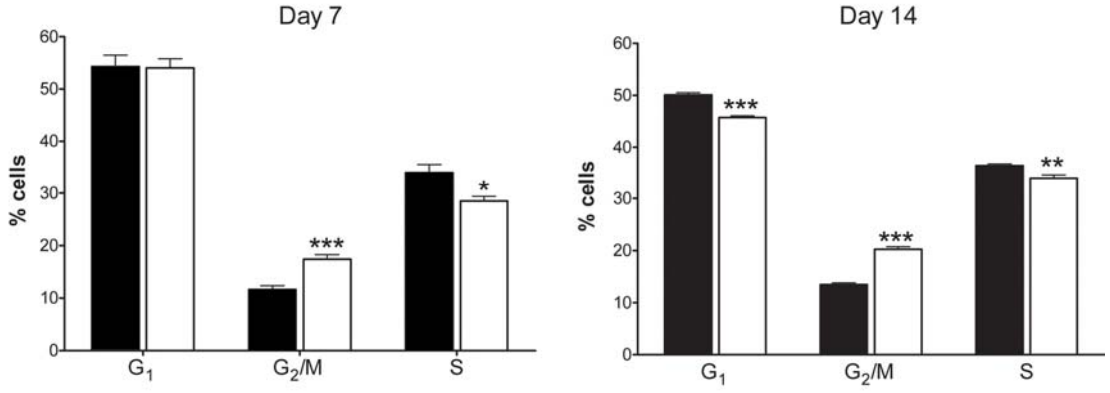

Figure 2.5. Effects of nicotinamide restriction on HaCaT keratinocytes cell cycle. Cell cycle analysis was assessed for 33 µM Nam (black) and 0 µM Nam (white). Bars represent the mean of triplicate analyses (± SEM) by PI fluorescence and flow cytometry. * $p < 0.05$, ** $p < 0.005$, *** $p < 0.0001$

DNA damage is increased in NAD-depleted HaCaT keratinocytes

Since PARP-1 is known to play an important role in response to DNA damage and has a relatively high K_m for NAD, we investigated whether NAD depletion in plays a role in DNA damage that may contribute to altered cell cycle progression. We examined HaCaT keratinocytes for DNA single strand breaks and alkali labile sites using the alkaline comet assay [122]. As seen in Figure 2.6A, no detectable differences in comet tail moments were apparent between control and NAD-depleted cells prior to the observed changes in proliferation and cell viability rates (day 7); however, by day 14, we observed a significant increase of tail moment in NAD-depleted cells from 10.5 ± 0.9 to 27.1 ± 1.9 ($p < 0.0001$). Addition of nicotinamide to restore NAD reversed the DNA damage as measured by comet tail moments (11.9 ± 1.1). Continuing with the trend observed in CF3s, no significant change was observed in the comet mean tail moment of restricted cells. Nicotinamide restricted CF3s present a 20.7 ± 4.1 mean tail moment, compared to 14.0 ± 1.5 in controls (n=3).

In addition to alkaline comet assay in HaCaTs, we also examined the response to double-strand breaks by phosphorylation of histone H2AX (γ-H2AX). Figure 2.6B shows how NAD depleted HaCaTs have an increased number of cells with γ-H2AX staining representing an increase in double strand DNA damage. Quantification of the number of γ-H2AX positive cells show that at day 7, 5.8% of control cells show signs of double-strand break damage versus 12.8% of NAD-depleted cells, a 121% increase. At day 14, under control conditions

2.3% are positive compared to a 12.9% under nicotinamide starvation, a 461% increase (Figure 2.6B). The increases in DNA damage observed both by alkaline comet assay and γ-H2AX likely contribute to the increased population doubling time that involves both increased cell death rates and G_2/M arrest described above.

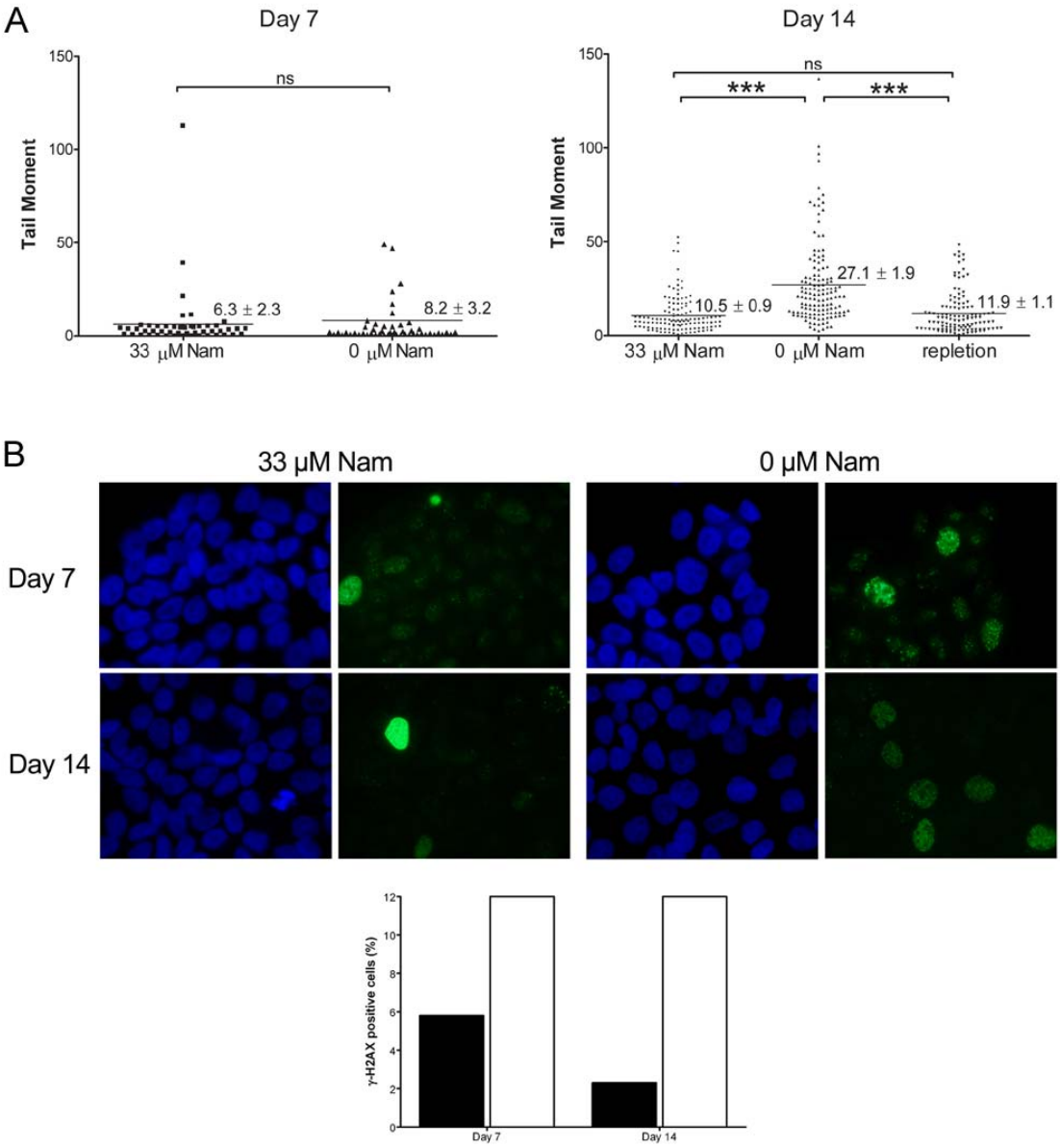

Figure 2.6. Effects of nicotinamide restriction on HaCaT keratinocytes DNA integrity. (A) DNA damage was analyzed by alkaline comet assay. Dots represent single cells (n=50, day 7; n=100, day 14); mean tail moment is shown by lines. * $p < 0.01$, ** $p < 0.001$, *** $p < 0.0001$ versus control (Student's *t*-test). (B) Double strand breaks were analyzed by γ-H2AX immunofluorescence and the number of γ-H2AX cells quantified in the bar graph. 33 μM Nam (black) and 0 μM Nam (white). Percentages were calculated from a sample of >300 cells.

NAD-depletion increases ROS in HaCaT keratinocytes

In an attempt to identify possible inducers of DNA damage in NAD-restricted cells, we observed ROS production. The first indication of an imbalanced ROS production in nicotinamide restricted HaCaTs was the increase in cell autofluorescence after 14 days of restriction, which was completely reversible upon nicotinamide repletion (Figure 2.7A). Nicotinamide-restricted CF3 do not display this increase in autofluorescence (Figure 2.7B). We quantified ROS in HaCaTs using the oxidation sensitive dye, DCF-DA, detected by flow cytometry as shown in Figure 2.8. ROS increased 4-fold in NAD-depleted cells by day 14, from 37 ± 24 to 182 ± 70 relative fluorescence units ($p < 0.0001$). Restoring NAD by addition of nicotinamide (repletion) completely reversed the ROS accumulation. Thus, nicotinamide restriction and the subsequent NAD depletion in HaCaTs resulted in ROS formation that is coincident with increased DNA damage, decreased viability and an increased accumulation of cells in G_2/M.

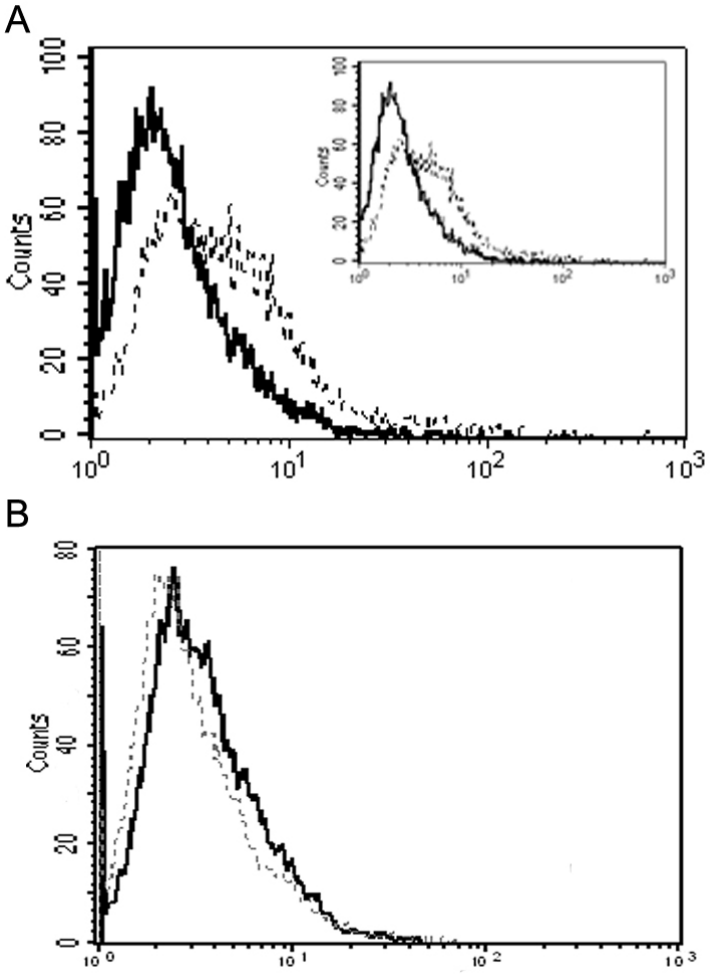

Figure 2.7. Increased autofluorescence in NAD-depleted HaCaT keratinocytes. Cellular autofluorescence was determined by flow cytometry analysis after 14 days of nicotinamide restriction. (A) HaCaT cells, Inset shows reversal of autofluorescence upon repletion (solid); (B) CF3 cells. 33 μM Nam (solid), 0 μM Nam (dashed).

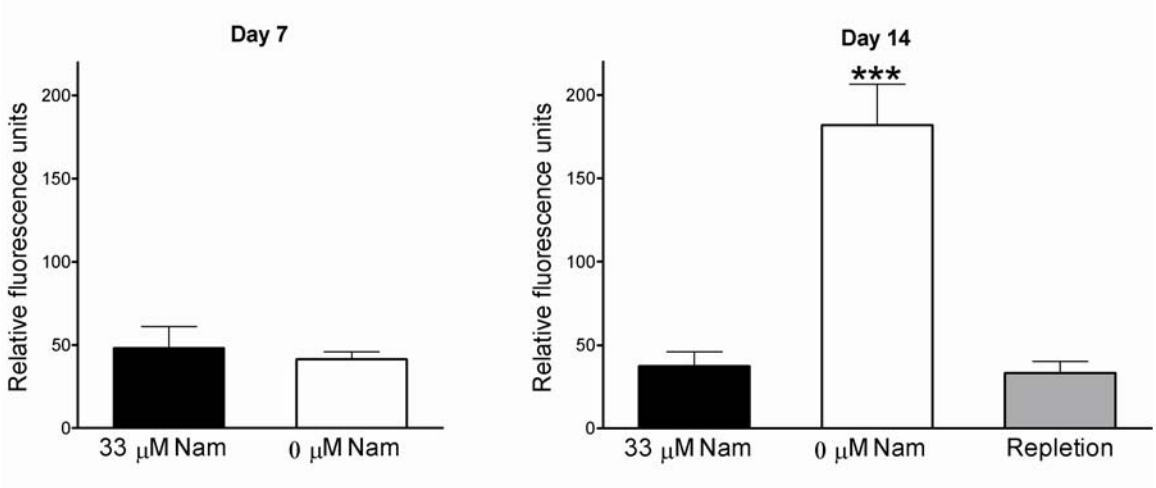

Figure 2.8. ROS accumulation in NAD-depleted HaCaT keratinocytes. Determination of intracellular ROS after 7 and 14 days. 33 μM Nam (black), 0 μM Nam (white), or repleted (gray). All values represent the mean of triplicate samples (± SEM). *** $p < 0.0001$ versus control (Student's *t*-test).

ROS accumulation and redox status in NAD^+-depleted HaCaT keratinocytes

Since NADPH is the ultimate source of reducing equivalents for cellular redox control and NADP(H) are synthesized from NAD, one possible explanation for the accumulation of ROS shown above in HaCaTs may be that NAD restriction results in NADPH content that is limiting for redox control. In order to assess if the levels of NADPH remaining in NAD-restricted cells are sufficient to maintain the redox state of the cell, we measured GSH/GSSG levels. As seen in Figure 2.9, we found that control cells GSH/GSSG levels are not significantly different than restricted cells, containing 146 ± 26 μM reduced GSH, 0.9 ± 0.32 μM GSSG, with a GSH/GSSG ratio of 155 ± 59 versus 172 ± 14 μM reduced GSH, 1.2 ± 0.01 μM GSSG, with a GSH/GSSG ratio of 141 ± 11 in restricted

cells at day 14. These data show that the increased levels of ROS observed are not a result of insufficient reducing equivalents in HaCaTs. Furthermore, in comparing the effects of nicotinamide restriction on the NAD and NADP nucleotide pools, the data show that NADP is preferentially maintained over NAD since the NAD pool is decreased to <1% while the NADP pool is maintained at 34% of control values (Table 2.1).

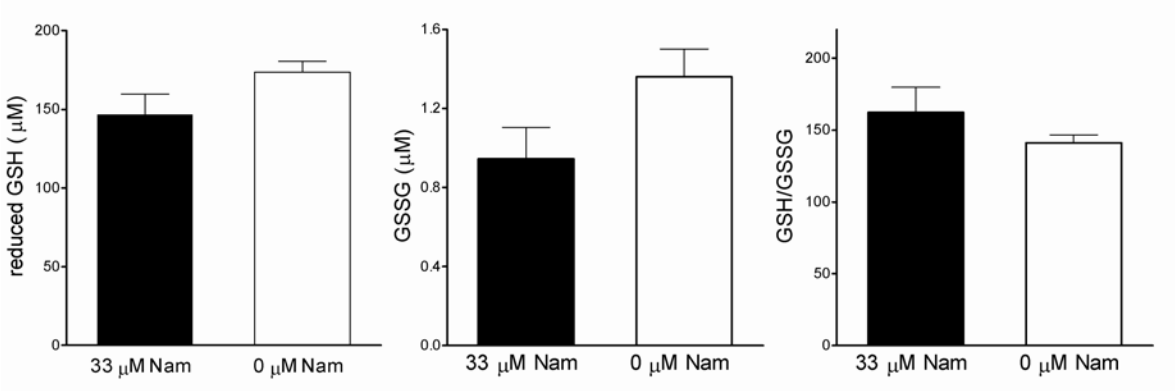

Figure 2.9. Glutathione levels in NAD-depleted HaCaT keratinocytes. Reduced GSH (left), GSSG (middle), and GSH/GSSG ratio quantification after 14 days of growth. 33 μM Nam (black) or 0 μM Nam (white). All values represent the mean of triplicate samples (± SEM).

NAD-depleted HaCaT keratinocytes have increased NOX activity

We hypothesized that the increased ROS levels observed in restricted HaCaTs are at least in part responsible for the DNA damage and decreased cell viability observed and; therefore, controlling the ROS production could decrease these effects. However, treatment with antioxidants including N-acetyl cysteine did not affect ROS accumulation in nicotinamide restricted cells (data not shown).

DNA microarray analyses revealed (Table 2.2) a 2-fold increase in the gene expression of NOX5 and a 4-fold increase for the NOX regulator $p67^{phox}$ (NCF2) in NAD-depleted cells, which was assessed also by qPCR, confirming increased expression at 8.7 ± 5.2-fold for the NOX5 gene and 4.4 ± 2.4-fold increase for the NCF2 gene (Table 2.2).

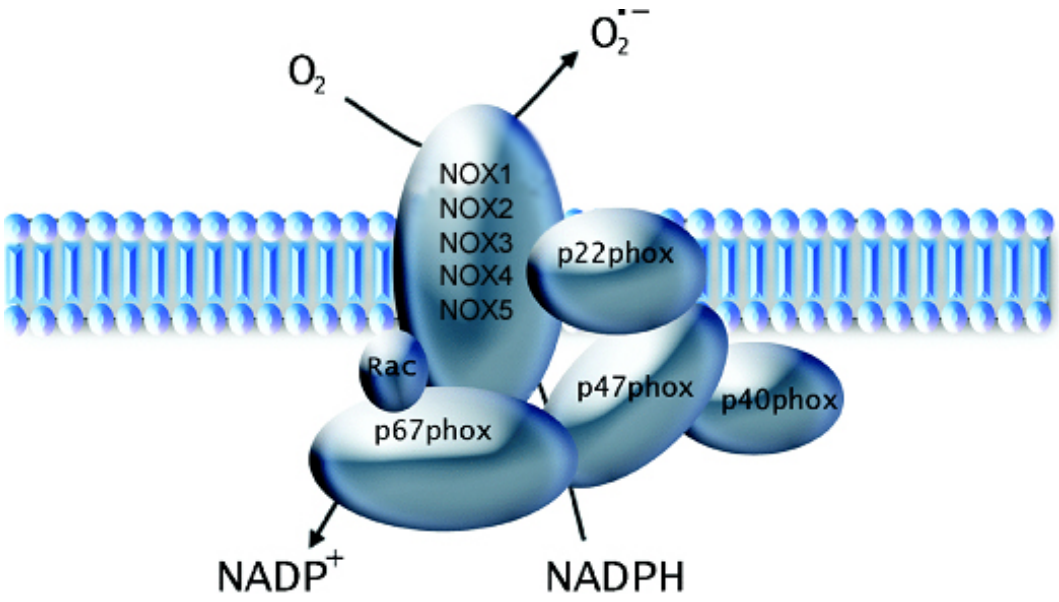

Figure 2.10. Schematic diagram of the structure of the active NADPH oxidase complex. The classical NADPH oxidase comprises a membrane-bound NOX/$p22^{phox}$ heterodimer and other subunits ($p67^{phox}$, $p47^{phox}$, $p40^{phox}$ and Rac) which associate with this complex in the activated enzyme [124].

Table 2.2. Microarray and qPCR results for gene expression following 14 days of nicotinamide restriction.

Gene	Genbank	Array	RT-PCR
NOX5	NM_024505	1.77	8.7 ± 5.18
$p67^{phox}$	NM_000433	3.64	4.4 ± 2.39
PAG	NM_014905	2.35	*n.a.*
IDH2	NM_002168	2.76	*n.a.*
GDH	NM_005271	1.71	*n.a.*

CodeLink Microaaray and qPCR results reported as fold change values relative to controls (33 μM Nam). Shown are mean ± SD of 3 replicates from 3 independent experiments. *n.a.*, not assayed.

Since NOX activity is a major source of ROS production in cells, we examined whether inhibiting NOX activity could block the ROS increase by treating NAD-depleted cells with the NOX inhibitor, apocynin. As shown in Figure 2.11, treatment with apocynin significantly reduced ROS from 179 ± 45 to 52 ± 4 ($p = 0.008$) relative fluorescence units, while in control cells ROS values were essentially unaffected (21 ± 8 vs. 11 ± 1, $p = 0.043$). Furthermore, treatment with apocynin significantly reversed the decrease in cell viability as shown in Figure 2.12. These data show that increased expression and activity of NOX is a significant contributor to the ROS accumulation in nicotinamide-restricted HaCaT keratinocytes, which in turn increases DNA damage and cell death.

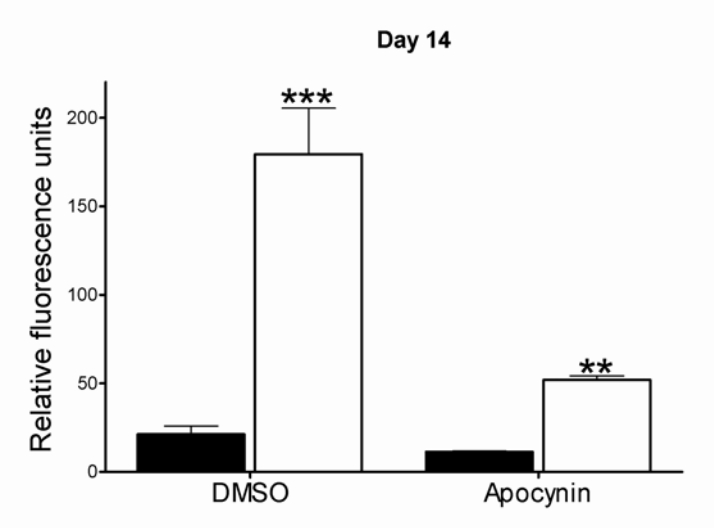

Figure 2.11. ROS accumulation reversal in NAD-depleted HaCaT keratinocytes. ROS after treatment with 0.3 mM apocynin. 33 μM Nam (black) or 0 μM Nam (white). All values represent the mean of triplicate samples (± SEM). ** $p < 0.001$, *** $p < 0.0001$ versus control (Student's *t*-test).

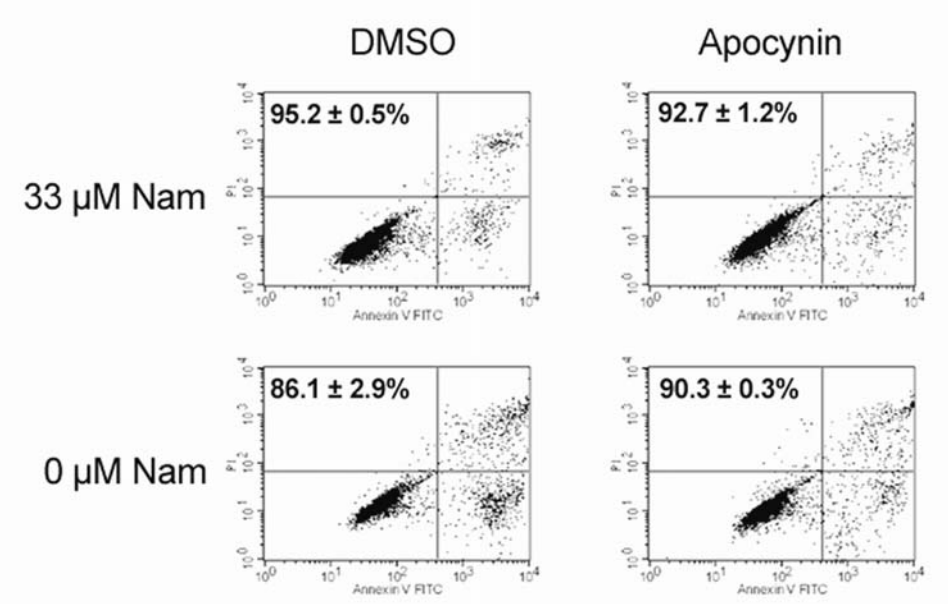

Figure 2.12. Cell viability is restored after ROS reversal in NAD-depleted HaCaT keratinocytes. Cell viability after treatment with 0.3 mM apocynin. 33 μM Nam (black), 0 μM Nam (white), or repleted (gray). All values represent the mean of triplicate samples (± SEM).

NAD-depleted HaCaT keratinocytes have increased sensitivity to glutaminase inhibition

Since the levels of NAD in niacin deficient cells are greatly reduced, it is likely that NAD-depleted cells are incapable of sustaining their energy requirements solely by glycolysis. Therefore, niacin deficient cells would require an additional carbon source. One such source available from the cell culture medium is glutamine. We hypothesized that if glutamine is a crucial carbon source for NAD-depleted cells, these cells would be far more sensitive than control cells if it was removed from the medium. Completely eliminating glutamine from the medium led to cell death both in control and depleted cells (data not shown), showing that glutamine is an essential nutrient for HaCaT keratinocytes. In the cell, glutamine is converted to glutamate and this is further converted to α-ketoglutarate to be used as a source of energy (Figure 2.14). We, therefore, decided to inhibit glutaminase, the enzyme responsible for converting glutamine to glutamate. As seen in Figure 2.13, NAD-depleted cells can not divide in the presence of the glutaminase inhibitor, DON, while control cells can.

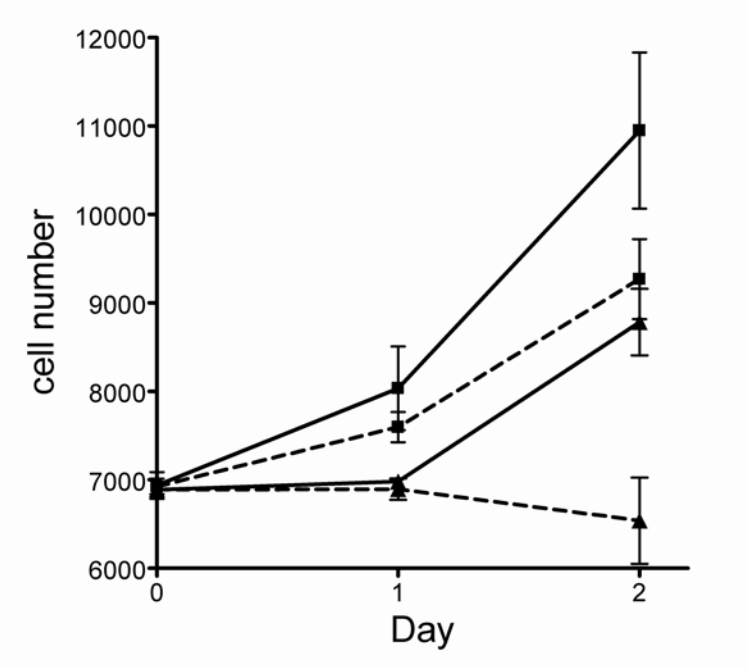

Figure 2.13. Effect of glutaminase inhibition on niacin deficient HaCaT keratinocytes. Growth rates of HaCaT cells grown under control (33 μM Nam, squares), or restricted (0 μM Nam, triangles) conditions in the presence (dotted line) or absence (continuous line) of DON. Values represent triplicate samples (Mean ± SEM).

Discussion

In these experiments, we developed a model to identify NAD-dependent pathways potentially important in early skin carcinogenesis. We show that nicotinamide restriction, and consequent NAD depletion, reversibly alters NAD(P)(H) pools, cell viability, cell cycle progression, and DNA stability. These alterations are affected at least in part by increased expression and activity of NOX leading to an accumulation of ROS which may provide a survival mechanism as has been shown in other cancer cells [125,126]. Similar studies of nicotinamide restriction using a variety of normal human diploid cells (i.e. primary mammary epithelial cells, skin, lung and breast fibroblasts) that have not been immortalized showed that cells can grow in restricted nicotinamide, but do not undergo the alteration in growth rate as shown here for HaCaT cells (Figure 2.3 and unpublished data). Even more relevant is the observation that NHEKs are unable to sustain growth under nicotinamide restriction conditions (Figure 2.3).

When cultured in medium containing no added nicotinamide, NHEK and HaCaT keratinocytes become depleted of NAD. In HaCaTs, NAD levels were maximally reduced after 4-5 population doublings (14 days). HaCaTs exhibit a slower growth following 7 days in medium with no added nicotinamide; however, they are able to grow indefinitely at a constant rate. These results confirm that human keratinocytes require the preformed vitamin, nicotinamide, in this case, to synthesize NAD utilizing the salvage pathway, as the synthesis of NAD from tryptophan through the *de novo* pathway seems to be absent. The data also

show that when niacin is limiting, NADP pools are preferentially maintained as would be needed for biosynthetic precursors in perpetually dividing cells. We hypothesize that the minimal NAD synthesized in the HaCaT keratinocytes during restriction may derive from pyridine nucleotides that are tightly bound to serum proteins in the fetal bovine serum and are not removed by exhaustive dialysis, and can be scavenged and utilized by the salvage pathways for NAD biosynthesis. The ability of various cultured cells to synthesize NAD under these conditions varies widely with human cells being more capable than mouse cells, and we have shown that HaCaTs are more capable than NHEKs.

The slower population doubling rate observed in the nicotinamide depleted cells results from both a G_2/M delay (Figure 2.5) and decreased cell viability (Figure 2.4). Accumulation of cells in the G_2/M-phase of cell cycle (Figure 2.5) in the nicotinamide depleted HaCaTs is consistent with the increase in DNA damage seen in these cells, as shown by the alkaline comet assay (Figure 2.6). These observations are in line with previous studies showing that inhibition of PARP-1, whose substrate is NAD^+, results in G_2/M arrest in a p53-independent manner [127-130]. Of particular interest is the observation that nicotinamide-restricted HaCaTs are able to proliferate indefinitely despite increased production of ROS and significant DNA damage. This is likely to cause instability in the genome, which may result in genetic alterations ultimately leading to progression of carcinogenesis.

Overproduction or insufficient scavenging of ROS can result in enhanced oxidative stress and DNA damage, which have been implicated in cancer initiation and promotion and is a particularly important down stream effector of UV damage [131,132]. Studies have documented significant generation of ROS in a variety of cells, including cancer cells, which is usually the consequence of mitochondrial respiration and NADPH-oxidase (NOX) activity [133-135]. The reduction–oxidation (redox) status of a cell can directly alter cell growth and development, proliferation and survival by modulation of signal transduction pathways [136,137]. In excess, ROS also can oxidatively damage DNA and other cellular macromolecules and lead to generation of a vicious cycle of stress through induction of reactive carbonyl species [22]. Since our data show that nicotinamide restriction maintains or increases the NADPH/total NADP ratio (Table 2.1), we hypothesized and demonstrated that the accumulation of ROS measured in restricted HaCaTs (Figure 2.8) is a result of increased NOX activity (Table 2.2) and that ROS accumulation and subsequent effects on cell survival and DNA damage could be reversed with the NOX inhibitor apocynin (Figures 2.11 and 2.12). In particular, we identified NOX5 as a NOX family member expressed in HaCaT keratinocytes and showed that its expression and that of its modulator, NCF2, are affected by NAD depletion (Table 2.2).

Nicotinamide-restricted HaCaTs divide indefinitely under conditions where NAD content of the cells is less than 1% of control cells (Table 2.1). The small amounts of residual NAD are likely to be compartmentalized in the mitochondria

in order to maintain fundamental functions such as energy metabolism and electron transport chain function. The low NAD impacts energy metabolism and utilization. Since NAD falls to extremely low levels, it is likely that utilization of glucose by glycolysis is not functional and that these cells use another carbon source for energy. As discussed below, glutamine is likely an important carbon source for nicotinamide-restricted cells. We have shown that while control cells proliferate in the presence of a glutaminase inhibitor, 6-diazo-5-oxo-L-norleucine, nicotinamide-restricted cells can not divide in the presence of this inhibitor, suggesting a strong dependence on glutamine for energy (Figure 2.13). Figure 2.14 describes a potential altered metabolic pathway for nicotinamide-restricted cells and suggests a possible role of NAD in limiting these ROS generating pathways in control cells. We observe that NADPH accumulates preferentially above all other pyridine nucleotides. Thus, glutamine in the culture medium is likely the major carbon source for nicotinamide-restricted cells as it can be converted to glutamate by phosphate-activated glutaminase (PAG), and we observed that the expression of PAG in nicotinamide-restricted HaCaTs increased 2-fold (Table 2.2). Glutamate dehydrogenase (GDH) can convert glutamate to the TCA cycle intermediate, α-ketoglutarate with generation of NADPH. This is one likely source for the observed NADPH generation under nicotinamide-restricted conditions. It is also interesting that recent reports suggest that SIRT3 and SIRT4, mitochondrial enzymes that use NAD^+ as a substrate, modulate energy metabolism by regulating the activity of acetyl-CoA

synthetase and GDH, respectively [91,138]. SIRT4 has been reported to downregulate GDH activity by ADP-ribosylation [91]. A decrease in available substrate for SIRT4 in nicotinamide-restricted cells may lead to upregulation of GDH, promoting utilization of glutamate as a source of energy, with the production of NADPH (Figure 2.14). The preferential generation of NADPH observed in nicotinamide-restricted cells may allow increased consumption by NOX leading to elevated ROS production and recycling of $NADP^+$ to be further reduced by GDH. Sustained production of NADPH could also be derived from $NADP^+$-specific isocitrate dehydrogenase (IDH2, Figure 2.14) whose expression is increased by 3-fold in nicotinamide-restricted cells (Table 2.2). The effect of nicotinamide restriction on ROS production is particularly relevant as it is thought that excessive oxidative damage to cellular macromolecules may play an important role in the initiation and promotion of carcinogenesis [139-142]. Glutamine utilization has been reported to be accompanied by ROS formation in immune cells [143] and implicated in cancer cell proliferation [144]. These findings suggest that NAD dependent pathways presented here modulate survival pathways that may limit ROS dependent signaling during early skin carcinogenesis.

The results of the experiments presented here suggest that niacin status (NAD^+ content) is a critical resistance factor for skin cells and raise the question of what are the limiting metabolic or signaling pathways involved. Our model can be used to help identify these NAD-dependent signaling pathways; and

furthermore, to determine how these pathways are altered in common environmental causes of skin cancer (i.e. UV).

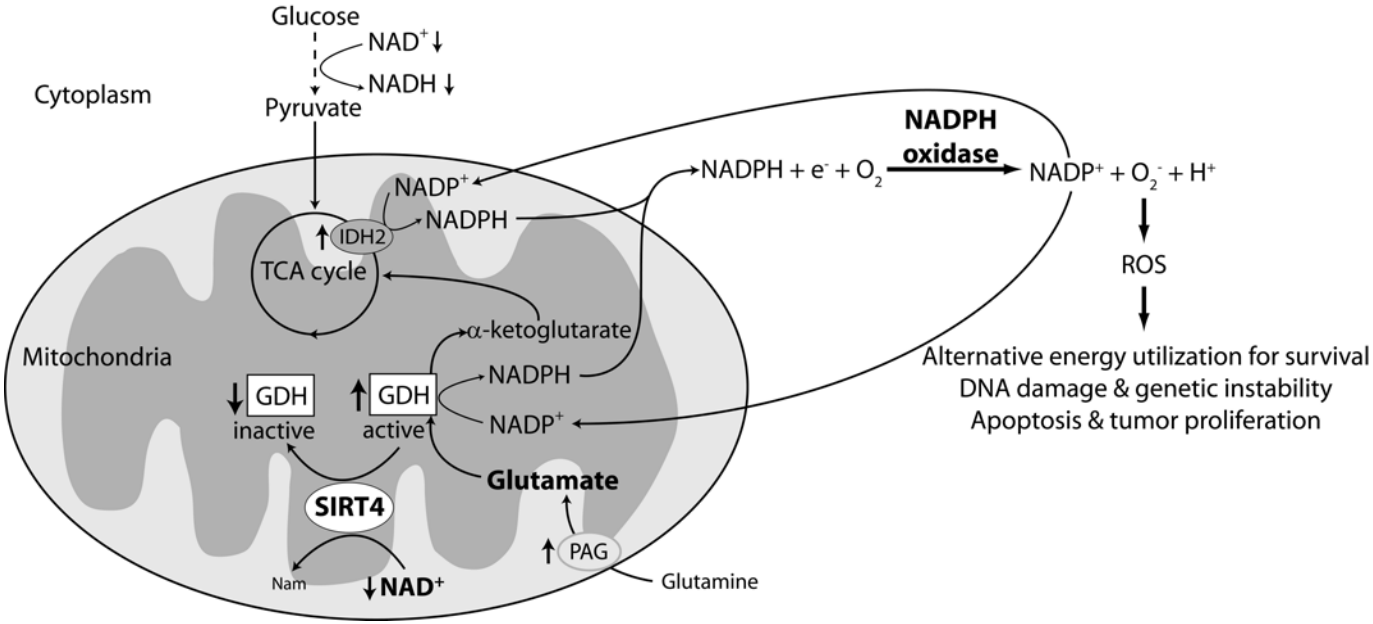

Figure 2.14. Proposed model of NOX activation in nicotinamide-restricted HaCaT keratinocytes. Under NAD-depleted conditions, the ability of the cell to use glycolysis as a source of energy is greatly reduced. Cells can utilize glutamate, synthesized from glutamine in the culture medium as an energy source. Glutamate dehydrogenase (GDH) coverts glutamate to α-ketoglutarate, with reduction of $NADP^+$ to NADPH. The activity of GDH may be regulated by SIRT4, which is dependent on NAD^+; therefore, under NAD-depleted conditions, GDH activity may be upregulated providing α-ketoglutarate as a carbon source for TCA cycle intermediates and energy production. Additional NADPH may be generated by IDH2. NADPH accumulation from these reactions could support NOX dependent ROS formation and recycling of $NADP^+$. In pre-cancerous cells, this ROS dependent signaling may lead to progression in carcinogenesis.

CHAPTER III

SIRTS EXPRESSION IN SKIN CELLS: RESPONSE TO PHOTODAMAGE

Abstract

Sirtuins (SIRTs) are a recently discovered family of NAD^+-dependent deacetylases whose known targets range from histones to transcription regulators. Through this activity, SIRTs have been shown to increase organism and tissue survival in diverse species, including mammals. Evidence indicates that NAD^+ metabolism and SIRTs contribute to mechanisms that influence cell survival under conditions of stress and toxicity. This is the first work identifying SIRT expression in human skin cells. These studies have also focused on elucidating SIRTs' roles in response to sun-induced damage. Here, we present evidence that all of the seven SIRTs are expressed in skin. We have also characterized the changes in SIRT gene expression induced in response to solar simulated light or singlet oxygen stress and how these responses vary between normal (NHEK) and initiated (HaCaT) keratinocytes and discuss the potential relevance in skin carcinogenesis.

Introduction

SIRTs are recently discovered NAD^+-depedent deacetylases that remove acetyl groups from acetylated lysine residues in proteins and in doing so, regulate the biological function of their targets [86]. SIRTs were first characterized in yeast as the “silent information regulator” class 2 (Sir2) protein [145]. In humans, there are at least seven Sir2-like proteins (SIRT1-7) with putative roles in diverse cellular functions, including gene silencing, DNA repair, apoptosis, and regulation of metabolism [113]. All SIRTs share a conserved catalytic domain which is reported to function as a NAD^+-dependent protein deacetylase and in some cases as a mono-ADP-ribosyltransferase [86-89].

Mammalian SIRTs have diverse cellular locations, target multiple substrates, and affect a wide range of cellular functions (Table 3.1). SIRT1 is localized to the nucleus and is the most extensively studied member of the SIRT family. It has been shown to play an important role in the regulation of cell fate and stress response in mammalian cells and has therefore been described as a guardian against cellular oxidative stress and DNA damage. SIRT1 promotes cell survival by inhibiting apoptosis or cellular senescence induced by stresses including DNA damage and oxidative stress. SIRT2 is a cytoplasmic protein which co-localizes both with chromatin during mitosis and microtubules in the cytoplasm [102]. SIRT2 plays an important role in the control of mitotic exit in the cell cycle where increased SIRT2 activity severely delays cell cycle progression through mitosis [103]. SIRT2 also acts as a mitotic checkpoint protein that

prevents chromosomal instability and the formation of hyperploid cells in early metaphase [104]. SIRT3 is a nuclear SIRT that translocates to the mitochondria upon cellular stress [105]. In the mitochondria, SIRT3's deacetylase activity has been linked with adaptative thermogenesis. SIRT3 expression is induced in mice in both white and brown adipose tissue by caloric restriction and in brown adipose tissue upon cold exposure [106]. SIRT3 also has been linked to longevity [107,108]. SIRT4 is located in the mitochondria and contains the conserved SIRT domain, but it apparently does not possess *in vitro* deacetylase activity [91]. SIRT4 has been shown to mono-ADP-ribosylate and inhibit glutamate dehydrogenase (GDH), a mitochondrial enzyme that converts glutamate to α-ketoglutarate [91]. GDH controls amino acid-stimulated insulin secretion by regulation of glutamine and glutamate oxidative metabolism. Inhibition of GDH activity by SIRT4 decreases insulin secretion in mouse pancreatic β-cells in response to amino acids [91]. SIRT5 is the least characterized member of the SIRT family and little is known about its activity. SIRT5 has been described as a mitochondrial protein [109] with weak deacetylase [101] and no ADP-ribosyltransferase activity [91]. SIRT6 is a nuclear protein associated with heterochromatin that promotes resistance to DNA damage and suppresses genomic instability in mouse cells, in association with a role in base excision repair (BER) [109,111]. SIRT6 deficient mice display multiple pathologies that resemble human aging including lymphopenia, loss of subcutaneous fat, decreased bone density, hypoglycemia, decreased IGF-1

levels, and premature death [111]. SIRT6 possess both ADP-ribosyl-transferase [90] and deacetylase activity [111]. Finally, SIRT7 is a widely expressed protein localized in the nucleolus that associates with condensed chromosomes during mitosis [109,112]. SIRT7 expression is abundant in tissues with high proliferation and low in non-proliferating tissues [112]. SIRT7 has been suggested to play a role as a positive regulator of RNA polymerase I transcription and may be required for cell viability in mammals [112]. SIRT7 interacts with RNA polymerase I and histones, and positively regulates the transcription of active rRNA genes (rDNA). Depletion of SIRT7 has been shown to stop cell proliferation and trigger apoptosis [112]. Like the rest of the SIRT family, the NAD binding core domain is conserved in SIRT7, but no deacetylase or ADP-ribosyltransferase activity has been demonstrated to date [112]. It has been suggested that SIRT7 regulates rDNA transcription in a NAD^+ dependent manner, such that the NAD^+/NADH ratio might modulate SIRT7 to link the cellular energy status with rRNA synthesis and ribosome production [113].

The exact biological functions of most of these SIRTs still remains partially characterized, especially in skin tissue, where the only previous report of SIRT activity focused on SIRT1 [146]. In this study, we have identified SIRT mRNA and protein expression both in human fibroblasts and keratinocytes. Furthermore, we have characterized the changes in SIRT expression following exposure to photodamage in the form of solar simulated light and singlet oxygen stress both in normal human keratinocytes (NHEK) and in immortalized human

keratinocytes (HaCaT). Since the genetic changes in HaCaT cells are frequently observed in skin cancers, the differences between NHEK and HaCaTs may have relevance to skin carcinogenesis.

Table 3.1. Sirtuins in mammals

Sirtuin	Activity	Location	Targets	Biology
SIRT1	Deacetylase	Nucleus	FOXO, p53, PGC-1α, H1, H3, H4, TAFI68, p300, Ku70, NF-κB, AceCS1, tat, PPARγ, MyoD, MEF2D	Cell survival, apoptosis, metabolism, transcription, differentiation, stress resistance
SIRT2	Deacetylase	Cytosol	tubulin, H4	Cell cycle
SIRT3	Deacetylase	Nucleus, Mitochondria	AceCS2, PGC-1α	Thermogenesis/metabolism
SIRT4	ADP-ribosyl-transferase	Mitochondria	Glutamate dehydrogenase	Insulin secretion/metabolism
SIRT5	Deacetylase	Mitochondria	Unknown	Unknown
SIRT6	ADP-ribosyl-transferase	Nucleus	DNA Polβ	DNA repair
SIRT7	Unknown	Nucleolus	RNA Pol I	rDNA transcription

Materials and Methods

Cell Culture and Growth Measurements

Normal human keratinocytes (NHEK cells, ATCC), were routinely cultured in Keratinocyte Medium 2 (KGM-2, Lonza) containing KGM-2 SingleQuots (Lonza). Normal human dermal fibroblasts (CF3, ATCC) and the established cell line of human epidermal keratinocytes (HaCaT cells), a gift from Dr. Norbert Fusenig (German Cancer Research Center, Heidelberg, Germany), were routinely cultured in Dulbecco's Modified Eagle Medium (DMEM) containing 10% fetal bovine serum. All cells were kept in a humidified atmosphere containing 5% CO_2 at 37°C.

qPCR

Total RNA was prepared from cultured HaCaT keratinocytes using the Rneasy purification system (Qiagen) according to the manufacturer's instructions. cDNA synthesis was performed with the TaqMan Reverse Transcription kit (Applied Biosystems) according to manufacturer's instructions using random hexamers and 1 μg of total RNA. For TaqMan-based qPCR expression profiling, 25 ng of each cDNA was added to the TaqMan Universal PCR Master Mix along with the TaqMan MGB probes according to the manufacturer's instructions (Applied Biosystems).

qPCR was performed essentially as described [123]. Primers and probes designed to specifically detect human SIRT1 (TaqMan Gene Expression Assay Hs0109006_m1), SIRT2 (TaqMan Gene Expression Assay HsHs00247263_m1),

SIRT3 (TaqMan Gene Expression Assay Hs00202030_m1), SIRT4 (TaqMan Gene Expression Assay Hs00202033_m1), SIRT5 (TaqMan Gene Expression Assay Hs00202043_m1), SIRT6 (TaqMan Gene Expression Assay Hs00213036_m1), and SIRT7 (TaqMan Gene Expression Assay Hs00213029_m1) transcripts were purchased from Applied Biosystems. Real-time fluorescence monitoring was performed with the ABI Prism 7900 (Applied Biosystems). Relative expression levels of the various transcripts were determined by comparison against the housekeeping gene, GAPDH. All expression measurements were performed in triplicate using three independently generated cDNA samples. Alterations in gene expression were considered significant at 1.5-fold change (increase or decrease), including standard error.

Irradiation

A kilowatt large area light source solar simulator (Model 91293; Oriel Corporation, Stratford, CT) was used, equipped with a 1000-W Xenon arc lamp power supply (Model 68920) and a VIS-IR bandpass blocking filter plus an atmospheric attenuation filter (output 290-400 nm plus residual 650-800 nm, for solar simulated light). The output was quantified using a dosimeter (Model IL1700; International Light Inc., Newburyport, MA), with an SED240 detector for UVB (range 265-310 nm, peak 285 nm) at a distance of 365 mm from the source, which was used for all experiments. At 365 mm from the source, solar-stimulated light (SSL) dose was 7.63 mJ cm^{-2} s^{-1} UVA and 0.40 mJ cm^{-2} s^{-1} UVB radiations.

For generation of singlet oxygen, photosensitization of 3.3 μM toluidine blue (TBL) was used in combination with a Sylvania 15-W Cool White light tube delivering visible light at an irradiance of 0.77 J/cm^2. The irradiance in the visible region (400-700 nm) was determined using a spectroradiometer, model 754, from Optronic Laboratories (Orlando, FL). Cells received visible radiation at a distance of 50 mm from the source through the polystyrene lids of cell culture dishes.

Western Blot Analyses

Protein extraction for SIRT detection and acetylation profile was performed using RIPA buffer (50 mM Tris-HCl pH 7.4, 1% NP-40, 0.25% Na-deoxycholate, 150 mM NaCl, 1mM EDTA, protease inhibitors). Western blot analysis was performed using a 10 or 15% SDS polyacrylamide gel, with transfer to a PDVF membrane (Millipore). Antibodies used were anti-acetyl lysine (Ab193, Abcam, Cambridge, MA), anti-SIRT1 (NB100-2132, Novus Biologicals, Littleton, CO) at 1:5000 dilution, 0.25 μg/mL anti-SIRT2 (ARP32384, Aviva Systems Biology, San Diego, CA), 0.25 μg/mL anti-SIRT3 (NB600-808, Novus Biologicals, Littleton, CO), 1 μg/mL anti-SIRT4 (NB100-1406, Novus Biologicals, Littleton, CO), 2 μg/mL anti-SIRT5 (ARP32390, Aviva Systems Biology, San Diego, CA), 2 μg/mL anti-SIRT6 (NB100-2524, Novus Biologicals, Littleton, CO), 0.5 μg/mL anti-SIRT7 (ARP32406, Aviva Systems Biology, San Diego, CA).

Results

SIRT proteins are expressed in skin cells

SIRT expression has been studied in various tissue types both in mice and humans, but has never been characterized in skin. In order to establish which members of the SIRT family are present in skin cells, we performed Western blot analyses with antibodies specific to the different SIRT family members (SIRT1-7) using total protein lysates from normal human keratinocytes (NHEK), immortalized human keratinocytes (HaCaT) and diploid human fibroblast (CF3). As seen in Figure 3.1, all SIRTs are expressed in CF3s, NHEKs and HaCaTs. SIRT1 showed as a double band of approximately 120 kDa, SIRT2 at 45 kDa, SIRT3 appeared as a doublet band (more clear when looking at HaCaTs) at about 30 kDa, SIRT4 at 40 kDa, SIRT5 also appeared as a doublet at around 35 kDa, SIRT6 showed at 40 kDa with a signal extending to 45 kDa in the case of HaCaTs, and SIRT7 at approximately 50 kDa. Doublet bands seen in SIRT1, 3 and 5, as well as the diffused band seen in SIRT6 are indicative of post-translational modifications such as phosphorylation which was been described to occur at least in SIRT1 [147].

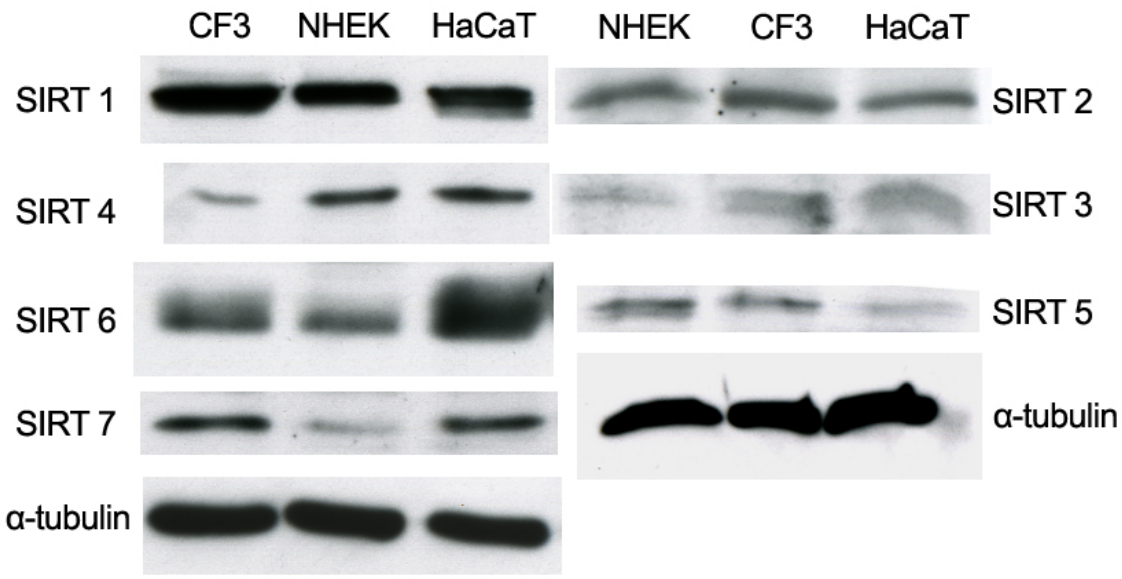

Figure 3.1. SIRT protein expression in skin cells. SIRT protein expression was detected by Western blotting using the specified SIRT peptide antibodies. To control for protein loading, all blots were probed with α-tubulin.

SIRT gene expression in skin cells

Since we observed that all SIRTs are being translated in skin cells, we performed qPCR gene expression analyses to measure SIRT mRNA expression in a quantitative way. Corroborating the data from the Western blot analyses, we detected gene expression of all 7 SIRT members in the three cell lines studied (Figure 3.2). SIRTs' mRNA levels shown in Figure 3.2 are expressed as the Ct differential normalized to GAPDH's mRNA in each cell type, which we used as housekeeping gene control. Expressing the data as Ct differential allows us to compare the relative abundance of each gene. A higher Ct differential reflects a lower total mRNA content of the specific gene and, therefore, a less abundant gene. Figure 3.2 shows that SIRT7 is the most abundant SIRT expressed in HaCaTs, while SIRT2 and SIRT6 are the most abundant SIRTs being expressed in NHEKs and CF3s. SIRT4 is the least abundant SIRT gene expressed in all three cell lines (Figure 3.2). Figure 3.3 presents the same data as a function of the fold difference compared to NHEK expression levels. Interestingly, both normal keratinocytes and diploid fibroblasts have similar expression levels for all SIRTs, except SIRT5 which showed 2.7–fold higher expression in NHEK cells (Figure 3.3). Also of interest is the observation that 5 of the 7 SIRTs have altered gene expression in HaCaT keratinocytes when compared to normal keratinocytes. All of these changes are increased expression: 2.5–fold in SIRT1, 3.7–fold in SIRT3, 2–fold in SIRT4, 1.5–fold in SIRT5, and 4–fold in SIRT7.

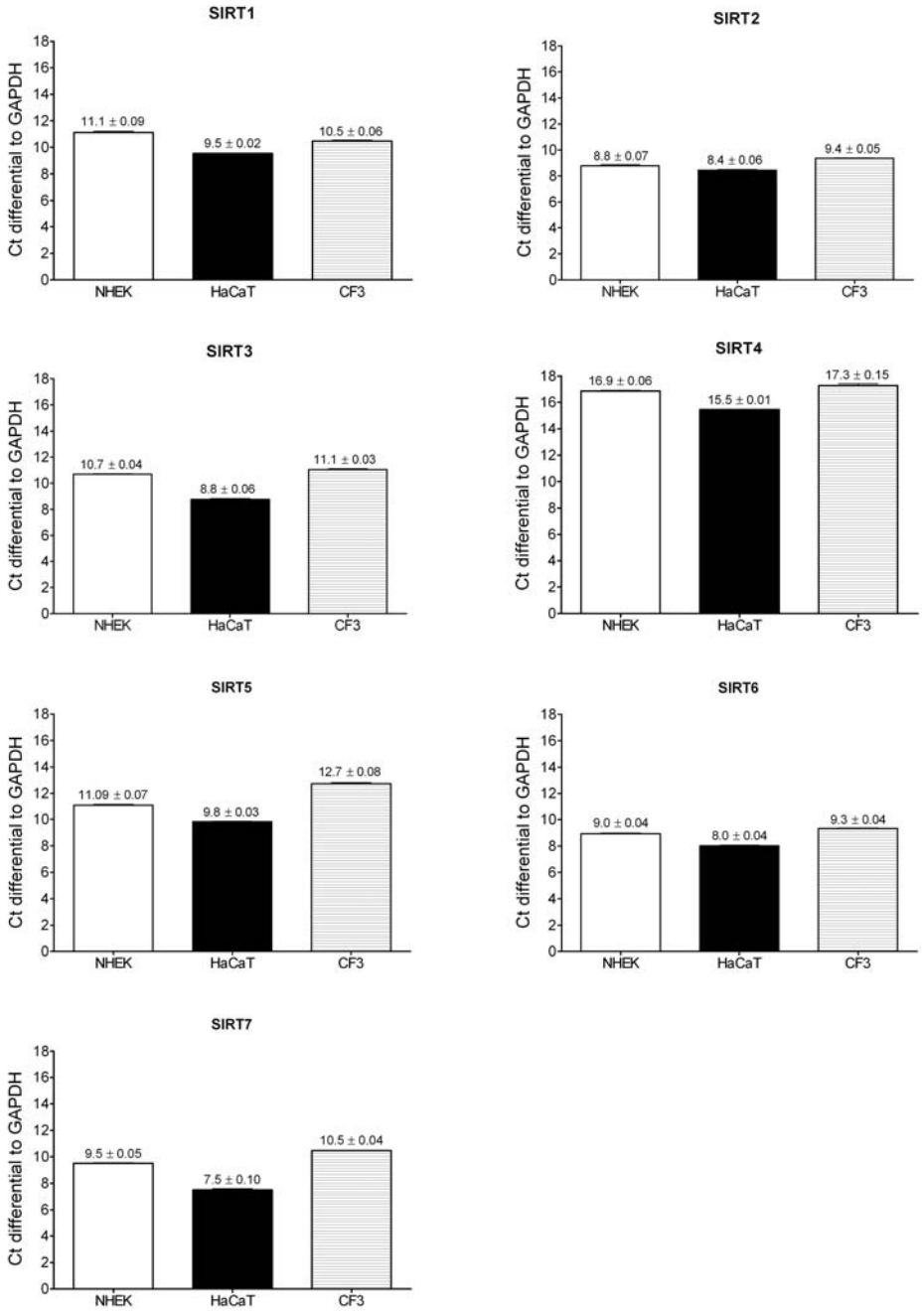

Figure 3.2. SIRTs gene expression in skin cells. SIRTs mRNA expression were measured using qPCR. Expression levels are expressed as Ct differential normalized to GAPDH expression (dCt). NHEK (white), HaCaT (black), and CF3 (striped). All values represent the mean of triplicate samples (± SEM).

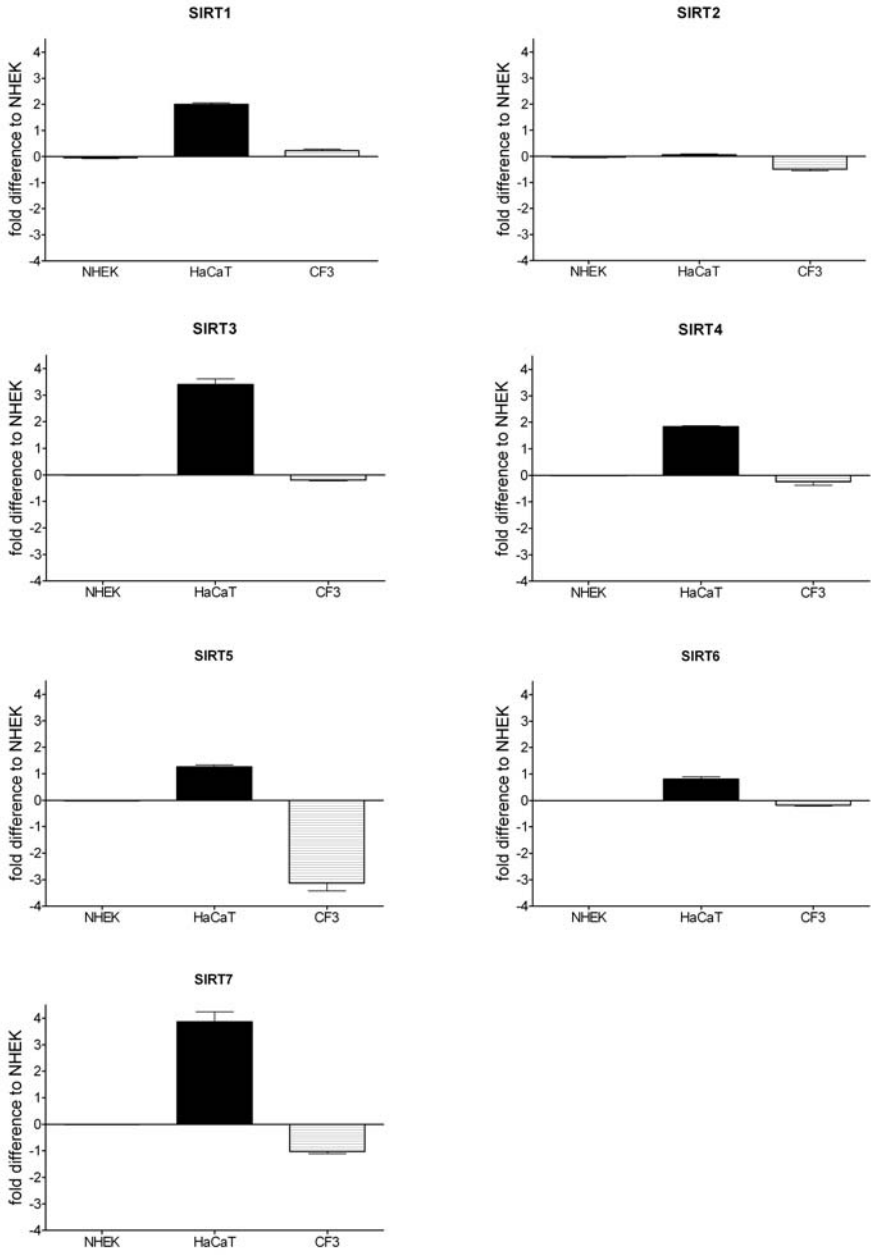

Figure 3.3. Relative SIRT gene expression in various skin cells. SIRTs mRNA expression were measured using qPCR. Gene expression levels shown are expressed as fold difference to NHEKs expression levels, previous normalization to GAPDH. NHEK (white), HaCaT (black) and CF3 (striped). All values represent the mean of triplicate samples (± SEM).

SIRT expression in response to photodamage in normal keratinocytes

SIRT1 and SIRT6 have been implicated as important regulators of cellular oxidative stress and DNA damage. As the roles of other SIRT family members are poorly characterized, it may well be that other SIRTs participate in responses following DNA damage. In order to determine whether SIRTs are involved in the response to photodamage in keratinocytes, we studied whether SIRT1-7 gene expression is altered following solar simulated light (SSL) and singlet oxygen stress (TBL), using qPCR. Figure 3.4 shows the time course of gene expression changes in NHEK cells upon SSL treatment. We observe that SIRT1 expression in these cells increases upon SSL induced DNA damage. This change is detectable at about 5-6 hours post treatment and increases up to a 6.7 ± 1.3–fold at 8 hours post-treatment. In contrast, SIRT3 and SIRT7 expressions are decreased at their minimum, 5.5 ± 2.5–fold and 7.5 ± 3.0–fold respectively, at 5 hours post-treatment. No significant changes were observed in the gene expression levels of SIRT2, SIRT4, SIRT5 and SIRT6 after SSL treatment.

The results in Figure 3.5 show that SIRT1 gene expression also increased (2.8 ± 0.5–fold) following TBL treatment. Under the latter conditions, inconclusive results are seen for SIRT4 and SIRT5 where there is a tendency towards decreased expression (1.8 ± 1.0 and 0.9 ± 0.4 –fold decreases, respectively), while expression of SIRT2, SIRT3, SIRT6, and SIRT7 were unaltered (Figure 3.5).

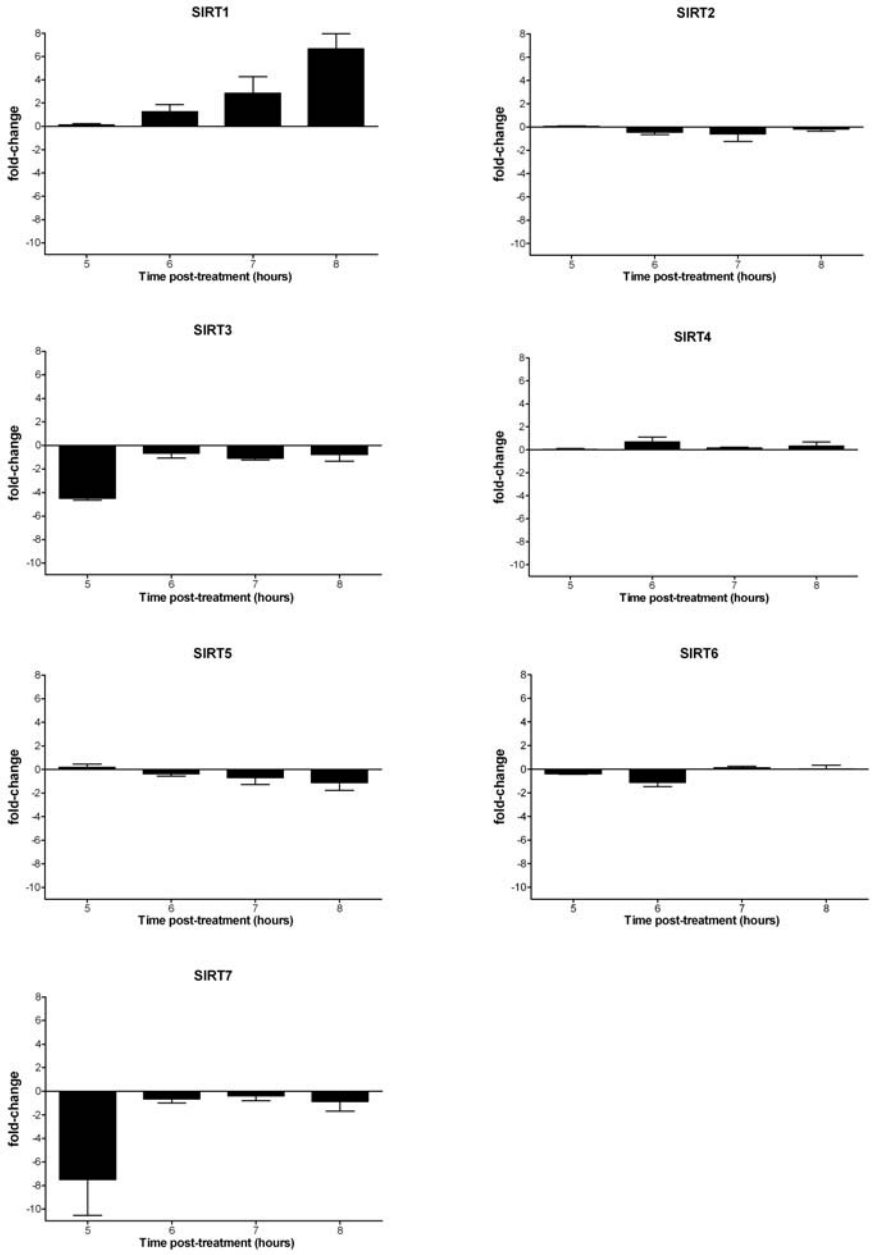

Figure 3.4. SIRT gene expression changes in NHEK cells upon SSL treatment. Time course of SIRT gene expression after solar simulated light treatment was measured using qPCR. Gene expression levels shown are expressed as fold-change relative to untreated NHEKs, previous normalization to GAPDH. All values represent the mean of three samples (± SEM).

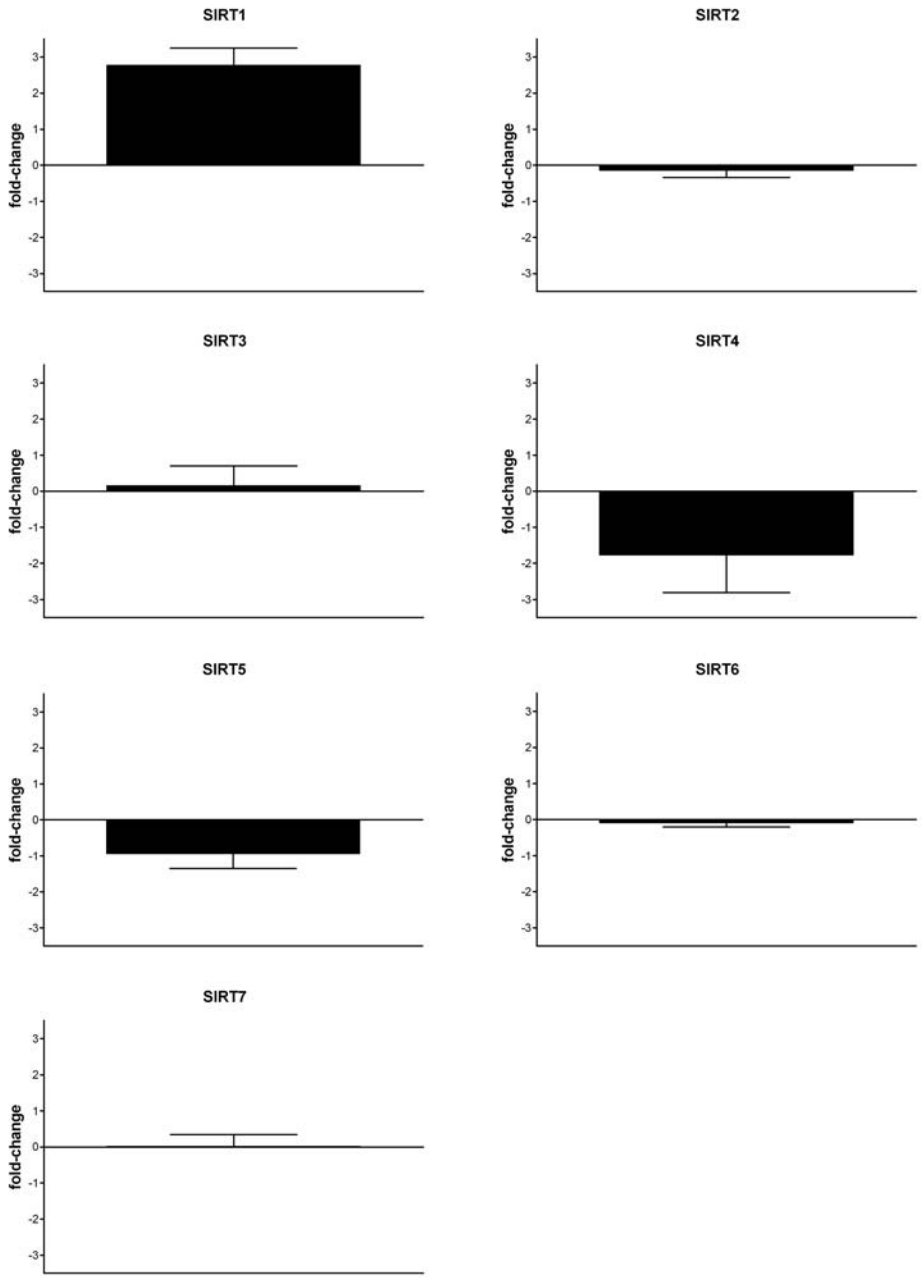

Figure 3.5. SIRT gene expression changes in NHEK cells upon TBL treatment. SIRT gene expression at 5 hours after singlet oxygen stress treatment was measured via qPCR. Gene expression levels shown are expressed as fold-change relative to untreated NHEKs, previous normalization to GAPDH. All values represent the mean of three samples (± SEM).

SIRT expression in response to photodamage in immortalized keratinocytes

We showed that HaCaT keratinocytes and NHEKs display different basal gene expression levels for various members of the SIRT family (Figure 3.2). Therefore, we studied the effect of photodamage on gene expression also in HaCaT keratinocytes to determine whether this immortalized cells respond to UV damage differently than NHEK cells. Figure 3.6 illustrates the fold changes observed in HaCaTs after treatment with SSL. As seen with NHEKs, SIRT3 decreases at 6 hours after SSL treatment (4.6 ± 2.6 –fold). A large change is observed also in SIRT6, with a 4.3 ± 1.1–fold decreased expression. Additionally, HaCaTs treated with SSL increase expression of SIRT4 (2.9 ± 0.1–fold) between 5 and 7 hours after treatment. In HaCaTs we don't detect the significant changes in SIRT1 and SIRT7 as we observed in NHEKs following SSL treatment.

HaCaTs exposed to TBL treatment increase expression of SIRT1 (2.9 ± 0.9) and SIRT4 (2.4 ± 1.1) (Figure 3.7) as was observed following SSL treatment. SIRT6 participation in the response to TBL treatment in HaCaTs wasn't clear as it either remained unchanged or was greatly reduced, leading to a standard deviation larger than the mean (1.8 ± 2.2 –fold decrease) suggesting that a dynamic response may be occurring and an extensive study of the time course may be required (Figure 3.7). Expression levels for SIRT2, SIRT3, SIRT5, and SIRT7 remained unaffected after TBL treatment (Figure 3.7), which are similar to SSL with the exception of SIRT3.

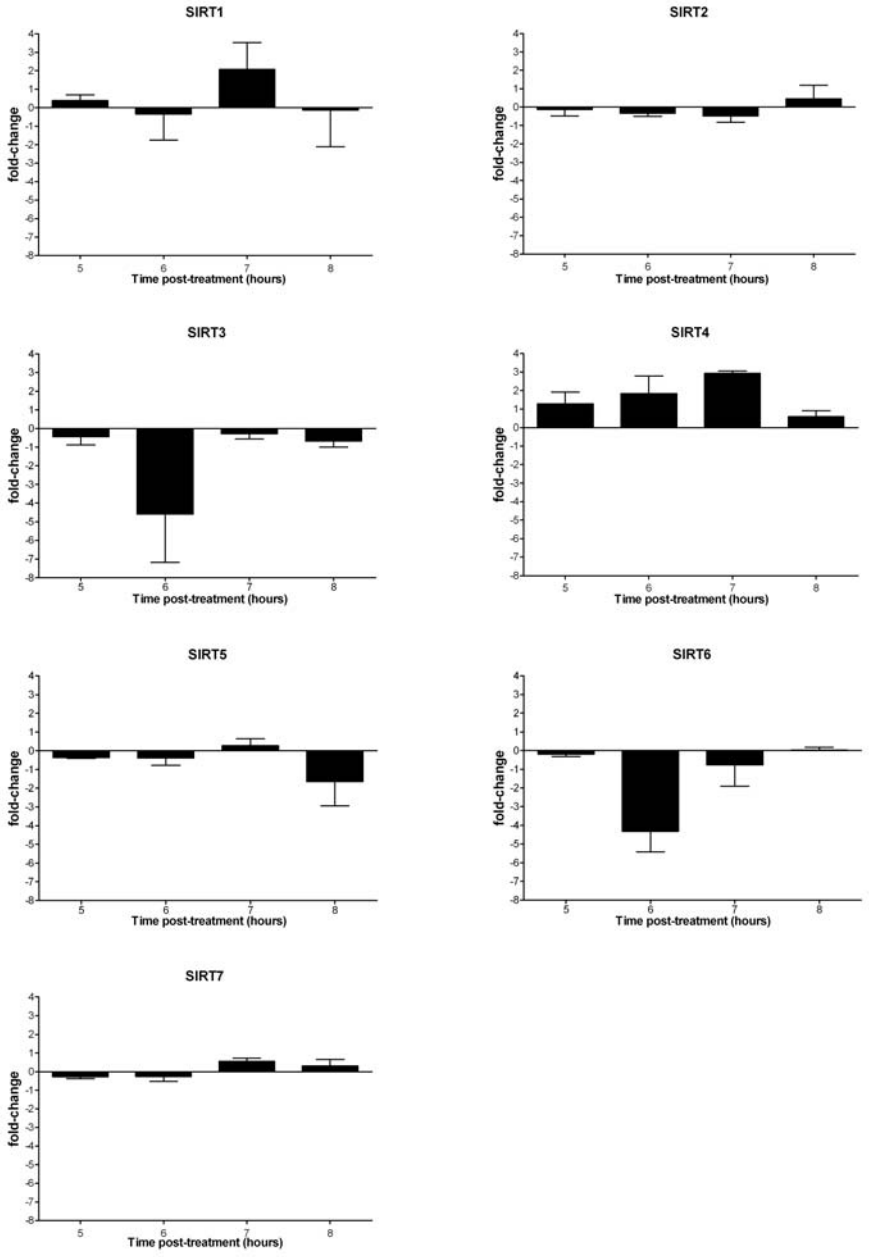

Figure 3.6. SIRT gene expression changes in HaCaT keratinocytes upon SSL treatment. Time course of SIRT gene expression after solar simulated light treatment was measured using qPCR. Gene expression levels shown are expressed as fold-change relative to untreated HaCaTs, previous normalization to GAPDH. All values represent the mean of seven samples (± SEM).

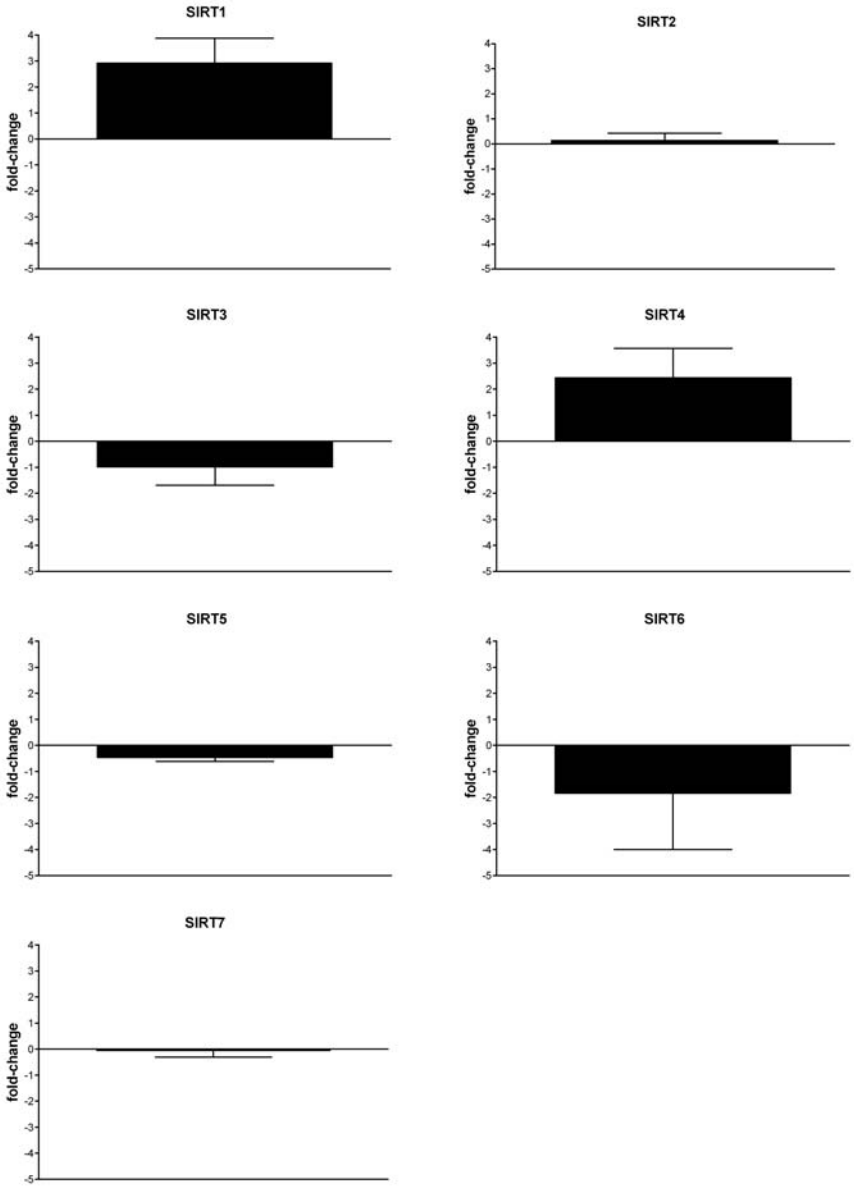

Figure 3.7. SIRT gene expression changes in HaCaT keratinocytes upon TBL treatment. SIRT gene expression at 5 hours after singlet oxygen stress treatment was measured via qPCR. Gene expression levels shown are expressed as fold-change relative to untreated HaCaTs, previous normalization to GAPDH. All values represent the mean of seven samples (± SEM).

Discussion

In this study, we have examined SIRT expression in human skin cells. We have identified the expression of all seven SIRT family members in fibroblasts (CF3) and both in normal (NHEK) and immortalized keratinocytes (HaCaT). We have shown in keratinocytes as a response to photodamage that the expression levels of several SIRTs is altered. Furthermore, these responses to photodamage differ between normal and initiated keratinocytes, which may be indicative of alterations potentially important in skin carcinogenesis.

We show that all of the seven SIRTs are widely expressed in skin cells. Using real time PCR as an approach to quantitatively compare SIRT expression in these skin cell types, we found that SIRT expression levels in CF3s and NHEKs are relatively similar, with the sole exception being SIRT5 which has an increased expression in NHEKs. The lack of knowledge about the targets and roles of SIRT5 makes it hard to speculate about the implications of this change, but it's likely to play a role in energy metabolism due to its localization in mitochondria. Of greater interest, however, is the comparison of SIRT expression between NHEKs and HaCaTs. The HaCaT cell line has been used as a substitute model for primary human keratinocytes since many features between these cells are similar [148-151]; however, distinct differences in the biology of HaCaT cells and primary human keratinocytes have also been described, including lack of intact p53 alleles and aberrant NF-κB signaling [116]. Adding to this list, we found SIRT1, SIRT3, SIRT4, SIRT5, and SIRT7 to be more highly

expressed in HaCaTs compared to NHEKs. This is of great interest as there is growing evidence that tumor cells become ‘addicted’ to SIRT overexpression [152]. Interestingly, the three mitochondrial SIRTs are overexpressed in HaCaTs. Mitochondria function in energy metabolism, and acetylation of key metabolic proteins may regulate changes in energy production in response to changes in the environment. The mitochondrial SIRTs likely play a role in the altered energy metabolism and response to oxidative stress in tumor cells [152]. In addition, SIRT1 is known to increase resistance to stress and is overexpressed in a number of cancers, SIRT3 is involved in increased longevity and SIRT7 supports the increased transcription required in tissues with high proliferation rates. Taken together, increased SIRT expression may be important in conferring adaptive advantages to HaCaTs allowing rapid proliferation and loss of checkpoints to promote continued propagation in the presence of accumulating mutations.

In studying the role of SIRTs in photodamage responses, we established that SIRT1 is upregulated in response to SSL (Figure 3.4) and TBL (Figure 3.5) in NHEK cells and in response to TBL (Figure 3.7) in HaCaTs. These results are not surprising as SIRT1 has been previously shown to modulate cellular stress response and survival [70,71,92-94,153]. Increased SIRT1 expression also correlates with increased DNA repair [154].

Table 3.2. Summary of SIRT changes upon photodamage

	NHEK		HaCaT	
Sirtuin	SSL	TBL	SSL	TBL
SIRT1	↑	↑	ns	↑
SIRT2	ns	ns	ns	ns
SIRT3	↓	ns	↓	ns
SIRT4	ns	~↓	↑	↑
SIRT5	ns	~↓	ns	ns
SIRT6	ns	ns	↓	ns
SIRT7	↓	ns	ns	ns

Gene expression changes as increase (↑), decrease (↓), trend to increase or decrease (~) or no significant change (ns) in gene expression.

Of interest is the observation that SIRT3 is silenced upon SSL-induced damage in NHEKs and HaCaTs. Recently, SIRT3 was reported to translocate from the nucleus to the mitochondria upon cellular stress (UV-irradiation and etoposide) [105]. This study also suggests that the nuclear function of SIRT3 is tightly regulated as the enzyme may have an extremely important and time-sensitive role in the nucleus. Therefore, our observation supports this hypothesis as suppressing SIRT3 expression upon cellular stress is analogous to maintaining SIRT3 excluded from the nucleus. If this is the case, SIRT3 expulsion from the nucleus might be dependent upon the type of cellular stress as we observed a decrease in SIRT3 expression only with SSL and not with TBL treatment.

We also observed downregulation of SIRT7 in NHEKs upon SSL treatment. SIRT7 has been shown to associate with active rRNA genes, where it interacts with RNA polymerase I (Pol I) and histones [112]. Depletion of SIRT7 results in a reduction of Pol I transcription which leads to inhibition of cellular proliferation and increased apoptosis [112]. Therefore, SIRT7 downregulation by SSL-induced damage may promote clearing of damaged cells by induction of apoptosis. The lack of a SIRT7 response in HaCaTs may provide a survival mechanism to these cells, allowing damaged cells to escape apoptosis and perhaps promoting genomic instability.

Upregulation of SIRT4 was only observed in HaCaT keratinocytes and it occurred in response to both SSL and TBL treatments. This mitochondrial enzyme regulates metabolism through inhibition of GDH [91]. We have previously shown (Chapter II) that under low intracellular levels of NAD^+, HaCaTs utilize glutamine as an alternative energy source and this promotes ROS production (Figure 2.13). Since DNA damaging agents are known to activate PARP activity, leading to consumption and depletion of NAD^+, it is possible that SIRT4 overexpression is a response mechanism to avoid excess generation of ROS that could lead to exacerbated cell death. This hypothesis is supported in Chapter IV, where we show that under niacin deficiency, which leads to NAD^+ depletion, HaCaTs overexpress SIRT4 in the absence of additional stress.

Surprisingly, the only change in gene expression observed for SIRT6 was a decrease upon SSL treatment in HaCaTs, opposite of expected. SIRT6 is

another SIRT shown to be involved in DNA damage response. Specifically, SIRT6 promotes resistance to DNA damage and suppresses genomic instability in mouse cells, in association with a role in base excision repair (BER) [109,111]. While the exact participation of SIRT6 in this process remains unclear, one would expect an increase in SIRT6 activity upon DNA damaging treatments. However, it should be noted that the lack of changes upon photodamage does not exclude participation of any of the SIRTs in processes involved in responses to cellular stress as these can be regulated at the protein levels rather than expression itself.

CHAPTER IV

NIACIN DEFICIENCY INCREASES SKIN SENSITIVITY TO PHOTODAMAGE

Abstract

Skin is constantly exposed to the DNA damaging effects of UV irradiation, and DNA repair is an important cellular defense mechanism against skin cancer development. Defects in DNA repair mechanisms are causal factors for skin cancer development. PARP-1 is an abundant nuclear enzyme involved in DNA damage responses, including repair, maintenance of genomic integrity, and signaling events for stress responses such as apoptosis. Upon activation by DNA damage, PARP-1 consumes NAD^+ as a substrate for synthesis of poly(ADP-ribose). SIRTs are another class of NAD^+ consuming enzymes that control genomic stability, DNA repair and transcription regulation. Therefore, the availability of NAD^+ is essential for DNA repair and genomic stability. Using our previously established model of intracellular NAD-modulation via niacin deprivation, we have studied the effects of NAD^+ depletion on human skin cell sensitivity to photodamage. We also studied how the expression and enzymatic function of SIRTs and PARPs might be disturbed by altering the availability of NAD^+ in skin cells with the intent to identify critical downstream signaling pathways in skin carcinogenesis. Here we show that niacin deficient HaCaT keratinocytes develop a severe sensitivity to solar simulated light (SSL) and singlet oxygen stress (TBL), which is reflected in increased DNA damage and

cell death. Our studies show that these alterations result from a combination of impaired PARP-1 and SIRTs catalytic activity.

Introduction

Skin cells are constantly exposed to endogenous and environmental agents that cause DNA damage. Sunlight, specifically ultraviolet (UV) radiation, has been established to be the main etiological factor for DNA damage in the skin. UV is subdivided into three wavelength components: UVA (320-400nm), UVB (280-320nm), and UVC (200-280nm), but only UVB and UVA are present in sunlight at ground level as UVC is absorbed by ozone. Most of the solar UV energy incident on human skin is in the deeply penetrating UVA region (90-99%) of the spectrum, and increasing experimental evidence supports a major role of UVA in skin photoaging and photocarcinogenesis [24,155-157]. Many skin chromophores and extracellular matrix proteins such as collagen and elastin are capable of absorbing UVA and have therefore been identified as potent UVA sensitizers of photooxidative stress. These endogenous sensitizers can generate radicals and reactive oxygen species (ROS) that can damage DNA, membranes, and other cellular constituents, which can ultimately induce skin carcinogenesis [158-160]. The carcinogenicity of UVB radiation is well established experimentally and, to a large extent, understood as a process of direct photochemical damage to DNA from which gene mutations arise. These lesions must be detected and removed by repair mechanisms or replaced by recombination. Genomic instability, including point mutations, deletions, chromosomal translocations and loss or gain of whole chromosomes, have been shown to initiate the cancer cell phenotype [161]. Recently, controversial

evidence has raised the possibility of an interaction between UVB and UVA. UVB-induced apoptosis is a protective measure by which survival of damaged cells is prevented. However, UVA has been shown to suppress this effect [30]. As a consequence, inhibition of UVB-induced apoptosis by UVA action may be a mechanism by which UVA augments UVB-mediated mutations and skin cancer formation or, alternatively, UVA may induce protective intracellular mechanisms that diminish UVB damage [24]. Therefore, the use of solar simulated light (SSL), a combination of UVA and UVB light, is the biologically relevant model to study the carcinogenic effects of UV radiation, since this is the form of light which causes human skin cancers.

Niacin deficiency in humans causes pellagra, a disease which is characterized by the four Ds: diarrhea, dementia, dermatitis, and death [37]. As suggested by the sun sensitivity observed in pellagra, models of UV exposure in rodents have shown that the skin is sensitized by niacin deficiency [162]. This sensitivity is thought to be due to reduced availability of NAD^+, resulting in impaired PARP-1 function and of DNA repair mechanisms. PARP-1 is an evolutionarily conserved nuclear enzyme that is activated when bound to single-strand DNA breaks [163]. PARP-1 uses NAD^+ as its substrate to synthesize poly(ADP-ribose) (PAR) and ADP-ribosylates different nuclear proteins, thereby exerting its role in the DNA damage surveillance network [164]. Extensive data can be found on the effects of NAD deficiency and its effect on PARP inhibition in the presence of DNA damage induced by chemical agents [165-167] and various

studies have shown PARP activation in response to UV irradiation [167-169]. In respect to the response to UV, PARP activation has been shown to participate in carcinogenesis, DNA repair and cell death. PARP inhibition during UVB-induced skin carcinogenesis in mice, acts as a co-carcinogen by accelerating the onset of tumors and increasing the severity of cancers [170]. PARP activation has also been linked to UVB-induced apoptosis in cultured cells and in mice skin [167,171]. Numerous studies have attempted to demonstrate that inhibition of PARP following UV damage would enhance the cytotoxic effects of UV, analogous to what has been shown with alkylating agent damage. However, no link has been drawn between PARP inhibition and cytotoxicity upon UV irradiation. In fact, a previous study suggests that PARP does not participate in the repair of UV-induced pyrimidine dimers [172]. Thus, the role of PARP activity during recovery from UV damage is not well defined. In this study, we have used NAD depletion to assist in identifying critical response pathways in keratinocytes following UV treatment.

Materials and Methods

Cell Culture

The established cell line of human epidermal keratinocytes (HaCaT cells), a gift from Dr. Norbert Fusenig (German Cancer Research Center, Heidelberg, Germany), was routinely cultured in Dulbecco's Modified Eagle Medium (DMEM) containing 10% fetal bovine serum and kept in a humidified atmosphere containing 5% CO_2 at 37°C. For NAD(P) modulation, cells were grown in a specially formulated DMEM (Gibco BRL) without nicotinamide, 10% dialyzed fetal bovine serum (Gibco BRL) and with addition of 33 μM nicotinamide (33 μM Nam) or without added nicotinamide (0 μM Nam).

Irradiation

A kilowatt large area light source solar simulator (Model 91293; Oriel Corporation, Stratford, CT) was used, equipped with a 1000-W Xenon arc lamp power supply (Model 68920) and a VIS-IR bandpass blocking filter plus an atmospheric attenuation filter (output 290-400 nm plus residual 650-800 nm, for solar simulated light). The output was quantified using a dosimeter (Model IL1700; International Light Inc., Newburyport, MA), with an SED240 detector for UVB (range 265-310 nm, peak 285 nm) at a distance of 365 mm from the source, which was used for all experiments. At 365 mm from the source, solar-stimulated light (SSL) dose was 4.152 J cm^{-2} UVA and 193.8 mJ cm^{-2} UVB radiations.

For generation of singlet oxygen stress, photosensitization of 3.3 μM toluidine blue (TBL) was used in combination with a Sylvania 15-W Cool White

light tube delivering visible light at an irradiance of 0.77 J/cm^2. The irradiance in the visible region (400-700 nm) was determined using a spectroradiometer, model 754, from Optronic Laboratories (Orlando, FL). Cells received visible radiation at a distance of 50 mm from the source through the polystyrene lids of cell culture dishes.

Cell death analysis

Cell death was determined by Annexin-V-fluorescein isothiocyanate/ propidium iodide dual staining of cells followed by flow cytometric analysis, as first described by Vermes et al [121]. HaCaT keratinocytes (100,000) were seeded on 35 mm dishes and 24 h later the medium was changed. Cells were harvested 24 h later, and cell staining was performed using an apoptosis detection kit according to the manufacturer's specifications (APO-AF; Sigma-Aldrich). In the figures shown, lower left quadrant (AnnexinV$^-$, PI$^-$) represents viable cells, lower right (AnnexinV$^+$, PI$^-$) is early apoptosis and upper right (AnnexinV$^+$, PI$^+$) is late apoptosis and necrosis.

Detection of intracellular oxidative stress by flow cytometry analysis

Intracellular reactive oxygen species (ROS) were analyzed by flow cytometry using dichlorofluorescein diacetate (DCF-DA; Sigma) as a specific dye probe which fluoresces upon oxidation by ROS. HaCaT keratinocytes were seeded at $1 \cdot 10^5$ cells per 35 mm dish. Cells loaded with DCF-DA (50 µg/ml) with light exclusion for 60 min were washed three times with PBS. Intracellular accumulation of fluorescent DCF-DA was measured (10,000 cells each) using a

FACScan flow cytometer (Becton-Dickinson, San Jose, California). Histograms were analyzed with the software program Cell Quest (Becton-Dickinson).

Comet assay

HaCaT keratinocytes were seeded at $1 \cdot 10^5$ per dish on 35 mm culture dishes (Sarstedt, Newton, NC) and left overnight to attach. Cells were removed by trypsinization and analyzed by alkaline single cell gel electrophoresis (comet assay) based on the method of Singh et al. [122]. Briefly, 100 µL of cells (100,000 cells/ml) suspended in PBS were mixed with 100 µL of 0.5% low melting point agarose (Sigma) and layered on CometSlides (Trevigen, Gaithersburg, MD). The mixture was allowed to solidify at 4ºC for 15 min on a metal plate. Cells were then exposed for 1 h at 4ºC to freshly prepared lysis buffer (2.5 M NaCl, 100 mM EDTA, 1% Triton, and 10 mM Tris, adjusted to pH 10 with NaOH). Following cell lysis, the slides were incubated with freshly prepared alkali buffer at room temperature for 40 min to allow DNA denaturation and unwinding. Then, the slides were placed in a horizontal electrophoresis box and filled with chilled, freshly prepared alkali buffer (300 mM NaOH, 1 mM EDTA, pH >13) at 4ºC and electrophoresis was carried out by a constant electric current of 300 mA for 23 min. After electrophoresis, the slides were neutralized with three 5 min washes in 0.4 mol/L Tris-HCl (pH 7.4). Finally, the slides were fixed in 100% ethanol for 5 min and stored in the dark at room temperature.

Quantification of DNA Damage

Immediately prior to imaging, comet slides were hydrated and stained by exposure to 1 mg/mL ethidium bromide for 15 min. Comets were analyzed using fluorescence based digital imaging system. Tail moments were calculated using Comet Assay Software Project (Casp) imaging software.

Western blot analyses

For poly(ADP-ribose) (PAR) modified protein detection, cell extracts were prepared using a lysis buffer consisting of 150 mM NaCl, 1% NP-40, 0.5% sodium deoxycholate, 0.1% SDS, 1 mM EDTA, 1 mM EGTA, 20% glycerol, 50 mM Tris-HCl, pH 7.5, and protease inhibitor mixture. After lysis, cell extracts were sonicated and loaded on 8% SDS-PAGE, followed by transfer to PDVF and immunoblotting using an anti-PAR SA-216 monoclonal (Biomol). Protein extraction for SIRT detection and acetylation profile was performed using RadioImmunoprecipitation assay (RIPA) buffer (50 mM Tris-HCl pH 7.4, 1% NP-40, 0.25% Na-deoxycholate, 150 mM NaCl, 1mM EDTA, protease inhibitors). Western blot analyses were performed using a 10 or 15% SDS polyacrylamide gel, and transferred to a PDVF membrane (Millipore). Antibodies used were anti-acetyl lysine (Ab193, Abcam, Cambridge, MA) at 1:1000 dilution, anti-SIRT1 (NB100-2132, Novus Biologicals, Littleton, CO) at 1:5000 dilution, 0.25 µg/mL anti-SIRT2 (ARP32384, Aviva Systems Biology, San Diego, CA), 0.25 µg/mL anti-SIRT3 (NB600-808, Novus Biologicals, Littleton, CO), 1 µg/mL anti-SIRT4 (NB100-1406, Novus Biologicals, Littleton, CO), 2 µg/mL anti-SIRT5 (ARP32390,

Aviva Systems Biology, San Diego, CA), 2 μg/mL anti-SIRT6 (NB100-2524, Novus Biologicals, Littleton, CO), 0.5 μg/mL anti-SIRT7 (ARP32406, Aviva Systems Biology, San Diego, CA).

Immunofluorescent detection of poly-ADP-ribose polymer

Cells were washed in phosphate buffer saline (PBS) and fixed in 5% formaldehyde in PBS for 30 min at room temperature (RT). Cells were then permeabilized with 0.4% Triton X-100 in PBS for 3 min at RT, washed with PBS and blocked with 3% BSA-PBS for 30 min at RT. Cells were then incubated for 1 hr at 37ºC in the presence of an anti-PAR monoclonal SA-216 antibody (Biomol) at 1:50 dilution, followed by 3 washes in PBS and incubation with a suitable secondary antibody conjugated with fluorescein (FITC) for 1 hr at 37ºC. Nuclear DNA was counterstained with DAPI and cells were examined at 60X magnification in a fluorescence microscope.

qPCR

Total RNA was prepared from cultured HaCaT keratinocytes using the Rneasy purification system (Qiagen) according to the manufacturer's instructions. cDNA synthesis was performed with the TaqMan Reverse Transcription kit (Applied Biosystems) according to manufacturer's instructions using random hexamers and 1 μg of total RNA. For TaqMan-based qPCR expression profiling, 25 ng of each cDNA was added to the TaqMan Universal PCR Master Mix along with the TaqMan MGB probes according to the manufacturer's instructions (Applied Biosystems).

qPCR was performed essentially as described [123]. Primers and probes designed to specifically detect human SIRT1 (TaqMan Gene Expression Assay Hs0109006_m1), SIRT2 (TaqMan Gene Expression Assay HsHs00247263_m1), SIRT3 (TaqMan Gene Expression Assay Hs00202030_m1), SIRT4 (TaqMan Gene Expression Assay Hs00202033_m1), SIRT5 (TaqMan Gene Expression Assay Hs00202043_m1), SIRT6 (TaqMan Gene Expression Assay Hs00213036_m1), and SIRT7 (TaqMan Gene Expression Assay Hs00213029_m1) transcripts were purchased from Applied Biosystems. Real-time fluorescence monitoring was performed with the ABI Prism 7900 (Applied Biosystems). Relative expression levels of the various transcripts were determined by comparison against the housekeeping gene, GAPDH. All expression measurements were performed in triplicate using three independently generated cDNA samples.

Results

NAD^+ as a resistance factor in photodamage

Our previous report showing the role of NAD^+ in maintenance of genomic integrity in keratinocytes (Chapter II) led us to examine whether NAD^+ depletion affects resistance of keratinocytes to photodamage. Using our previously described model of niacin restriction, which leads to NAD depletion, we performed alkaline comet assays on cells exposed to solar simulated light (SSL) or singlet oxygen stress (TBL), a well known form of indirect damage following UV exposure. We quantified DNA damage measuring a combination of breaks directly induced by SSL or TBL and those formed indirectly during repair processes. As seen in Figure 4.1, HaCaT keratinocytes with low intracellular NAD^+ are significantly more sensitive to the cytotoxic effects of these DNA-damaging agents. As early as day 7 after initiation of nicotinamide restriction, we observe an increase in mean tail moment from 13.1 ± 0.9 in controls to 21.1 ± 1.6 in NAD-depleted HaCaTs treated with TBL ($p < 0.001$, Figure 4.1C). As seen in Figure 4.1A, no significant change was observed when cells were treated with SSL at this degree of NAD^+ depletion, with mean tail moment values of 37.7 ± 8.8 in controls vs. 57.7 ± 11.5 in depleted cells ($p = 0.08$). After 14 days of nicotinamide restriction, we observe a marked increase in the sensitivity to photodamage. Treatment with SSL induces a significant increase in mean tail moment from 34.4 ± 7.4 in controls to 81.2 ± 9.6 in NAD-depleted HaCaTs ($p < 0.0001$, Figure 4.1B). Similarly, TBL treatment significantly increases the mean

tail moments from 10.5 ± 0.9 in controls to 27.1 ± 1.9 in NAD-depleted cells ($p < 0.0001$, Figure 4.1C). However, the increase in DNA damage seen in NAD-depleted HaCaTs upon TBL sensitization is comparable to normal cells when you compare the increase in DNA damage to their respective controls. The increased sensitivity observed is thought to be due to reduced availability of NAD^+, resulting in impaired function of NAD^+ dependent enzymes including PARP-1 and downstream targets involved in recovery from DNA damage. Nicotinamide repletion reverses the increased DNA damage observed in depleted cells as assessed by comet analysis to that observed in control cells (Figure 4.1, repletion).

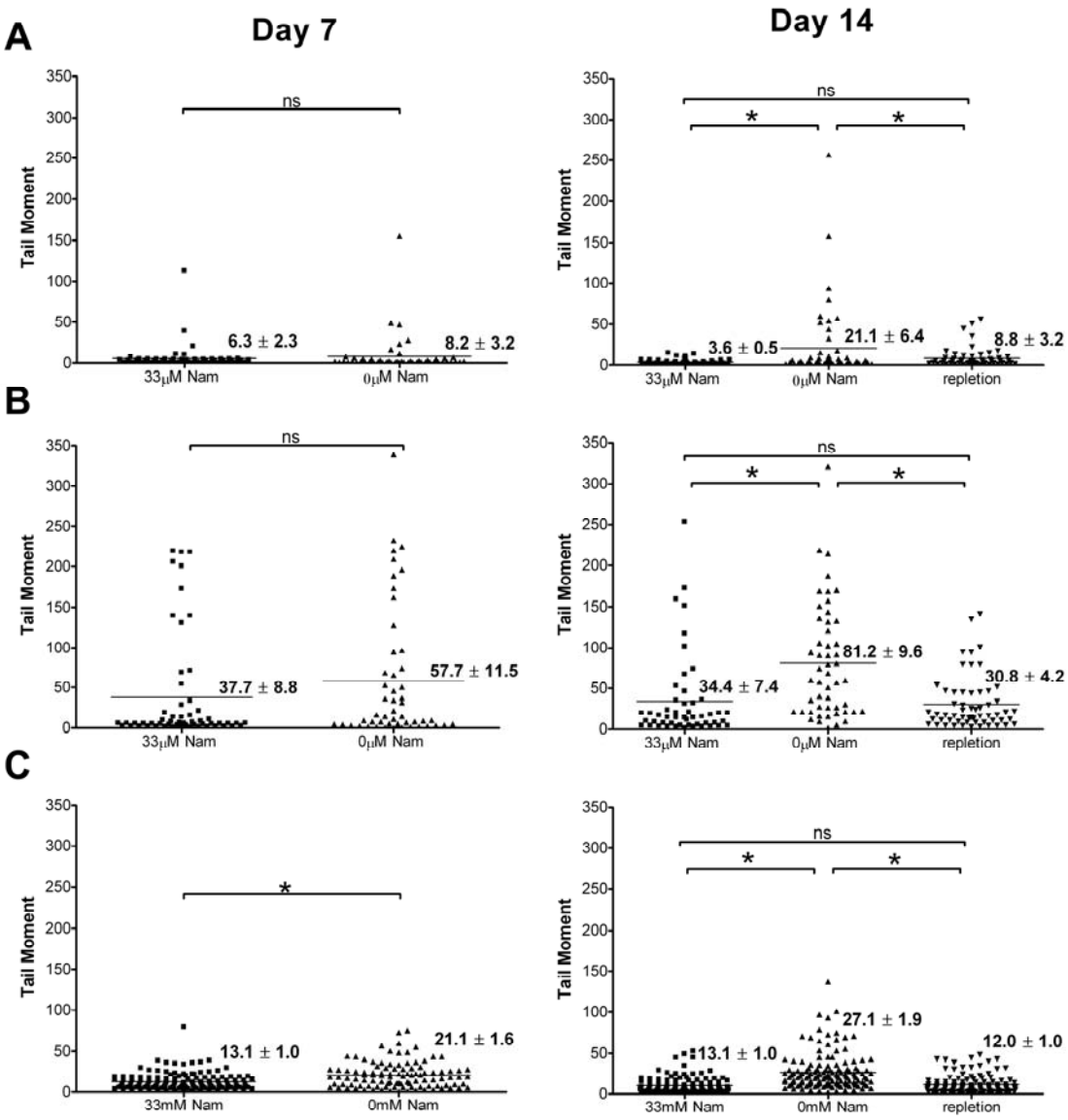

Figure 4.1. Effect of photodamage on DNA integrity in niacin-deficient HaCaTs keratinocytes. DNA damage in HaCaT keratinocytes grown in the presence (33 μM Nam) or absence (0 μM Nam) of niacin was analyzed by alkaline comet assay. Dots represent single cells; mean tail moment lines are shown for: (A) untreated, (B) SSL treatment, and (C) TBL treatment. *ns*, non significant difference; *, denotes significant differences, by unpaired t test, $p < 0.001$.

NAD^+-restriction and ROS accumulation in photodamaged HaCaT keratinocytes

Our previous observations showing that nicotinamide restricted cells accumulate ROS in the absence of additional stress led us to examine the effects of SSL and TBL on ROS formation since these treatments also are known to generate ROS. As shown in Figure 4.2, upon both SSL and TBL damage, intracellular ROS increased both in control and NAD-depleted cells indicating that these treatments are ROS generators, as expected. Interestingly, the levels of ROS accumulation upon photodamage are not significantly different between the two cell culture conditions at day 7. However, by day 14, a robust increase in ROS is observed in NAD-depleted HaCaTs compared to their control counterparts. Under SSL treatment, control keratinocytes show an increase in ROS of 16.7 ± 9.2 relative fluorescence units (RFU) compared to untreated control cells. NAD-depleted cells show an increase in ROS of 35.1 ± 25.0 RFU compared to untreated deficient cells under the same SSL treatment. The same trend is observed with TBL treatment where we observed a 14.0 ± 14.1 RFU increase compared to untreated control cells. In depleted cells ROS was significantly higher, reaching 44.2 ± 22.6 RFU compared to untreated depleted cells. These increases in ROS observed in depleted cells are completely reversible by addition of nicotinamide (repletion).

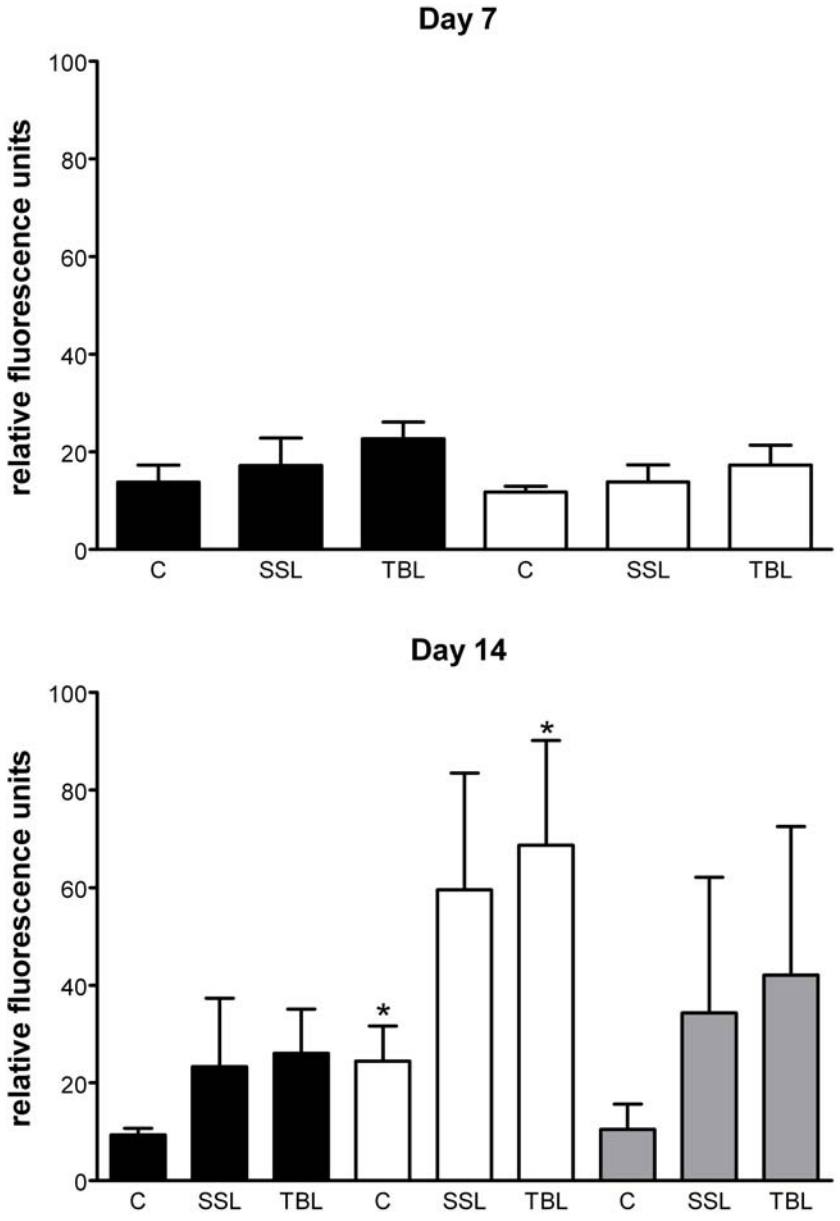

Figure 4.2. ROS accumulation in NAD-depleted HaCaT keratinocytes upon photodamage. Determination of intracellular ROS after 7 and 14 days of niacin deficienty. 33 μM Nam (black), 0 μM Nam (white), or repleted (gray). All values represent the mean of triplicate samples (± SEM). * $p < 0.05$ versus control. (Student's t-*t*est).

NAD^+-restriction increases apoptosis in photodamaged HaCaT keratinocytes

To further characterize the consequences of the increased sensitivity of NAD-depletion to photodamage in HaCaTs, we measured induction of cell death following treatment with SSL or TBL. The viability of HaCaT keratinocytes grown for 7 days under NAD-depletion is not significantly different than control cells upon photodamage. After 14 days of nicotinamide depletion, the increased DNA damage induced by photodamage (Figure 4.1) is reflected in a significant increase in cell death both for SSL, 9.1 ± 2.1% increase cell death in controls versus 19.66 ± 2.5% cell death in NAD-depleted cells ($p < 0.05$), and TBL treatment, 6.6 ± 1.2% increased cell death in controls versus 19.4 ± 5.9% in NAD-depleted cells ($p<0.05$) (Figure 4.3). These effects are completely reversible upon addition of nicotinamide and restoration of NAD^+ (Figure 4.3).

Interestingly, as shown in Figure 4.3, the increase in DNA damage observed by alkaline comet assay with TBL treatment (Figure 4.1) did not lead to an increase in cell death. This indicates that the degree of NAD^+ depletion at day 7 is still able to sustain DNA repair, but at a slower rate, which is completely lost after 14 days of NAD^+ depletion.

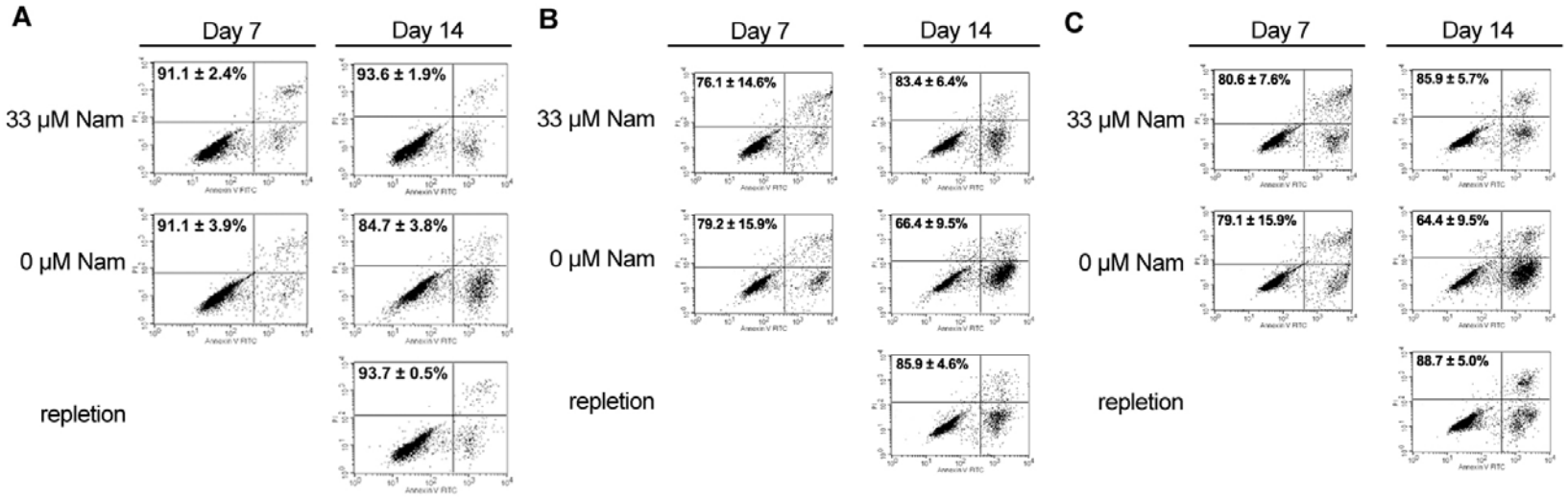

Figure 4.3. Effects of photodamage on viability of nicotinamide-deficient HaCaT keratinocytes. Cell viability was quantified for HaCaTs grown in the presence (33 μM Nam) or absence (0 μM Nam) of niacin using Annexin-V/PI Facs analysis. (A) before treatment; and 24 hr after treatment as described in materials and methods with (B) SSL; (C) TBL. Numbers shown represent percentage of viable cells from triplicate samples (Mean ± SEM).

Poly-ADP-ribosylation is impaired in NAD^+-restricted cells

Previous studies have shown that low NAD^+ following niacin deficiency led to an impaired DNA damage response from PARPs (specifically PARP-1 and PARP-2) [49]. To verify that impaired PARP function is a contributing factor to the increased sensitivity observed in our niacin-deficient cells exposed to photodamage, we studied PARP catalytic activation by detection of its product, PAR-modified proteins. Polymer immunoblotting using an antibody for PAR shows proteins, including PARP, modified by PAR chains which appear between 100-200 kDa [54,173,174]. Using our 14-day depletion model, we observed that in TBL-treated control keratinocytes, the signal for PAR was clearly present 1 hour post-treatment and was maintained during the 3 hours studied (Figure 4.4). In SSL-irradiated control keratinocytes, the signal for PAR appeared after 2 hours and increased at 3 hours post-treatment. In contrast, niacin-depleted cells show no PAR-modified proteins (Figure 4.4).

The above results were corroborated using indirect immunofluorescence in HaCaT cells using the same antibody against PAR. As seen in Figure 4.5, upon SSL treatment a light ubiquitous PAR signal is observed in NAD-sufficient but not in NAD-deficient HaCaTs. Consistent with a greater PARP activation signal observed in the Western blot analyses upon TBL treatment, we observe a stronger nuclear PAR staining in control cells than in SSL treated cells. Under nicotinamide restricted conditions, no nuclear staining is seen in TBL treated cells. These results indicate that the intracellular NAD^+ remaining in HaCaT

keratinocytes is insufficient to generate an adequate DNA damage response from PARP following photodamage. These data show that PAR formation and PARP activation occur upon SSL and TBL treatment and are absent in NAD depleted cells.

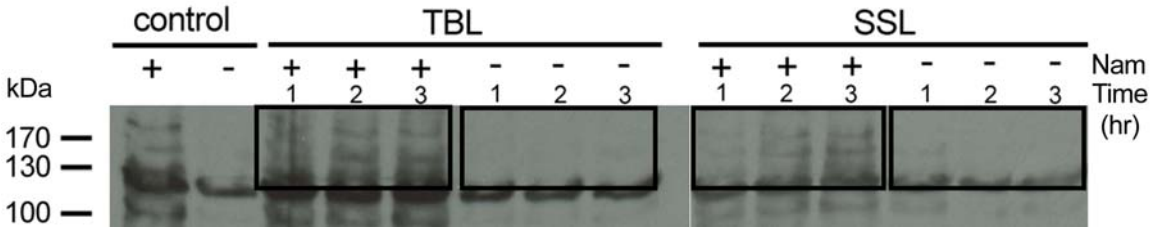

Figure 4.4. Effect of niacin deficiency on PARP activation by photodamage. Polymer immunoblotting of HaCaT keratinocytes grown for 14 days in 33 μM Nam (+) or 0 μM Nam (-) and exposed to photodamage. Extracts of cells treated with singlet oxygen stress (TBL) or solar simulated light (SSL) were Western blotted for using the PAR antibody SA-216.

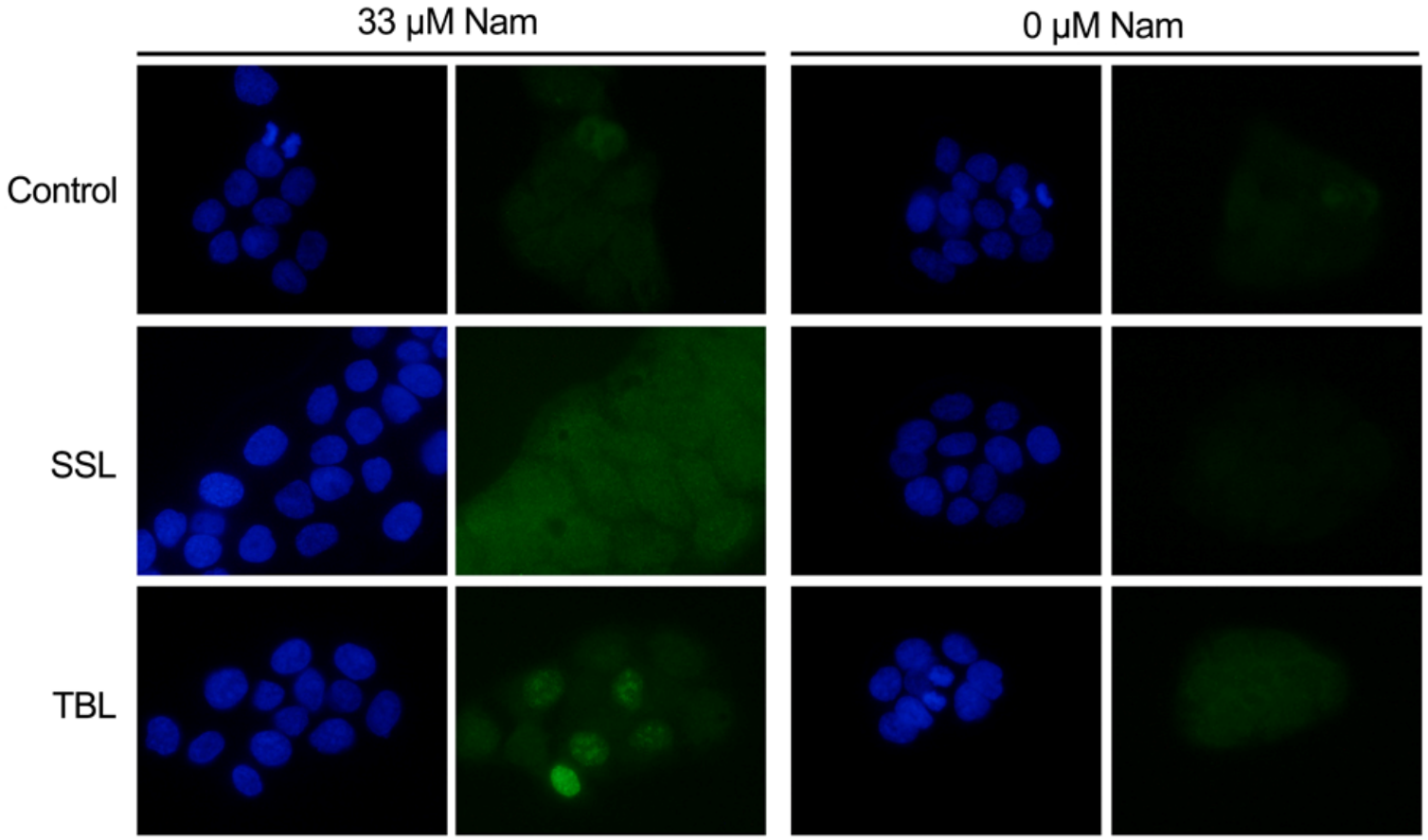

Figure 4.5. PAR formation is impaired in NAD^+-deficient cells. PAR formation was measured in HaCaTs grown in the presence (33 μM Nam) or absence (0 μM Nam) of niacin using immunofluorescence 2hrs after treatment with solar simulated light (SSL); singlet oxygen stress (TBL) and untreated cells (control).

SIRT expression in response to metabolic stress in HaCaT keratinocytes

The dependence of SIRTs on their substrate, NAD^+, suggests a link of SIRT activity to changing metabolic conditions. To further understand this link, we have studied the effect of niacin deficiency and the resulting NAD depletion on SIRT gene expression. We had previously shown that all seven SIRTs (SIRT1-7) are expressed in HaCaTs (Chapter III). Here we show that all SIRT proteins are also expressed in niacin-deficient cells (Figure 4.6). For a more quantitative approach, we measured SIRT gene expression using qPCR. Figure 4.7 shows the effects of niacin depletion on SIRT gene expression in HaCaTs to that of HaCaTs grown under control conditions. All SIRTs are expressed at similar levels in niacin deficient cells when compared to controls, except for SIRT4. Interestingly, SIRT4 expression is significantly increased by 3.7 ± 1.4–fold, potentially linking SIRT4 expression to response to oxidative stress.

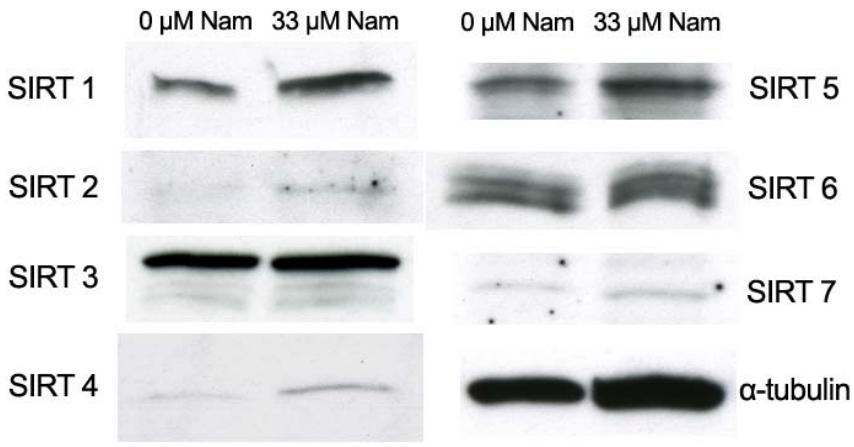

Figure 4.6. SIRT protein expression in niacin-deficient HaCaT keratinocytes. SIRT protein expression was detected by Western blotting using the specified SIRT peptide antibodies. To control for protein loading, blots were probed with α-tubulin.

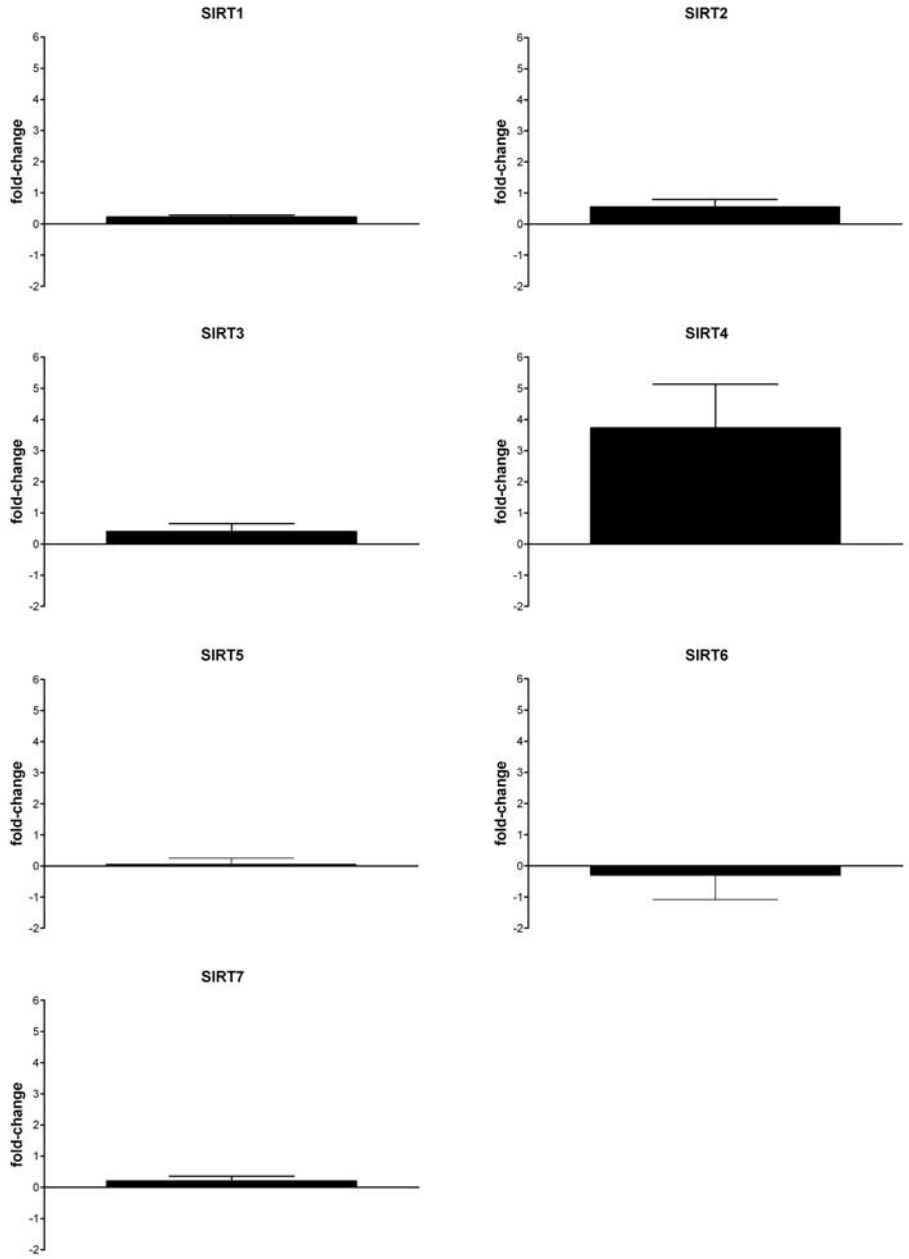

Figure 4.7. SIRT gene expression changes in HaCaT keratinocytes upon niacin deficiency. SIRT expression after NAD-depletion was measured using qPCR. Expression levels shown are expressed as fold-change compared to control HaCaTs. All values represent the mean of 4-9 samples (± SEM).

SIRT response to photodamage is altered by niacin deficiency

To determine how niacin deficiency might affect the gene expression responses of SIRTs upon photodamage, we exposed NAD-depleted HaCaTs to SSL and TBL and compared the expression of SIRTs to their untreated controls. Figures 4.8 and 4.9 show the expression levels of SIRTs after treatment with SSL and TBL, respectively, relative to untreated cells. We had previously demonstrated (Chapter III) that in HaCaTs grown under optimal niacin conditions, treatment with SSL induced upregulation of SIRT4 and downregulation of SIRT3 and SIRT6, while TBL induced upregulation of both SIRT1 and SIRT4. Interestingly, under niacin deficient conditions we observe that SIRT gene expression after photodamage is mostly abrogated, with an upregulation of SIRT1 expression being the only significant response after TBL treatment (1.5 ± 0.6–fold increase) and no significant changes were observed following SSL in niacin deficiency. A trend for decreased SIRT5 expression was observed although this showed a lot of variance and did not reach significance.

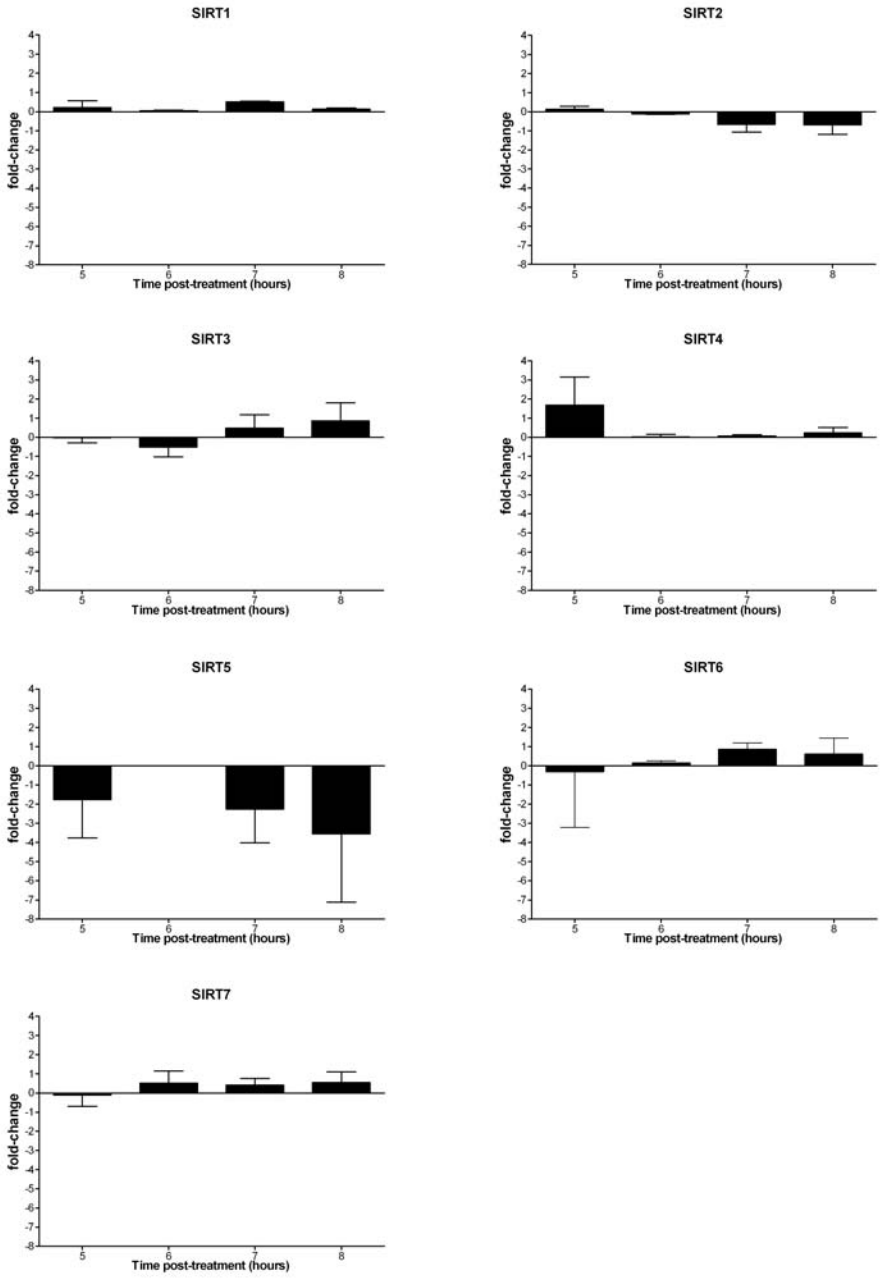

Figure 4.8. SIRT gene expression changes in niacin-deficient HaCaT keratinocytes upon SSL treatment. Time course of SIRT expression after SSL treatment was measured using qPCR. Expression levels shown are calculated as fold-change relative to untreated niacin-deficient HaCaTs. All values represent the mean of 2-6 samples (± SEM).

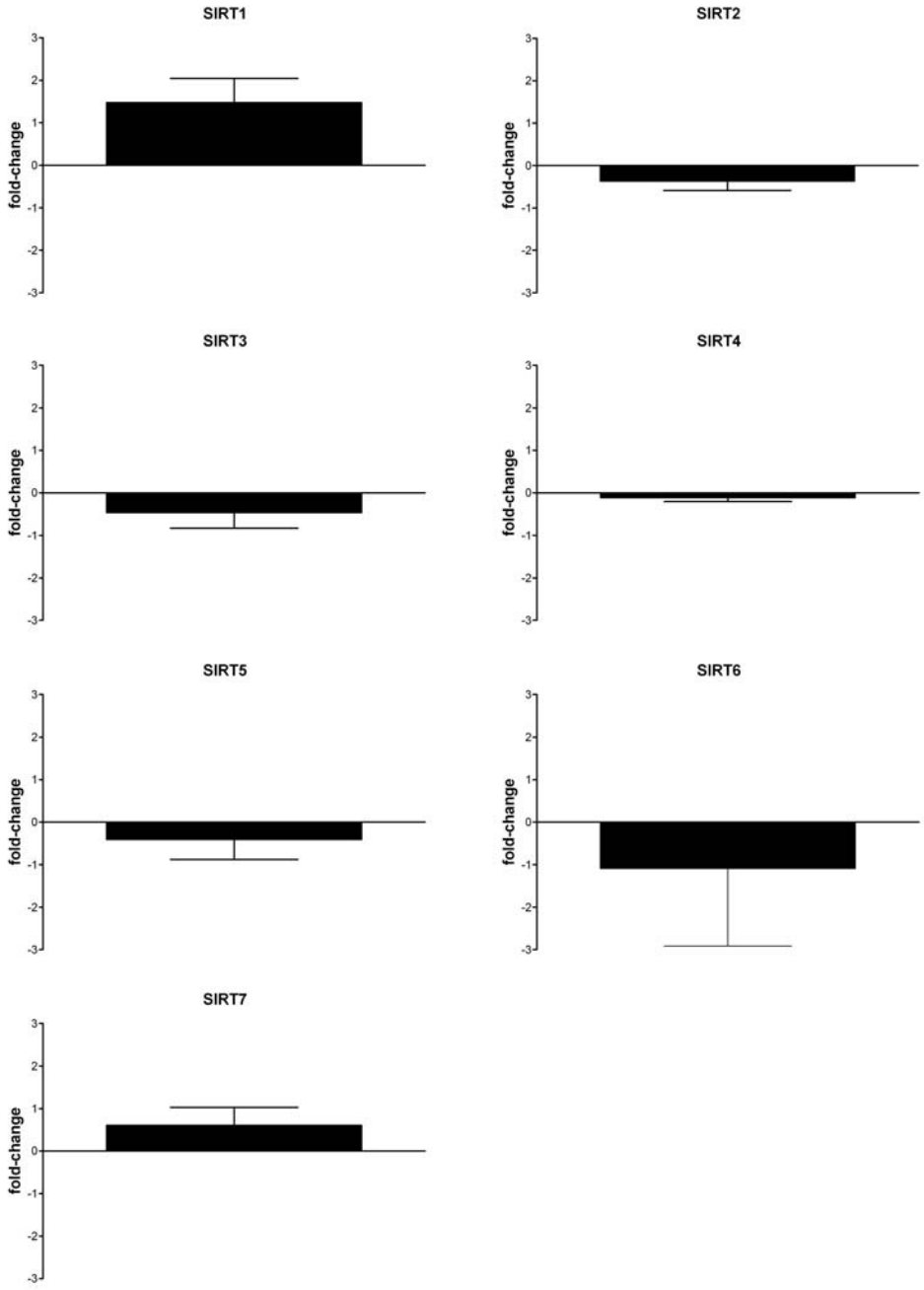

Figure 4.9. SIRT gene expression changes in niacin-deficient HaCaT keratinocytes upon TBL treatment. SIRT expression 5 hours after TBL treatment was measured using qPCR. Expression levels shown are calculated as fold-change relative to untreated niacin-deficient HaCaTs. All values represent the mean of 4-9 samples (± SEM).

Niacin deficiency alters SIRTs deacetylase activity

Since the activity of SIRTs depends on the availability of NAD^+, we predict that niacin deficiency and consequent NAD^+ depletion would lead to inhibition of the deacetylation activity of SIRTs. Using an antibody against acetylated lysine residues, we studied the acetylation profile of cellular proteins from HaCaT keratinocyte cultures grown in normal and niacin deficient media and compared them to cells grown in the presence of known SIRT inhibitors (25 μM sirtinol, 50 μM splitomycin and 5 mM Nam). As seen in Figure 4.10, niacin-deficient HaCaTs show significantly more acetylated protein compared to control cells. Furthermore, niacin deprivation is much more effective in increasing the acetylated state of proteins than any of the SIRT inhibitors used. Since SIRTs are the only known enzymes that involve post-translational acetylation modifications dependent on NAD^+, it is safe to conclude that, as expected, niacin-deficient cells have impaired SIRT activity, leading to a hyperacetylated state.

Next, we employed a proteomics approach to identify the proteins differentially acetylated during niacin deficiency. Using two dimensional Western blot analyses using the same antibody against acetylated lysine residues used before, we looked for spots where increased acetylation is present in niacin deficient cells compared to controls. In Figure 4.11 we highlight five different spots of interest. In Figure 4.10 we had observed a large hyperacetylated protein of approximately 72 kDa, which also seems to appear in the two dimensional Western blot on Figure 4.11; therefore, we chose to identify the proteins

corresponding to that signal using the Coomasie blue stained gel. The results of the mass spectrometry analyses identified the protein as albumin. Albumin is a protein routinely used as a target to test the deacetylase activity of SIRTs; however, the biological relevance of this finding is unknown. Other spots identified were unable to be identified due to the reduced quantities found in the Coomasie blue stained gel from where proteins need to be isolated. However, optimization of this technique can be of great use to identify novel SIRT targets.

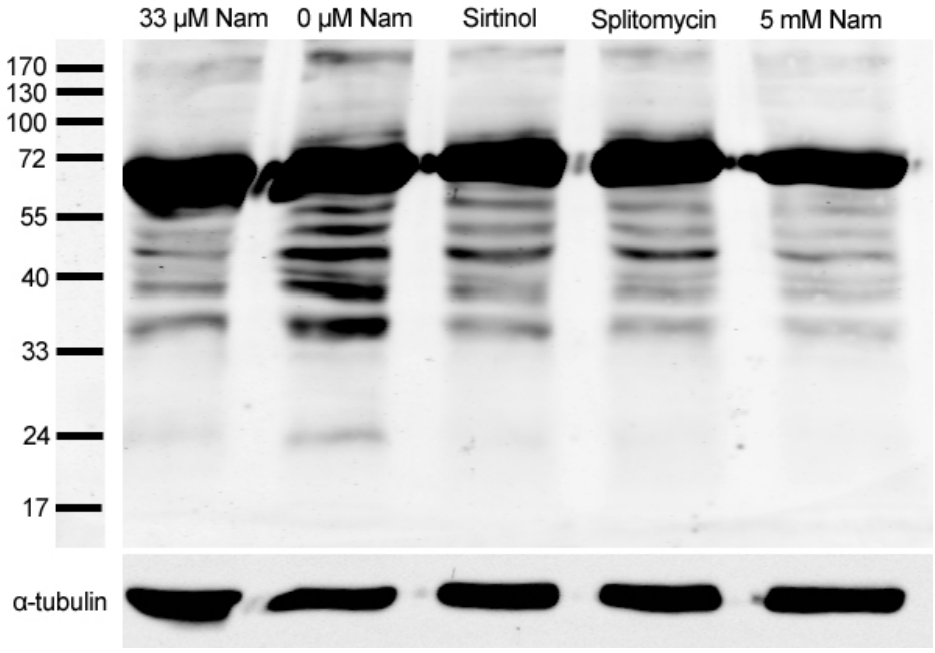

Figure 4.10. Niacin deficiency increases protein acetylation in HaCaT keratinocytes. Acetylation of cellular proteins using Western Blot analysis using an antibody against acetyl-lysine. HaCaT keratinocytes grown in normal (33 μM Nam) or deficient (0 μM Nam) niacin media, treated with SIRT inhibitors: 25 μM sirtinol, 50 μM splitomycin or 5 mM Nam. Bottom: α-tubulin used as protein loading control for each condition.

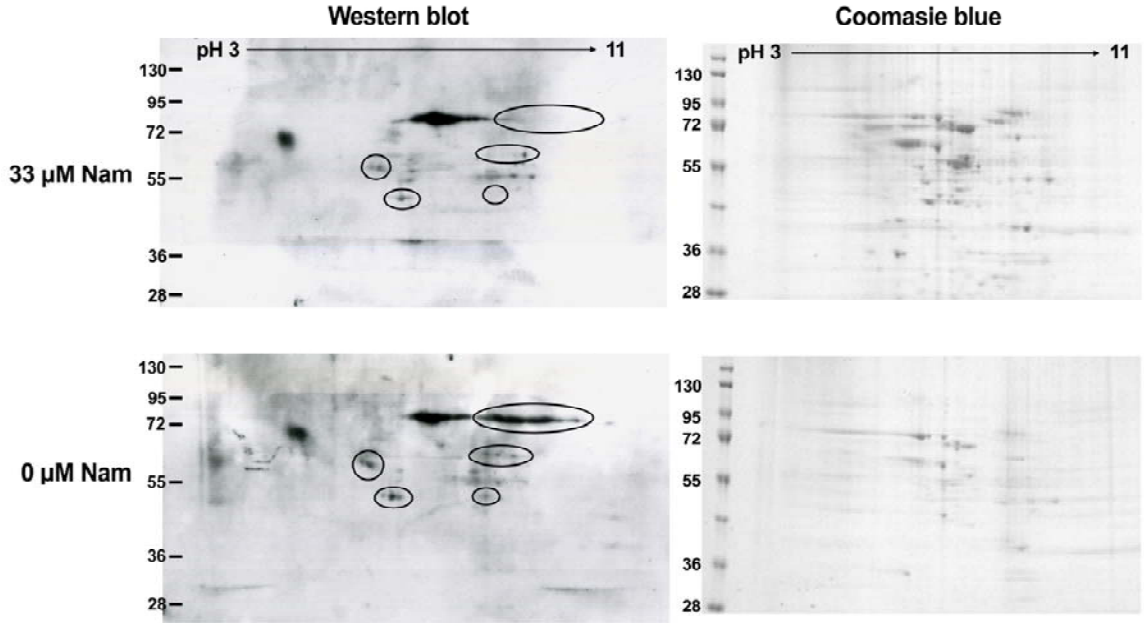

Figure 4.11. 2-D Western blot analysis of protein acetylation in niacin deficient HaCaT keratinocytes. (Left) 2-D Western Blot analyses of acetylated cellular proteins using an antibody against acetyl-lysine. (Right) 2-D gel analyses of total protein content of cell lysates stained with Coomasie blue. HaCaT keratinocytes grown in normal (33 µM Nam) or deficient (0 µM Nam) niacin media. Circles represent proteins of interest hyperacetylated under niacin deficiency.

Discussion

Using our previously described model of NAD-depletion by niacin restriction, we have shown that upon photodamage, either SSL or TBL, deficient HaCaT keratinocytes exhibit increased DNA damage which ultimately leads to small increases in cell death. These data provide evidence that both PARP and SIRT inhibition due to unavailability of their substrate, NAD^+, leads to altered responses upon photodamage.

We observed that NAD-depleted cells are highly sensitized to SSL and TBL treatment at day 14, showing increased DNA damage shown by their increased comet assay mean tail moments (Figure 4.1). At day 7, we only observed a significant increase in DNA damage in cells treated with TBL. Interestingly, cell viability after treatment at 7 days of niacin deprivation shows no significant difference from cells grown under control conditions. This observation might reflect a delay in repair as previously reported [175]. PARP binds to DNA strand breaks induced directly or indirectly by repair processes. During base excision repair, a strand break is created as part of the repair mechanism that is recognized by PARP, initiating the synthesis of poly(ADP-ribose) and leading to changes surrounding the strand break that help to organize the repair process. Once the synthesis of poly(ADP-ribose) on PARP has become extensive enough that anionic repulsion allows it to leave the strand break, completion of repair can occur [175]. At day 7 of niacin deprivation, where NAD^+ levels are kept at 10% of controls (Table 2.1), NAD^+ is limiting for PARP function and, therefore, delays

repair. However, at day 14, the time at which NAD^+ drops below 1% of controls, PARP becomes catalytically inactive (as seen in Figures 4.4 and 4.5), precluding excision repair and increasing apoptosis (Figure 4.3).

Contributing to the increased sensitivity to photodamage, SIRT activity was shown to be impaired by niacin deficiency in HaCaTs (Figure 4.10). The repercussions of a hyperacetylated state in the nucleus due to impaired SIRT function are discussed below. In addition to a lack of SIRT activity under niacin deprivation, we observe that SIRT4 is upregulated. This mitochondrial enzyme regulates metabolism through inhibition of GDH [91]. We have previously shown (Chapter II) that under low intracellular levels of NAD^+, HaCaTs utilize glutamine as an alternative energy source and this promotes ROS production (Figure 2.13). It is possible that SIRT4 expression is regulated by NAD and therefore SIRT4 overexpression is a response to control energy metabolism under limiting NAD^+. Since the absence of active SIRT4 leads to a constitutively active GDH activity which indirectly induces ROS formation, an increase in SIRT4 might be an attempt to increase regulation of GDH and control ROS formation. Other unknown mitochondrial targets for SIRT4 might also play roles in advantageous regulation of metabolism in these cells. In HaCaTs grown under optimal niacin, we have observed an increase of SIRT4 expression upon SSL and TBL treatment. The increased SIRT4 gene expression with niacin deprivation alone may explain the lack of change in this gene observed when the cells are exposed to photodamage as it may reach maximal stress-induced expression with niacin

deprivation. However, we also observe a lack of change in SIRT3 expression and a decrease in the magnitude of the response in SIRT1 in deficient HaCaTs compared to controls.

PARP inhibition by substrate deprivation not only can explain the increase cell death due to unrepaired DNA damage, but also can explain the increase in DNA strand breaks in two ways. First, as mentioned before, unavailability of NAD^+ leads to a catalytically inactive PARP that can have a dominant negative influence on DNA repair, leading to unrepaired DNA breaks produced by endonucleases in the DNA repair process. Second, PARP-1 functions both as a structural component of chromatin and a modulator of chromatin structure through its intrinsic enzymatic activity, promoting the formation of compact, transcriptionally repressed chromatin structures [52]. Therefore, PARP inhibition would lead to a more relaxed chromatin, which would become more prone to DNA damage. NAD^+ is also consumed by SIRTs to deacetylate histones, among other targets. Histone deacetylation leads to a more compact chromatin structure and gene silencing. It also appears to protect sensitive areas of chromatin, such as telomeres, against translocation events and to play a role in extended life span associated with caloric restriction [117]. Taken together, niacin deficiency could lead to a more open DNA structure, with more active gene expression and greater sensitivity to damage and translocation events [74].

Previous studies have been unable to show a correlation between PARP inhibition and enhanced cytotoxicity upon UV irradiation. Here, we have shown

that PARP inhibition through limiting substrate not only increases DNA damage but also correlates with increased cell death. The difference between our observations and previous results may lie in our cell model since HaCaTs are immortalized, have mutated p53, aberrant NF-κB signaling, and under niacin deprivation may be more vulnerable due to the need to make ROS as a survival mechanism. Our data demonstrate a combined effect of PARP and SIRT inhibition following UV damage. These data support the idea that niacin deficient skin is more sensitive to sunlight and early in initiation, niacin deficiency might promote tumor progression both by altering PARP activity and SIRT functions. Furthermore, these data have identified specific SIRTs that likely play a role following DNA damage and on which further studies are warranted.

CHAPTER V
NICOTINIC ACID RECEPTOR EXPRESSION IN HUMAN KERATINOCYTES: A NEW ROLE IN SKIN?

Abstract

Identified as important pharmacological targets for the treatment of dyslipidemia and prevention of coronary heart disease, the nicotinic acid receptor in humans is encoded by two genes, HM74 and HM74A. Expression of these receptors has been reported in adipose tissue, where they negatively regulate hydrolysis of adipocyte triglycerides, skin Langerhans cells and macrophages and mediate skin flushing, a side effect of pharmacological niacin administration. Our studies using skin cell models show that HM74 and HM74A receptors are expressed in human keratinocytes but not fibroblasts. These findings are based on immunocytochemical analyses of human skin cells and immunohistochemical analyses of human skin sections using an antibody specific to HM74 and HM74A, as well as by quantitative reverse transcriptase-PCR analyses of human skin cells. Since expression of HM74 and HM74A in keratinocytes is not believed to be involved in blood lipid regulation or skin flushing, alternative functions of the receptor expressed uniquely in the stratum corneum are suggested.

Introduction

The use of niacin as a chemopreventive agent for the treatment of early signs of skin cancer requires defining which chemical form of the vitamin is more beneficial. Both nicotinic acid and nicotinamide serve as precursor of coenzymes NAD and NADP. However, some evidence indicates that high concentrations of nicotinamide, but not nicotinic acid, have inhibitory effects on NAD-dependent protein deacetylases (SIRTs) and poly(ADP-ribose) polymerases (PARPs) [176,177]. Furthermore, nicotinic acid appears to be a better candidate for therapeutic use since it has additional biological effects unrelated to those as a vitamin. Pharmacological doses of nicotinic acid administered orally have been shown to reduce total levels of cholesterol in the plasma and provide effective elevation of HDL, a protective effect that to date has not been reproduced by any other drug [178]. In recent years, nicotinic acid was found to bind to an orphan G-protein coupled receptor, HM74A [179]. This discovery has provided the possibility of gaining further insight into the mechanism of action by which nicotinic acid can elevate HDL and modulate numerous biological phenomena.

Human nicotinic acid receptors HM74 (also referred to as GPR109B) and HM74A (also referred to as GPR109A in humans and PUMA-G in mice) are two very similar G protein-coupled receptors (GPCR) of the seven-transmembrane type. These two receptors are encoded by separate genes in tandem organization where the HM74 gene encodes a protein with a carboxyterminal extension of 24 amino acids as compared to HM74A [180]. HM74A has recently

been identified as an important pharmacological target for the treatment of dyslipidemia as it binds nicotinic acid with high affinity [181-184]. HM74A is expressed in adipose tissue where, upon binding of its ligand, it has been shown to inhibit the activity of adenylyl cyclases, resulting in lowered cAMP levels. As a consequence, the hydrolysis of triglycerides and the release of free fatty acids into the bloodstream are reduced. This leads to the positive impact of elevating HDL and reducing LDL cholesterol observed upon nicotinic acid intake. For this reason, nicotinic acid is the most effective drug in use for lowering of lipidemia, increasing HDL cholesterol levels, and preventing coronary heart disease [185].

Amongst various tissues, HM74A is also expressed in skin macrophages and Langerhans cells where it has been reported to mediate an intense flushing and burning sensation of the skin in response to nicotinic acid, the common side effect of high-dose niacin intake [186]. In order to circumvent this problem our lab has developed the esterified niacin derivative, lauryl nicotinate, for transdermal delivery of the drug through the skin, providing controlled rates of delivery that alleviate the flushing response during therapy to modulate serum cholesterol levels. During mechanistic studies of lauryl nicotinate, Dr. Hyuntae Kim and collaborators discovered that niacin causes the release of leptin and downstream signaling of leptin has profound effects on epidermal renewal, wound healing and hair follicle biology in skin (Figure 5.1). These findings led to an investigation of niacin derivatives that target delivery of niacin to skin cells and the functions of niacin in skin biology (Figure 5.2). Of interest to the studies of this dissertation

was the fact that niacin stimulates skin differentiation, consistent with a role in cancer prevention. In order to determine whether the beneficial effects to skin [82,187] observed by topical application of niacin are mediated by signaling through the nicotinic acid receptor, we raised the question of whether skin cells express this receptor and where in the skin is it expressed.

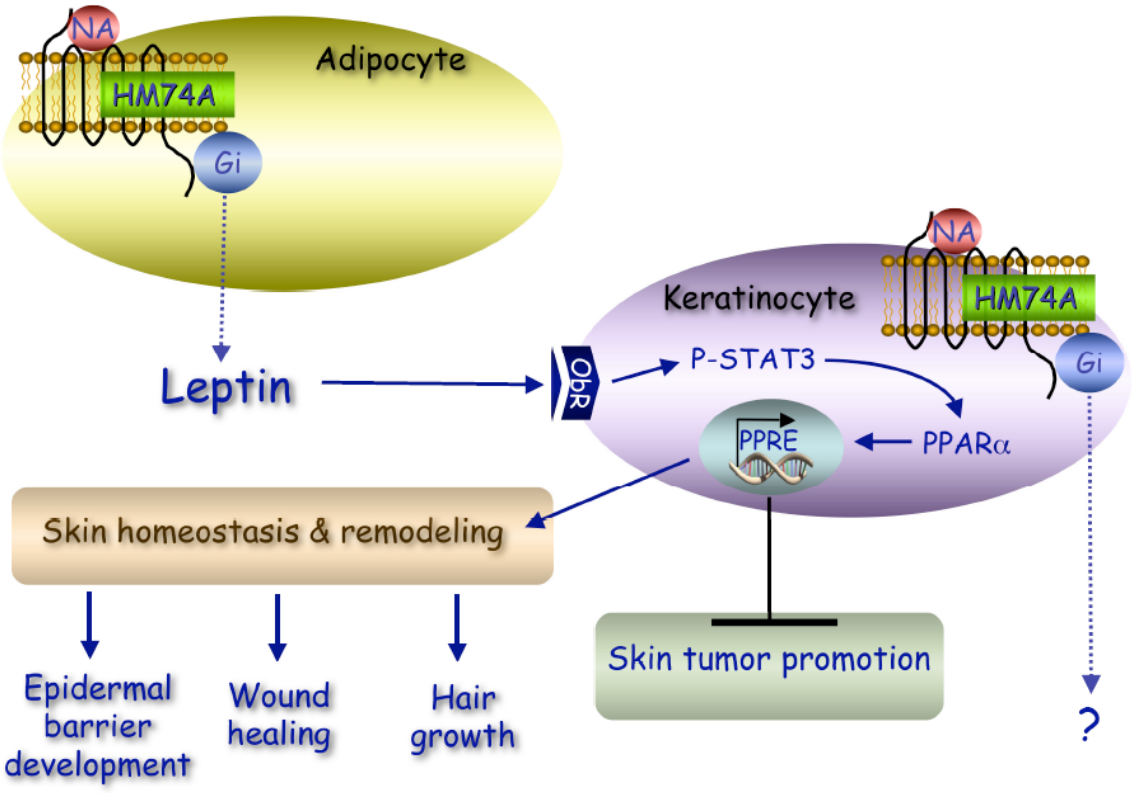

Figure 5.1. Leptin as an intermediate in nicotinic acid receptor signaling in skin. Binding of niacin to the nicotinic acid receptor causes the release of leptin and signaling downstream of leptin stimulates skin homeostasis and remodeling and suppressed skin tumor promotion.

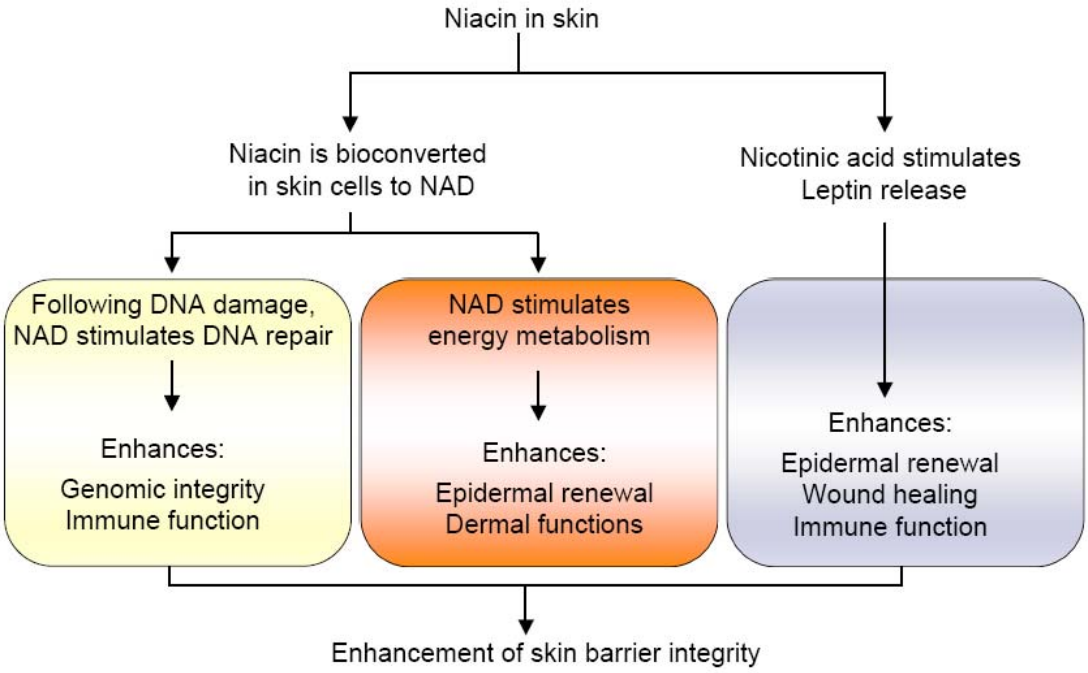

Figure 5.2. Nutrient and drug effects of nicotinic acid in skin damage and skin cancer. Niacin functions both as a G-protein coupled receptor agonist important in skin differentiation and as a precursor for NAD whose substrate roles for PARPs, SIRTs and energy metabolism all contribute significantly to photo-resistance in human skin cells.

Materials and Methods

Cell culture

HeLa cells (substrain S3) (ATCC), low-passage populations of CF3 human fibroblasts (ATCC), and human immortalized keratinocytes (HaCaT) a gift from Dr. Norbert Fusenig (German Cancer Research Center, Heidelberg, Germany) [114] were routinely cultured in Dulbecco's Modified Eagle Medium (DMEM) containing 10% bovine calf serum. Normal human keratinocytes (NHEK, ATCC) were routinely cultured in Keratinocyte Medium 2 (KGM-2, Lonza) containing KGM-2 SingleQuots (Lonza). All cells were kept in a humidified atmosphere containing 5% CO_2 at 37°C.

qPCR

Total RNA was prepared from cultured cells using the RNeasy purification system (Qiagen) according to the manufacturer's instructions. cDNA synthesis was performed with the TaqMan Reverse Transcription kit (Applied Biosystems) using random hexamers and 1 µg of total RNA. For TaqMan-based real-time PCR expression profiling, 25 ng of cDNA each was added to the TaqMan Universal PCR Master Mix along with the TaqMan MGB probes according to the manufacturer's instructions (Applied Biosystems).

qPCR was performed essentially as described [123]. Primers and probes designed to specifically detect the human HM74 (TaqMan Gene Expression Assay Hs02341102_s1) and HM74A (TaqMan Gene Expression Assay Hs02341584_s1) transcripts were purchased from Applied Biosystems. Real-

time fluorescence monitoring was performed with the ABI Prism 7900 (Applied Biosystems). Relative expression levels of the various transcripts were determined by comparison against the housekeeping gene, GAPDH. Quantitative expression was determined creating a standard curve with plasmid DNA template for each of the genes. All expression measurements were performed in triplicate using three independently generated cDNA samples. Real time RT-PCR product amplification sizes for HM74 (83 bp) and HM74A (97 bp) were verified using 2.5% agarose gel electrophoresis.

Western blot analyses

Monolayers of transfected or nontransfected cells were first washed with PBS and then directly scraped off the plates, both in the presence of protease inhibitors phenylmethylsulfonyl fluoride (PMSF) and complete protease inhibitor cocktail (Roche). After SDS-polyacrylamide electrophoresis and semidry electrotransfer to PDVF membranes, proteins were detected using a final concentration of 0.5 µg/mL of affinity-purified rabbit antisera raised against synthetic peptide 201 (Sigma Genosys) corresponding to an amino acid sequence that is identical in HM74 and HM74A (Ab201: MNRHHLQDHFLEIDKKNC). The peptide used for generation of Ab201 was also used for blocking antibody solutions for specificity testing in immunofluorescence or immunoblotting experiments. For this purpose, either a 10-fold (i.e. 3.33 µM = 6.709 µg/ml) or 100-fold (i.e. 33.33 µM = 67.09 µg/ml) molar excess of the synthetic peptide in 3% BSA/PBS was preincubated at 4°C (overnight) or room

temperature (one hour) with the corresponding antibody and then centrifuged at 3000 x g for 15 min. The supernatant was then used in parallel with the corresponding standard primary antibody solution in immunostaining or immunoblotting protocol in order to allow for specificity assessment. Donkey anti-rabbit antibodies (Jackson) coupled to fluorescein isothiocyanate (FITC) or horseradish peroxidase (HRP) were used as secondary antibodies for immunofluorescence or western blot detection, respectively, of the primary antibodies.

Immunofluorescence analyses

Cells grown on coverslips were fixed using 5% formaldehide made fresh from stabilized 37.5% stock solution (Sigma) and then subjected to a standard immunostaining protocol. Briefly, coverslips were incubated with 0.5 µg/mL of purified antibody solution for 1 hour at 37°C or 4°C overnight in a humid chamber, then washed 3 – 5 times in PBS for 5 min each and then incubated with FITC-conjugated donkey anti-rabbit secondary antibody solution (1:100) in 3% BSA/PBS (w/v) for 45 min at 37°C. After 3 – 5 washing steps in PBS, coverslips were mounted on slides using vectashield (Vector laboratories) containing 1 µg/ml DAPI and then analyzed. Human skin paraffin sections were dewaxed and blocked with 3% BSA/PBS for 1 hour at room temperature prior to incubation with antibody solutions of various concentrations using the same standard immunostaining protocol as outlined above.

Results

Skin cells express the nicotinic acid receptor genes

Nicotinic acid receptor expression has been observed in various cell types, but has never been characterized in skin, except for Langerhans cells in which it has been shown to be present and the source of prostaglandin D signaling in response to niacin [188]. In order to establish whether the nicotinic acid receptor is expressed in non-immune skin cells, we performed quantitative reverse-transcriptase-PCR. Figure 5.3 shows the number of HM74 and HM74A mRNA copies found in diploid human fibroblasts (CF3), normal human keratinocytes (NHEK), and immortalized human keratinocytes (HaCaT). This figure shows that both HM74 and HM74A are being expressed in skin cells. However, HM74A is a more abundant form of the receptor than HM74. We found that in CF3 cells, HM74A has approximately 30% higher expression than HM74, in NHEK cells the mRNA levels of HM74A are 300% higher than HM74, and in HaCaTs this difference reaches 400%. Interestingly, the expression of both receptors is much higher in keratinocytes than fibroblasts. Furthermore, the expression is significantly increased in HaCaTs compared to NHEKs.

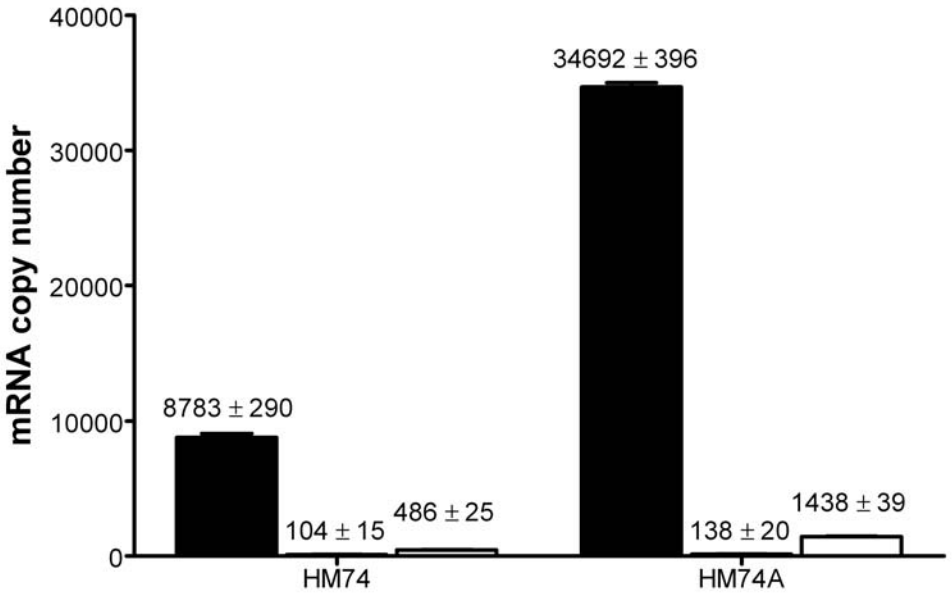

Figure 5.3. Nicotinic acid receptor gene expression in skin cells. Copy numbers of HM74 and HM74A mRNA in skin cells normalized to GAPDH expression as determined by qPCR analyses. HaCaTs (black), NHEK (white), and CF3 (striped). All values represent the mean of triplicate samples (± SEM).

The nicotinic acid receptor is expressed and translated in keratinocytes

Using an antibody raised for the specific detection of both HM74 and HM74A, we studied the protein expression of the nicotinic acid receptor in skin cells. Western blot analyses of fibroblasts and keratinocytes showed endogenous expression of the HM74/A receptors (Figure 5.4, left) with the specific band being competitively blocked by pre-incubation with the peptide against which the antibody was raised (Figure 5.4, right). As a positive control, we used an adipocyte cell lysate, as adipocytes have been shown to express high levels of the HM74/A receptor [185]. Consistent with our qPCR results, Western blot analysis shows that HaCaTs have significantly higher levels of nicotinic acid receptor than CF3s, in which protein was undetectable. Human niacin receptors have a predicted relative molecular weight of 42 kDa. However, the detected specific band was approximately 30 kDa in size, independent of the experimental conditions which included the use of a variety of protease inhibitors (data not shown). Whether this indicates that the receptor is an inherently unstable protein with a possible high turnover or is the product of alternative splicing is currently under investigation.

Immunocytochemistry studies further support our previous observations of endogenous nicotinic acid receptor expression being significantly higher in keratinocytes compared to fibroblasts. Figure 5.5 shows a strong signal that localizes to the membrane of HaCaT cells. On the other hand, expression of the nicotinic acid receptor was absent or below detection in fibroblasts as was

expected from the Western blots analyses (Figure 5.6). As performed with the Western blot analyses, the specificity of the nicotinic acid receptor signal was determined by peptide competition.

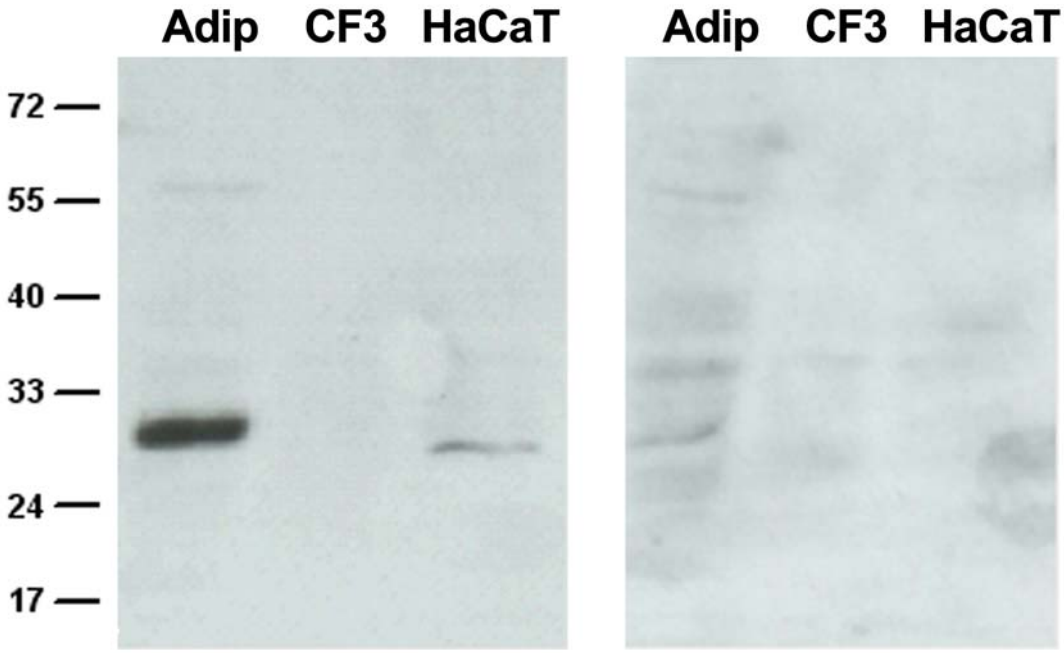

Figure 5.4. Endogenous nicotinic acid receptor expression in skin cells. Left: Nicotinic acid receptor expression in fibroblasts (CF3) and keratinocytes (HaCaT) was detected by Western blot analyses using an antibody that recognizes both HM74 and HM74A. Right: Peptide competition of the antibody signal to prove specificity. Normal human adipocytes (Adip) were used as positive control.

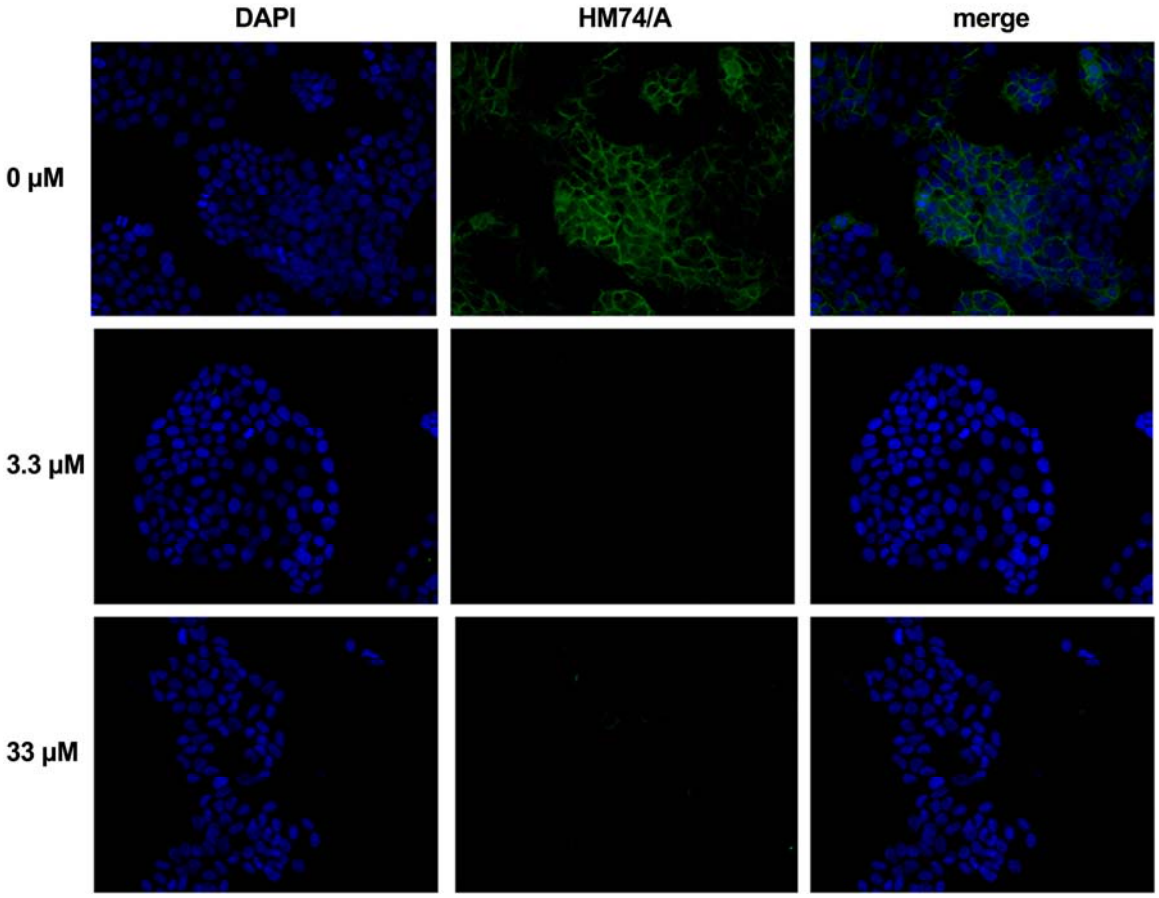

Figure 5.5. Immunodetection of endogenous nicotinic acid receptor expression in HaCaT keratinocytes. Nicotinic acid receptor (HM74/A) was detected in HaCaT keratinocytes. Increasing concentration (shown on the left) of blocking peptide was used for competition of antibody binding to show specificity. Nuclei co-stain is also shown (DAPI).

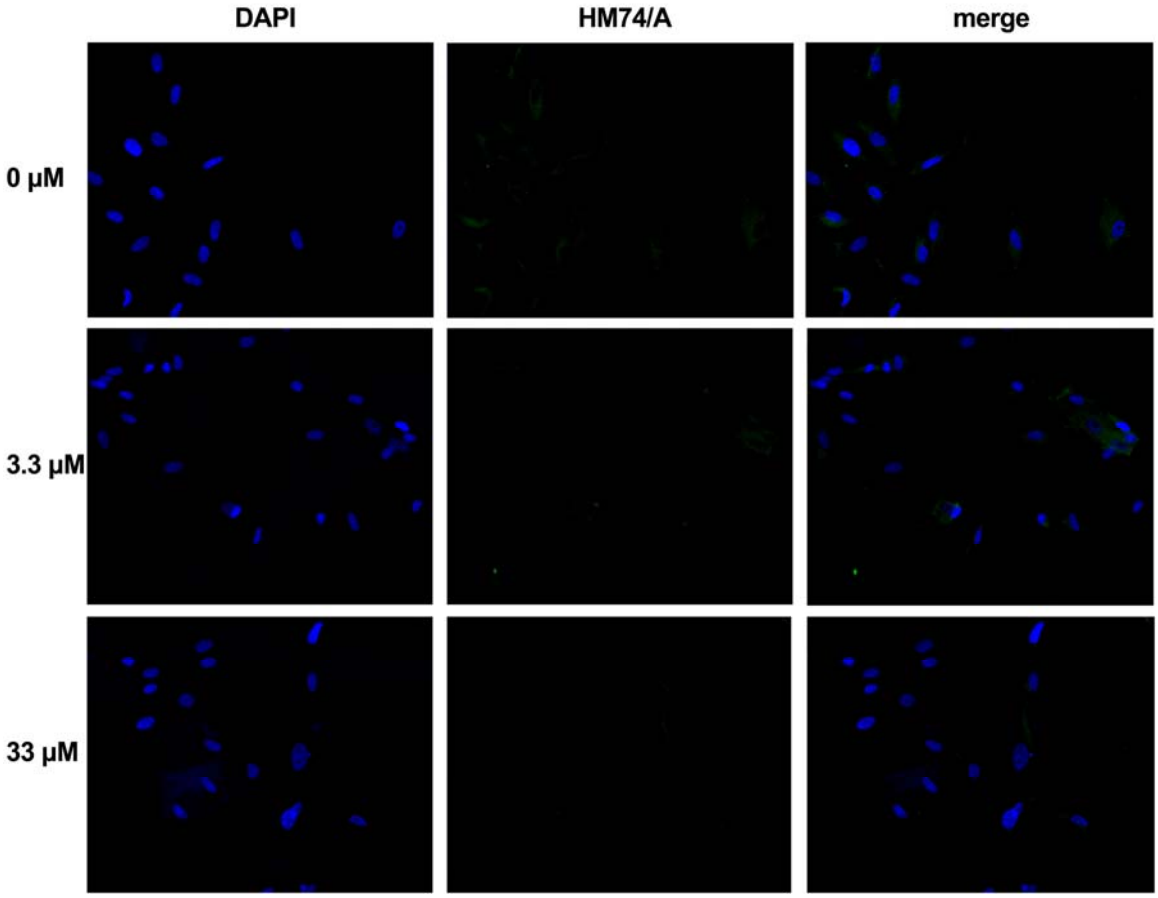

Figure 5.6. Nicotinic acid receptor is absent in CF3 fibroblasts. Nicotinic acid receptor (HM74/A) was undetected in CF3 fibroblasts. Increasing concentration (shown on the left) of blocking peptide was used for competition of antibody binding to show specificity. Nuclei co-stain is also shown (DAPI).

In situ analysis of the nicotinic acid receptor in human skin

To verify that the observations in cultured skin cells correlate with what is found in human skin, we performed immunofluorescence analyses using human skin sections. Consistent with our previous data, Figure 5.7 shows strong signals in the epidermis while the underlying dermal fibroblasts were not stained by the nicotinic acid receptor antibody. This is the first report of an *in situ* analysis of nicotinic acid expression at the protein level in human skin and substantial evidence indicates that keratinocytes strongly express these receptors.

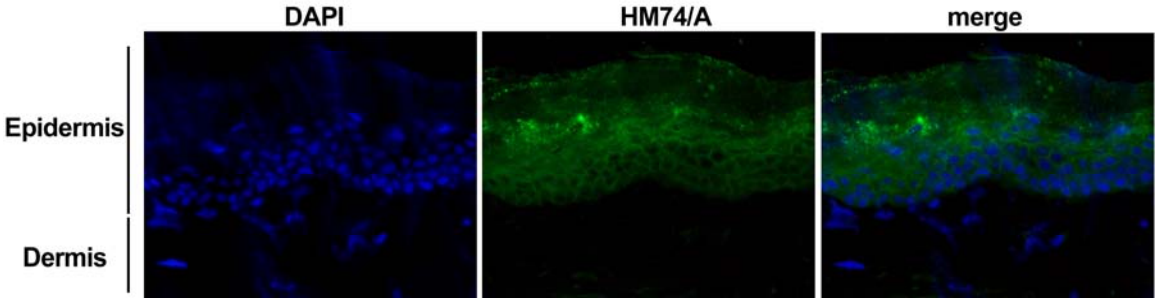

Figure 5.7. Nicotinic acid receptor expression in human skin sections. Nicotinic acid receptor (HM74/A) was detected in skin sections. Specific immunofluorescence signals indicate high expression levels of niacin receptor molecules in the epidermis, but nearly undetectable levels in the dermal layer of the skin that are predominantly formed by fibroblasts. Nuclei co-stain is also shown (DAPI).

Discussion

In this study, we have examined the expression of the nicotinic acid receptor in human skin cells. Here, we have identified for the first time that HM74 and HM74A are expressed in human skin keratinocytes, mainly in the keratinocyte differentiation zone of the stratum corneum in the epidermis.

We have shown that the HM74 and HM74A genes are expressed in skin cells. Using qPCR to quantify the mRNA levels in human diploid fibroblasts (CF3s), normal human keratinocytes (NHEKs) and immortalized keratinocytes (HaCaTs), we found that nicotinic acid receptor gene expression is present in all these skin cell types with HM74A being the more abundant form of the receptor. We also noted that the expression levels in keratinocytes are significantly higher than in fibroblasts. Furthermore, we found that HaCaTs expressed significantly higher levels of both HM74 and HM74A than NHEKs. Understanding the implications of such an increase in immortalized keratinocytes requires the elucidation of the role of nicotinic acid in the skin, which remains unknown.

Using a specific antibody previously developed by our lab that recognizes both forms of the nicotinic acid receptor, we showed that endogenous receptors are detectable in HaCaT keratinocytes but absent or marginally present in CF3 fibroblasts. In line with this result, histological sections of human skin were strongly stained for HM74/A in the keratinocyte differentiation zone of the stratum corneum in the epidermis, but no detectable staining was present in the dermis.

The finding that keratinocytes express HM74 and HM74A presents an opportunity for understanding novel roles for the nicotinic acid receptor. Several observations have shown that topical application of a nicotinic acid derivative has beneficial effects on skin barrier integrity by increasing the thickness of the epidermis and in particular of the stratum corneum, reducing transepidermal water loss and enhancing specific markers of differentiation [82,187]. It has also been proposed that topical application of nicotinic acid enhances wound healing by stimulation of leptin secretion (Figure 5.1) [189]. The presence of the nicotinic acid receptor in the same area where these effects are taking place points towards the possibility that signaling through this receptor is responsible for the enhanced differentiation and leptin secretion being observed. Whether leptin is derived from adipocytes in the subcutaneous layers, from keratinocytes or both, remains to be determined. Further research will be necessary to define the exact mechanisms mediating the effects of topical niacin and whether they are mediated via the niacin receptor and/or leptin. This is particularly exciting after finding that the receptors are expressed differentially in skin with preferential expression in human epidermal keratinocytes. The nicotinic acid receptor thus represents a potential target for developing skin cancer prevention agents.

CHAPTER VI

CONCLUSIONS

Niacin deficiency in humans causes sun sensitivity, indicative of DNA repair problems [74]. In fact, animal models of niacin deficiency demonstrate genomic instability [76] and increased cancer development in sensitive tissues including skin [162]. However, the maintenance and regulation of cellular NAD(P)(H) content and its influence on cell function are poorly understood. Therefore, the development of a cell culture model that allows assessment of pathways regulated by NAD(P) content is crucial to identify NAD-dependent signaling events that may be critical in early skin carcinogenesis.

We developed a model to identify the NAD-dependent pathways potentially important in early skin carcinogenesis. Our model confirmed that human keratinocytes require the preformed vitamin, niacin, to synthesize NAD utilizing the salvage pathway, as the synthesis of NAD from tryptophan through the *de novo* pathway seems to be absent. Using this model, we showed that nicotinamide restriction, and consequent NAD depletion, reversibly alters NAD(P)(H) pools, increases apoptosis, induces G_2/M cell cycle arrest, and decreases DNA stability. These alterations are affected at least in part by increased expression and activity of NOX leading to an accumulation of ROS, which may provide a survival mechanism as has been shown in other cancer cells [125,126,139-142]. Our data also support the hypothesis that glutamine is a likely alternative energy source during niacin deficiency. Glutamine utilization has

been reported to be accompanied by ROS formation in immune cells [143] and implicated in cancer cell proliferation [144]. These findings suggest that NAD dependent pathways presented here modulate survival pathways that may limit ROS dependent signaling during early skin carcinogenesis.

We also examined the expression of the NAD^+-dependent protein deacetylases, SIRTs, in human skin cells. We are the first to identify the expression of all seven SIRT family members in fibroblasts (CF3) and both in normal (NHEK) and immortalized keratinocytes (HaCaT). Of interest, we found that SIRT1, SIRT3, SIRT4, SIRT5, and SIRT7 are overexpressed in HaCaTs, supporting the line of thought that HaCaTs may be a model of initiated keratinocytes, since tumor cells have been shown to require SIRT overexpression [152]. We also showed that in response to photodamage, the expression of several SIRTs is altered in keratinocytes. Furthermore, we showed that SIRTs responses to photodamage differ between normal (NHEK) and initiated keratinocytes (HaCaT), which may be indicative of alterations potentially important in skin carcinogenesis.

Furthermore, we have also shown that NAD-depleted HaCaT keratinocytes are more sensitive to photodamage, either as solar simulated light (SSL) or singlet oxygen stress (TBL). We observed that both PARPs and SIRTs are inhibited by the unavailability of their substrate, NAD^+, leading to unrepaired DNA damage upon photodamage and subsequent increase in cell death. PARP inhibition would lead to a more relaxed chromatin, which would become more

prone to DNA damage. NAD^+ is also consumed by SIRTs to deacetylate histones, among other targets. Histone deacetylation leads to a more compact chromatin structure and gene silencing [117]. Taken together, niacin deficiency could lead to a more open DNA structure, with more active gene expression and greater sensitivity to damage and translocation events [74]. These data demonstrate that both SIRTs and PARPs are critical following DNA damage and show which SIRTs are likely the critical ones.

Finally, we examined the expression of the nicotinic acid receptor in human skin cells. We have identified for the first time that HM74 and HM74A are expressed in human skin keratinocytes, mainly in the keratinocyte differentiation zone of the stratum corneum in the epidermis. This study provides a further link to niacin's role as a potential skin cancer prevention agent and suggests that the nicotinic acid receptor as a potential target for skin cancer prevention drugs. Furthermore, finding that keratinocytes express the nicotinic acid receptors supports the idea that niacin plays an important role in preventing skin disease as signaling through this receptor may be responsible for the enhanced skin differentiation and wound healing observed upon niacin treatment [82,187].

Together our data shows that niacin deficiency drives keratinocytes during early carcinogenesis to proliferate and survive under conditions that promote genomic instability and DNA damage, thus driving the carcinogenesis process in skin. Therefore, niacin has potential as a chemopreventive agent used for treatment of early skins of skin cancer (e.g. actinic keratoses) as it would sustain

proper DNA damage repair and maintenance of genomic stability, as well as drive skin differentiation to create a proper skin barrier and function.

REFERENCES

1. Kricker, A., Armstrong, B.K. and English, D.R. (1994) Sun exposure and non-melanocytic skin cancer. *Cancer Causes Control*, **5**, 367-92.

2. Jemal, A., Siegel, R., Ward, E., Murray, T., Xu, J. and Thun, M.J. (2007) Cancer statistics, 2007. *CA Cancer J Clin*, **57**, 43-66.

3. Einspahr, J.G., Stratton, S.P., Bowden, G.T. and Alberts, D.S. (2002) Chemoprevention of human skin cancer. *Crit Rev Oncol Hematol*, **41**, 269-85.

4. Frankel, D.H., Hanusa, B.H. and Zitelli, J.A. (1992) New primary nonmelanoma skin cancer in patients with a history of squamous cell carcinoma of the skin. Implications and recommendations for follow-up. *J Am Acad Dermatol*, **26**, 720-6.

5. Karagas, M.R., Stukel, T.A., Greenberg, E.R., Baron, J.A., Mott, L.A. and Stern, R.S. (1992) Risk of subsequent basal cell carcinoma and squamous cell carcinoma of the skin among patients with prior skin cancer. Skin Cancer Prevention Study Group. *Jama*, **267**, 3305-10.

6. Preston, D.S. and Stern, R.S. (1992) Nonmelanoma cancers of the skin. *N Engl J Med*, **327**, 1649-62.

7. Robinson, J.K. (1987) What are adequate treatment and follow-up care for nonmelanoma cutaneous cancer? *Arch Dermatol*, **123**, 331-3.

8. Rowe, D.E., Carroll, R.J. and Day, C.L., Jr. (1989) Long-term recurrence rates in previously untreated (primary) basal cell carcinoma: implications for patient follow-up. *J Dermatol Surg Oncol*, **15**, 315-28.

9. Silverberg, E. and Lubera, J.A. (1988) Cancer statistics, 1988. *CA Cancer J Clin*, **38**, 5-22.

10. Chen, J.G., Fleischer, A.B., Jr., Smith, E.D., Kancler, C., Goldman, N.D., Williford, P.M. and Feldman, S.R. (2001) Cost of nonmelanoma skin cancer treatment in the United States. *Dermatol Surg*, **27**, 1035-8.

11. Weber, R.S., Lippman, S.M. and McNeese, M.D. (1990) Advanced basal and squamous cell carcinomas of the skin of the head and neck. *Cancer Treat Res*, **52**, 61-81.

12. Blum, H. (1948) Sunlight as a causal factor in cancer of the skin in man. *JNCI*, 247-58.

13. Emmett, E.A. (1973) Ultraviolet radiation as a cause of skin tumors. *CRC Crit Rev Toxicol*, **2**, 211-55.

14. Fitzpatrick, T.B., Pathak, M.A., Magnus, I.A., Curwen, W.L.. (1963) Abnormal reactions of man to light. *Annu Rev Med*, 195-214.

15. Kwa, R.E., Campana, K. and Moy, R.L. (1992) Biology of cutaneous squamous cell carcinoma. *J Am Acad Dermatol*, **26**, 1-26.

16. Ananthaswamy, H.N. and Pierceall, W.E. (1990) Molecular mechanisms of ultraviolet radiation carcinogenesis. *Photochem Photobiol*, **52**, 1119-36.

17. Melnikova, V.O. and Ananthaswamy, H.N. (2005) Cellular and molecular events leading to the development of skin cancer. *Mutat Res*, **571**, 91-106.

18. DiGiovanni, J. (1992) Multistage carcinogenesis in mouse skin. *Pharmacol Ther*, **54**, 63-128.

19. Tornaletti, S., Rozek, D. and Pfeifer, G.P. (1993) The distribution of UV photoproducts along the human p53 gene and its relation to mutations in skin cancer. *Oncogene*, **8**, 2051-7.

20. Ziegler, A., Leffell, D.J., Kunala, S., Sharma, H.W., Gailani, M., Simon, J.A., Halperin, A.J., Baden, H.P., Shapiro, P.E., Bale, A.E. and et al. (1993) Mutation hotspots due to sunlight in the p53 gene of nonmelanoma skin cancers. *Proc Natl Acad Sci U S A*, **90**, 4216-20.

21. Bowden, G.T. (2004) Prevention of non-melanoma skin cancer by targeting ultraviolet-B-light signalling. *Nat Rev Cancer*, **4**, 23-35.

22. Wondrak, G.T., Jacobson, M.K. and Jacobson, E.L. (2006) Endogenous UVA-photosensitizers: mediators of skin photodamage and novel targets for skin photoprotection. *Photochem Photobiol Sci*, **5**, 215-37.

23. Kappes, U.P., Luo, D., Potter, M., Schulmeister, K. and Runger, T.M. (2006) Short- and long-wave UV light (UVB and UVA) induce similar mutations in human skin cells. *J Invest Dermatol*, **126**, 667-75.

24. Runger, T.M. (2007) How different wavelengths of the ultraviolet spectrum contribute to skin carcinogenesis: the role of cellular damage responses. *J Invest Dermatol*, **127**, 2103-5.

25. Decraene, D., Agostinis, P., Pupe, A., de Haes, P. and Garmyn, M. (2001) Acute response of human skin to solar radiation: regulation and function of the p53 protein. *J Photochem Photobiol B*, **63**, 78-83.

26. Avkin, S., Sevilya, Z., Toube, L., Geacintov, N., Chaney, S.G., Oren, M. and Livneh, Z. (2006) p53 and p21 regulate error-prone DNA repair to yield a lower mutation load. *Mol Cell*, **22**, 407-13.

27. Baade, P.D., Balanda, K.P. and Lowe, J.B. (1996) Changes in skin protection behaviors, attitudes, and sunburn: in a population with the highest incidence of skin cancer in the world. *Cancer Detect Prev*, **20**, 566-75.

28. Graham, S., Marshall, J., Haughey, B., Stoll, H., Zielezny, M., Brasure, J. and West, D. (1985) An inquiry into the epidemiology of melanoma. *Am J Epidemiol*, **122**, 606-19.

29. Wolf, P., Donawho, C.K. and Kripke, M.L. (1994) Effect of sunscreens on UV radiation-induced enhancement of melanoma growth in mice. *J Natl Cancer Inst*, **86**, 99-105.

30. Ibuki, Y., Allanson, M., Dixon, K.M. and Reeve, V.E. (2007) Radiation sources providing increased UVA/UVB ratios attenuate the apoptotic effects of the UVB waveband UVA-dose-dependently in hairless mouse skin. *J Invest Dermatol*, **127**, 2236-44.

31. Fu, C.S., Swendseid, M.E., Jacob, R.A. and McKee, R.W. (1989) Biochemical markers for assessment of niacin status in young men: levels of erythrocyte niacin coenzymes and plasma tryptophan. *J Nutr*, **119**, 1949-55.

32. Jacob, R.A., Swendseid, M.E., (1996) Niacin. In Ziegler, E.E., Filer, L.J. (ed.), *Present Knowledge in Nutrition*. ILSI Press, Washington, DC, pp. 184-190.

33. Warburg, O., Christian, W., Griese, A. (1935) Wasserstoffübertragendes Co-Ferment, seine Zusammensetsung und Wirkungsweise. *Biochem. Z.*, **282**, 157-165.

34. Chambon, P., Weill, J.D. and Mandel, P. (1963) Nicotinamide mononucleotide activation of new DNA-dependent polyadenylic acid synthesizing nuclear enzyme. *Biochem Biophys Res Commun*, **11**, 39-43.

35. Rusinko, N. and Lee, H.C. (1989) Widespread occurrence in animal tissues of an enzyme catalyzing the conversion of NAD+ into a cyclic metabolite with intracellular Ca2+-mobilizing activity. *J Biol Chem*, **264**, 11725-31.

36. Lee, H.C., Walseth, T.F., Bratt, G.T., Hayes, R.N. and Clapper, D.L. (1989) Structural determination of a cyclic metabolite of NAD+ with intracellular Ca2+-mobilizing activity. *J Biol Chem*, **264**, 1608-15.

37. Major, R.H. (1944) Don Gasper Casal, Francois Thiery and pellagra. *Bull Hist Med* **16**, 351–361.

38. Spies, T.D. (1950) Clinical nutrition. In Joliffe, N., Tisdall, F., Cannon, P.R. (ed.). Hoeber, pp. 531.

39. Lu, J.Y., Yu, C.L. and Wu, M.Z. (2001) Pellagra in an immunocompetent patient with cytomegalovirus colitis. *Am J Gastroenterol*, **96**, 932-4.

40. Darvay, A., Basarab, T., McGregor, J.M. and Russell-Jones, R. (1999) Isoniazid induced pellagra despite pyridoxine supplementation. *Clin Exp Dermatol*, **24**, 167-9.

41. Castiello, R.J. and Lynch, P.J. (1972) Pellagra and the carcinoid syndrome. *Arch Dermatol*, **105**, 574-7.

42. Rapaport, M.J. (1985) Pellagra in a patient with anorexia nervosa. *Arch Dermatol*, **121**, 255-7.

43. Stevens, H.P., Ostlere, L.S., Begent, R.H., Dooley, J.S. and Rustin, M.H. (1993) Pellagra secondary to 5-fluorouracil. *Br J Dermatol*, **128**, 578-80.

44. Murray, M.F., Langan, M. and MacGregor, R.R. (2001) Increased plasma tryptophan in HIV-infected patients treated with pharmacologic doses of nicotinamide. *Nutrition*, **17**, 654-6.

45. Pitche, P., Kombate, K. and Tchangai-Walla, K. (1999) [Prevalence of HIV infection in patients with pellagra and pellagra-like erythemas]. *Med Trop (Mars)*, **59**, 365-7.

46. Ziegler, M. (2000) New functions of a long-known molecule. Emerging roles of NAD in cellular signaling. *Eur J Biochem*, **267**, 1550-64.

47. Hassa, P.O., Haenni, S.S., Elser, M. and Hottiger, M.O. (2006) Nuclear ADP-ribosylation reactions in mammalian cells: where are we today and where are we going? *Microbiol Mol Biol Rev*, **70**, 789-829.

48. Jacobson, M.K. and Jacobson, E.L. (1999) Discovering new ADP-ribose polymer cycles: protecting the genome and more. *Trends Biochem Sci*, **24**, 415-7.

49. Durkacz, B.W., Omidiji, O., Gray, D.A. and Shall, S. (1980) (ADP-ribose)n participates in DNA excision repair. *Nature*, **283**, 593-6.

50. Satoh, M.S. and Lindahl, T. (1992) Role of poly(ADP-ribose) formation in DNA repair. *Nature*, **356**, 356-8.

51. Oliver, F.J., Menissier-de Murcia, J. and de Murcia, G. (1999) Poly(ADP-ribose) polymerase in the cellular response to DNA damage, apoptosis, and disease. *Am J Hum Genet*, **64**, 1282-8.

52. Kim, M.Y., Mauro, S., Gevry, N., Lis, J.T. and Kraus, W.L. (2004) NAD+-dependent modulation of chromatin structure and transcription by nucleosome binding properties of PARP-1. *Cell*, **119**, 803-14.

53. Rolli, V., Armin, R., Augustin, A., Schulz, G., Menisser-de Murcia, J., de Murcia, G. (2000) Poly(ADP-ribose) polymerase:structure and function. In Shall, S., de Murcia, G. (ed.), *Poly ADP-ribosylation reactions: From DNA damage and stress signaling to cell death*. Oxford University Press, Oxford, pp. 36-67.

54. Yu, S.W., Wang, H., Poitras, M.F., Coombs, C., Bowers, W.J., Federoff, H.J., Poirier, G.G., Dawson, T.M. and Dawson, V.L. (2002) Mediation of poly(ADP-ribose) polymerase-1-dependent cell death by apoptosis-inducing factor. *Science*, **297**, 259-63.

55. Balard, B. and Giacomoni, P.U. (1989) Nicotinamide adenosine dinucleotide level in dimethylsulfate-treated or UV-irradiated mouse epidermis. *Mutat Res*, **219**, 71-9.

56. Farzaneh, F., Zalin, R., Brill, D. and Shall, S. (1982) DNA strand breaks and ADP-ribosyl transferase activation during cell differentiation. *Nature*, **300**, 362-6.

57. Lubet, R.A., McCarvill, J.T., Putman, D.L., Schwartz, J.L. and Schechtman, L.M. (1984) Effect of 3-aminobenzamide on the induction of

toxicity and transformation by ethyl methanesulfonate and methylcholanthrene in BALB/3T3 cells. *Carcinogenesis*, **5**, 459-62.

58. Takahashi, S., Nakae, D., Yokose, Y., Emi, Y., Denda, A., Mikami, S., Ohnishi, T. and Konishi, Y. (1984) Enhancement of DEN initiation of liver carcinogenesis by inhibitors of NAD+ ADP ribosyl transferase in rats. *Carcinogenesis*, **5**, 901-6.

59. Lubet, R.A., McCarvill, J.T., Schwartz, J.L., Putman, D.L. and Schechtman, L.M. (1986) Effects of 3-aminobenzamide on the induction of morphologic transformation by diverse compounds in Balb/3T3 cells in vitro. *Carcinogenesis*, **7**, 71-5.

60. Kupper, J.H., Muller, M., Jacobson, M.K., Tatsumi-Miyajima, J., Coyle, D.L., Jacobson, E.L. and Burkle, A. (1995) trans-dominant inhibition of poly(ADP-ribosyl)ation sensitizes cells against gamma-irradiation and N-methyl-N'-nitro-N-nitrosoguanidine but does not limit DNA replication of a polyomavirus replicon. *Mol Cell Biol*, **15**, 3154-63.

61. Tsutsumi, M., Masutani, M., Nozaki, T., Kusuoka, O., Tsujiuchi, T., Nakagama, H., Suzuki, H., Konishi, Y. and Sugimura, T. (2001) Increased susceptibility of poly(ADP-ribose) polymerase-1 knockout mice to nitrosamine carcinogenicity. *Carcinogenesis*, **22**, 1-3.

62. Menissier de Murcia, J., Ricoul, M., Tartier, L., Niedergang, C., Huber, A., Dantzer, F., Schreiber, V., Ame, J.C., Dierich, A., LeMeur, M., Sabatier, L., Chambon, P. and de Murcia, G. (2003) Functional interaction between PARP-1 and PARP-2 in chromosome stability and embryonic development in mouse. *Embo J*, **22**, 2255-63.

63. Schreiber, V., Ame, J.C., Dolle, P., Schultz, I., Rinaldi, B., Fraulob, V., Menissier-de Murcia, J. and de Murcia, G. (2002) Poly(ADP-ribose) polymerase-2 (PARP-2) is required for efficient base excision DNA repair in association with PARP-1 and XRCC1. *J Biol Chem*, **277**, 23028-36.

64. Augustin, A., Spenlehauer, C., Dumond, H., Menissier-De Murcia, J., Piel, M., Schmit, A.C., Apiou, F., Vonesch, J.L., Kock, M., Bornens, M. and De Murcia, G. (2003) PARP-3 localizes preferentially to the daughter centriole and interferes with the G1/S cell cycle progression. *J Cell Sci*, **116**, 1551-62.

65. Kickhoefer, V.A., Siva, A.C., Kedersha, N.L., Inman, E.M., Ruland, C., Streuli, M. and Rome, L.H. (1999) The 193-kD vault protein, VPARP, is a novel poly(ADP-ribose) polymerase. *J Cell Biol*, **146**, 917-28.

66. Smith, S., Giriat, I., Schmitt, A. and de Lange, T. (1998) Tankyrase, a poly(ADP-ribose) polymerase at human telomeres. *Science*, **282**, 1484-7.

67. Cook, B.D., Dynek, J.N., Chang, W., Shostak, G. and Smith, S. (2002) Role for the related poly(ADP-Ribose) polymerases tankyrase 1 and 2 at human telomeres. *Mol Cell Biol*, **22**, 332-42.

68. Cohen, H.Y., Miller, C., Bitterman, K.J., Wall, N.R., Hekking, B., Kessler, B., Howitz, K.T., Gorospe, M., de Cabo, R. and Sinclair, D.A. (2004) Calorie restriction promotes mammalian cell survival by inducing the SIRT1 deacetylase. *Science*, **305**, 390-2.

69. Denu, J.M. (2005) Vitamin B3 and sirtuin function. *Trends Biochem Sci*, **30**, 479-83.

70. Vaziri, H., Dessain, S.K., Ng Eaton, E., Imai, S.I., Frye, R.A., Pandita, T.K., Guarente, L. and Weinberg, R.A. (2001) hSIR2(SIRT1) functions as an NAD-dependent p53 deacetylase. *Cell*, **107**, 149-59.

71. Motta, M.C., Divecha, N., Lemieux, M., Kamel, C., Chen, D., Gu, W., Bultsma, Y., McBurney, M. and Guarente, L. (2004) Mammalian SIRT1 represses forkhead transcription factors. *Cell*, **116**, 551-63.

72. Jacobson, E.L., Shieh, W.M. and Huang, A.C. (1999) Mapping the role of NAD metabolism in prevention and treatment of carcinogenesis. *Mol Cell Biochem*, **193**, 69-74.

73. Jacobson, E.L., Giacomoni, P.U., Roberts, M.J., Wondrak, G.T. and Jacobson, M.K. (2001) Optimizing the energy status of skin cells during solar radiation. *J Photochem Photobiol B*, **63**, 141-7.

74. Kirkland, J.B. (2003) Niacin and carcinogenesis. *Nutr Cancer*, **46**, 110-8.

75. Gensler, H.L., Williams, T., Huang, A.C. and Jacobson, E.L. (1999) Oral niacin prevents photocarcinogenesis and photoimmunosuppression in mice. *Nutr Cancer*, **34**, 36-41.

76. Spronck, J.C. and Kirkland, J.B. (2002) Niacin deficiency increases spontaneous and etoposide-induced chromosomal instability in rat bone marrow cells in vivo. *Mutat Res*, **508**, 83-97.

77. Zhang, J.Z., Henning, S.M. and Swendseid, M.E. (1993) Poly(ADP-ribose) polymerase activity and DNA strand breaks are affected in tissues of niacin-deficient rats. *J Nutr*, **123**, 1349-55.

78. Spronck, J.C., Nickerson, J.L. and Kirkland, J.B. (2007) Niacin Deficiency Alters p53 Expression and Impairs Etoposide-Induced Cell Cycle Arrest and Apoptosis in Rat Bone Marrow Cells. *Nutr Cancer*, **57**, 88-99.

79. Spronck, J.C., Bartleman, A.P., Boyonoski, A.C. and Kirkland, J.B. (2003) Chronic DNA damage and niacin deficiency enhance cell injury and cause unusual interactions in NAD and poly(ADP-ribose) metabolism in rat bone marrow. *Nutr Cancer*, **45**, 124-31.

80. Boyonoski, A.C., Gallacher, L.M., ApSimon, M.M., Jacobs, R.M., Shah, G.M., Poirier, G.G. and Kirkland, J.B. (1999) Niacin deficiency increases the sensitivity of rats to the short and long term effects of ethylnitrosourea treatment. *Mol Cell Biochem*, **193**, 83-7.

81. Jacobson, E.L. (1993) Niacin deficiency and cancer in women. *J Am Coll Nutr*, **12**, 412-6.

82. Jacobson, E.L., Kim, H., Kim, M., Williams, J.D., Coyle, D.L., Coyle, W.R., Grove, G., Rizer, R.L., Stratton, M.S. and Jacobson, M.K. (2007) A topical lipophilic niacin derivative increases NAD, epidermal differentiation and barrier function in photodamaged skin. *Exp Dermatol*, **16**, 490-9.

83. Weitberg, A.B. (1989) Effect of nicotinic acid supplementation in vivo on oxygen radical-induced genetic damage in human lymphocytes. *Mutat Res*, **216**, 197-201.

84. Weitberg, A.B. and Corvese, D. (1990) Niacin prevents DNA strand breakage by adenosine deaminase inhibitors. *Biochem Biophys Res Commun*, **167**, 514-9.

85. Denu, J.M. (2003) Linking chromatin function with metabolic networks: Sir2 family of NAD(+)-dependent deacetylases. *Trends Biochem Sci*, **28**, 41-8.

86. Frye, R.A. (1999) Characterization of five human cDNAs with homology to the yeast SIR2 gene: Sir2-like proteins (sirtuins) metabolize NAD and may have protein ADP-ribosyltransferase activity. *Biochem Biophys Res Commun*, **260**, 273-9.

87. Imai, S., Armstrong, C.M., Kaeberlein, M. and Guarente, L. (2000) Transcriptional silencing and longevity protein Sir2 is an NAD-dependent histone deacetylase. *Nature*, **403**, 795-800.

88. Landry, J., Sutton, A., Tafrov, S.T., Heller, R.C., Stebbins, J., Pillus, L. and Sternglanz, R. (2000) The silencing protein SIR2 and its homologs are NAD-dependent protein deacetylases. *Proc Natl Acad Sci U S A*, **97**, 5807-11.

89. Smith, J.S., Brachmann, C.B., Celic, I., Kenna, M.A., Muhammad, S., Starai, V.J., Avalos, J.L., Escalante-Semerena, J.C., Grubmeyer, C., Wolberger, C. and Boeke, J.D. (2000) A phylogenetically conserved NAD+-dependent protein deacetylase activity in the Sir2 protein family. *Proc Natl Acad Sci U S A*, **97**, 6658-63.

90. Liszt, G., Ford, E., Kurtev, M. and Guarente, L. (2005) Mouse Sir2 homolog SIRT6 is a nuclear ADP-ribosyltransferase. *J Biol Chem*, **280**, 21313-20.

91. Haigis, M.C., Mostoslavsky, R., Haigis, K.M., Fahie, K., Christodoulou, D.C., Murphy, A.J., Valenzuela, D.M., Yancopoulos, G.D., Karow, M., Blander, G., Wolberger, C., Prolla, T.A., Weindruch, R., Alt, F.W. and Guarente, L. (2006) SIRT4 Inhibits Glutamate Dehydrogenase and Opposes the Effects of Calorie Restriction in Pancreatic beta Cells. *Cell*, **126**, 941-54.

92. Langley, E., Pearson, M., Faretta, M., Bauer, U.M., Frye, R.A., Minucci, S., Pelicci, P.G. and Kouzarides, T. (2002) Human SIR2 deacetylates p53 and antagonizes PML/p53-induced cellular senescence. *Embo J*, **21**, 2383-96.

93. Luo, J., Nikolaev, A.Y., Imai, S., Chen, D., Su, F., Shiloh, A., Guarente, L. and Gu, W. (2001) Negative control of p53 by Sir2alpha promotes cell survival under stress. *Cell*, **107**, 137-48.

94. Brunet, A., Sweeney, L.B., Sturgill, J.F., Chua, K.F., Greer, P.L., Lin, Y., Tran, H., Ross, S.E., Mostoslavsky, R., Cohen, H.Y., Hu, L.S., Cheng, H.L., Jedrychowski, M.P., Gygi, S.P., Sinclair, D.A., Alt, F.W. and Greenberg, M.E. (2004) Stress-dependent regulation of FOXO transcription factors by the SIRT1 deacetylase. *Science*, **303**, 2011-5.

95. Daitoku, H., Hatta, M., Matsuzaki, H., Aratani, S., Ohshima, T., Miyagishi, M., Nakajima, T. and Fukamizu, A. (2004) Silent information regulator 2

potentiates Foxo1-mediated transcription through its deacetylase activity. *Proc Natl Acad Sci U S A*, **101**, 10042-7.

96. van der Horst, A., Tertoolen, L.G., de Vries-Smits, L.M., Frye, R.A., Medema, R.H. and Burgering, B.M. (2004) FOXO4 is acetylated upon peroxide stress and deacetylated by the longevity protein hSir2(SIRT1). *J Biol Chem*, **279**, 28873-9.

97. Picard, F., Kurtev, M., Chung, N., Topark-Ngarm, A., Senawong, T., Machado De Oliveira, R., Leid, M., McBurney, M.W. and Guarente, L. (2004) Sirt1 promotes fat mobilization in white adipocytes by repressing PPAR-gamma. *Nature*, **429**, 771-6.

98. Cohen, H.Y., Lavu, S., Bitterman, K.J., Hekking, B., Imahiyerobo, T.A., Miller, C., Frye, R., Ploegh, H., Kessler, B.M. and Sinclair, D.A. (2004) Acetylation of the C terminus of Ku70 by CBP and PCAF controls Bax-mediated apoptosis. *Mol Cell*, **13**, 627-38.

99. Fulco, M., Schiltz, R.L., Iezzi, S., King, M.T., Zhao, P., Kashiwaya, Y., Hoffman, E., Veech, R.L. and Sartorelli, V. (2003) Sir2 regulates skeletal muscle differentiation as a potential sensor of the redox state. *Mol Cell*, **12**, 51-62.

100. Rodgers, J.T., Lerin, C., Haas, W., Gygi, S.P., Spiegelman, B.M. and Puigserver, P. (2005) Nutrient control of glucose homeostasis through a complex of PGC-1alpha and SIRT1. *Nature*, **434**, 113-8.

101. North, B.J., Marshall, B.L., Borra, M.T., Denu, J.M. and Verdin, E. (2003) The human Sir2 ortholog, SIRT2, is an NAD+-dependent tubulin deacetylase. *Mol Cell*, **11**, 437-44.

102. Vaquero, A., Scher, M.B., Lee, D.H., Sutton, A., Cheng, H.L., Alt, F.W., Serrano, L., Sternglanz, R. and Reinberg, D. (2006) SirT2 is a histone deacetylase with preference for histone H4 Lys 16 during mitosis. *Genes Dev*, **20**, 1256-61.

103. Dryden, S.C., Nahhas, F.A., Nowak, J.E., Goustin, A.S. and Tainsky, M.A. (2003) Role for human SIRT2 NAD-dependent deacetylase activity in control of mitotic exit in the cell cycle. *Mol Cell Biol*, **23**, 3173-85.

104. Inoue, T., Hiratsuka, M., Osaki, M., Yamada, H., Kishimoto, I., Yamaguchi, S., Nakano, S., Katoh, M., Ito, H. and Oshimura, M. (2007) SIRT2, a tubulin deacetylase, acts to block the entry to chromosome condensation in response to mitotic stress. *Oncogene*, **26**, 945-57.

105. Scher, M.B., Vaquero, A. and Reinberg, D. (2007) SirT3 is a nuclear NAD+-dependent histone deacetylase that translocates to the mitochondria upon cellular stress. *Genes Dev*, **21**, 920-8.

106. Shi, T., Wang, F., Stieren, E. and Tong, Q. (2005) SIRT3, a mitochondrial sirtuin deacetylase, regulates mitochondrial function and thermogenesis in brown adipocytes. *J Biol Chem*, **280**, 13560-7.

107. Rose, G., Dato, S., Altomare, K., Bellizzi, D., Garasto, S., Greco, V., Passarino, G., Feraco, E., Mari, V., Barbi, C., BonaFe, M., Franceschi, C., Tan, Q., Boiko, S., Yashin, A.I. and De Benedictis, G. (2003) Variability of the SIRT3 gene, human silent information regulator Sir2 homologue, and survivorship in the elderly. *Exp Gerontol*, **38**, 1065-70.

108. Bellizzi, D., Dato, S., Cavalcante, P., Covello, G., Di Cianni, F., Passarino, G., Rose, G. and De Benedictis, G. (2007) Characterization of a bidirectional promoter shared between two human genes related to aging: SIRT3 and PSMD13. *Genomics*, **89**, 143-50.

109. Michishita, E., Park, J.Y., Burneskis, J.M., Barrett, J.C. and Horikawa, I. (2005) Evolutionarily conserved and nonconserved cellular localizations and functions of human SIRT proteins. *Mol Biol Cell*, **16**, 4623-35.

110. Mahlknecht, U., Ho, A.D., Letzel, S. and Voelter-Mahlknecht, S. (2006) Assignment of the NAD-dependent deacetylase sirtuin 5 gene (SIRT5) to human chromosome band 6p23 by in situ hybridization. *Cytogenet Genome Res*, **112**, 208-12.

111. Mostoslavsky, R., Chua, K.F., Lombard, D.B., Pang, W.W., Fischer, M.R., Gellon, L., Liu, P., Mostoslavsky, G., Franco, S., Murphy, M.M., Mills, K.D., Patel, P., Hsu, J.T., Hong, A.L., Ford, E., Cheng, H.L., Kennedy, C., Nunez, N., Bronson, R., Frendewey, D., Auerbach, W., Valenzuela, D., Karow, M., Hottiger, M.O., Hursting, S., Barrett, J.C., Guarente, L., Mulligan, R., Demple, B., Yancopoulos, G.D. and Alt, F.W. (2006) Genomic instability and aging-like phenotype in the absence of mammalian SIRT6. *Cell*, **124**, 315-29.

112. Ford, E., Voit, R., Liszt, G., Magin, C., Grummt, I. and Guarente, L. (2006) Mammalian Sir2 homolog SIRT7 is an activator of RNA polymerase I transcription. *Genes Dev*, **20**, 1075-80.

113. Dali-Youcef, N., Lagouge, M., Froelich, S., Koehl, C., Schoonjans, K. and Auwerx, J. (2007) Sirtuins: the 'magnificent seven', function, metabolism and longevity. *Ann Med*, **39**, 335-45.

114. Boukamp, P., Petrussevska, R.T., Breitkreutz, D., Hornung, J., Markham, A. and Fusenig, N.E. (1988) Normal keratinization in a spontaneously immortalized aneuploid human keratinocyte cell line. *J Cell Biol*, **106**, 761-71.

115. Lehman, T.A., Modali, R., Boukamp, P., Stanek, J., Bennett, W.P., Welsh, J.A., Metcalf, R.A., Stampfer, M.R., Fusenig, N., Rogan, E.M. and et al. (1993) p53 mutations in human immortalized epithelial cell lines. *Carcinogenesis*, **14**, 833-9.

116. Lewis, D.A., Hengeltraub, S.F., Gao, F.C., Leivant, M.A. and Spandau, D.F. (2006) Aberrant NF-kappaB activity in HaCaT cells alters their response to UVB signaling. *J Invest Dermatol*, **126**, 1885-92.

117. Lin, S.J., Ford, E., Haigis, M., Liszt, G. and Guarente, L. (2004) Calorie restriction extends yeast life span by lowering the level of NADH. *Genes Dev*, **18**, 12-6.

118. Jacobson, E.L. and Jacobson, M.K. (1997) Tissue NAD as a biochemical measure of niacin status in humans. *Methods Enzymol*, **280**, 221-30.

119. Jacobson, E.L., Lange, R.A. and Jacobson, M.K. (1979) Pyridine nucleotide synthesis in 3T3 cells. *J Cell Physiol*, **99**, 417-25.

120. Krishan, A. (1975) Rapid flow cytofluorometric analysis of mammalian cell cycle by propidium iodide staining. *J Cell Biol*, **66**, 188-93.

121. Vermes, I., Haanen, C., Steffens-Nakken, H. and Reutelingsperger, C. (1995) A novel assay for apoptosis. Flow cytometric detection of phosphatidylserine expression on early apoptotic cells using fluorescein labelled Annexin V. *J Immunol Methods*, **184**, 39-51.

122. Singh, N.P., McCoy, M.T., Tice, R.R. and Schneider, E.L. (1988) A simple technique for quantitation of low levels of DNA damage in individual cells. *Exp Cell Res*, **175**, 184-91.

123. Gibson, U.E., Heid, C.A. and Williams, P.M. (1996) A novel method for real time quantitative RT-PCR. *Genome Res*, **6**, 995-1001.

124. Ray, R. and Shah, A.M. (2005) NADPH oxidase and endothelial cell function. *Clin Sci (Lond)*, **109**, 217-26.

125. Chamulitrat, W., Schmidt, R., Tomakidi, P., Stremmel, W., Chunglok, W., Kawahara, T. and Rokutan, K. (2003) Association of gp91phox homolog Nox1 with anchorage-independent growth and MAP kinase-activation of transformed human keratinocytes. *Oncogene*, **22**, 6045-53.

126. Dreher, D. and Junod, A.F. (1996) Role of oxygen free radicals in cancer development. *Eur J Cancer*, **32A**, 30-8.

127. Jacobson, E.L., Meadows, R. and Measel, J. (1985) Cell cycle perturbations following DNA damage in the presence of ADP-ribosylation inhibitors. *Carcinogenesis*, **6**, 711-4.

128. Masutani, M., Nozaki, T., Wakabayashi, K. and Sugimura, T. (1995) Role of poly(ADP-ribose) polymerase in cell-cycle checkpoint mechanisms following gamma-irradiation. *Biochimie*, **77**, 462-5.

129. Schreiber, V., Hunting, D., Trucco, C., Gowans, B., Grunwald, D., De Murcia, G. and De Murcia, J.M. (1995) A dominant-negative mutant of human poly(ADP-ribose) polymerase affects cell recovery, apoptosis, and sister chromatid exchange following DNA damage. *Proc Natl Acad Sci U S A*, **92**, 4753-7.

130. Saldeen, J., Tillmar, L., Karlsson, E. and Welsh, N. (2003) Nicotinamide- and caspase-mediated inhibition of poly(ADP-ribose) polymerase are associated with p53-independent cell cycle (G2) arrest and apoptosis. *Mol Cell Biochem*, **243**, 113-22.

131. Cerutti, P.A. (1985) Prooxidant states and tumor promotion. *Science*, **227**, 375-81.

132. Cerutti, P., Ghosh, R., Oya, Y. and Amstad, P. (1994) The role of the cellular antioxidant defense in oxidant carcinogenesis. *Environ Health Perspect*, **102 Suppl 10**, 123-9.

133. Cross, A.R. and Jones, O.T. (1991) Enzymic mechanisms of superoxide production. *Biochim Biophys Acta*, **1057**, 281-98.

134. Nisimoto, Y., Otsuka-Murakami, H. and Lambeth, D.J. (1995) Reconstitution of flavin-depleted neutrophil flavocytochrome b558 with 8-mercapto-FAD and characterization of the flavin-reconstituted enzyme. *J Biol Chem*, **270**, 16428-34.

135. Cheng, G., Cao, Z., Xu, X., van Meir, E.G. and Lambeth, J.D. (2001) Homologs of gp91phox: cloning and tissue expression of Nox3, Nox4, and Nox5. *Gene*, **269**, 131-40.

136. Esposito, F., Ammendola, R., Faraonio, R., Russo, T. and Cimino, F. (2004) Redox control of signal transduction, gene expression and cellular senescence. *Neurochem Res*, **29**, 617-28.

137. Martin, K.R. and Barrett, J.C. (2002) Reactive oxygen species as double-edged swords in cellular processes: low-dose cell signaling versus high-dose toxicity. *Hum Exp Toxicol*, **21**, 71-5.

138. Hallows, W.C., Lee, S. and Denu, J.M. (2006) Sirtuins deacetylate and activate mammalian acetyl-CoA synthetases. *Proc Natl Acad Sci U S A*, **103**, 10230-5.

139. Ames, B.N. (2001) DNA damage from micronutrient deficiencies is likely to be a major cause of cancer. *Mutat Res*, **475**, 7-20.

140. Williams, G.M. and Jeffrey, A.M. (2000) Oxidative DNA damage: endogenous and chemically induced. *Regul Toxicol Pharmacol*, **32**, 283-92.

141. Cooke, M.S., Evans, M.D., Dizdaroglu, M. and Lunec, J. (2003) Oxidative DNA damage: mechanisms, mutation, and disease. *Faseb J*, **17**, 1195-214.

142. Loft, S. and Poulsen, H.E. (1996) Cancer risk and oxidative DNA damage in man. *J Mol Med*, **74**, 297-312.

143. Pithon-Curi, T.C., Levada, A.C., Lopes, L.R., Doi, S.Q. and Curi, R. (2002) Glutamine plays a role in superoxide production and the expression of p47phox, p22phox and gp91phox in rat neutrophils. *Clin Sci (Lond)*, **103**, 403-8.

144. Mates, J.M., Perez-Gomez, C., Nunez de Castro, I., Asenjo, M. and Marquez, J. (2002) Glutamine and its relationship with intracellular redox status, oxidative stress and cell proliferation/death. *Int J Biochem Cell Biol*, **34**, 439-58.

145. Ivy, J.M., Klar, A.J. and Hicks, J.B. (1986) Cloning and characterization of four SIR genes of Saccharomyces cerevisiae. *Mol Cell Biol*, **6**, 688-702.

146. Dal Farra, C. and Domloge, N. (2006) SIRT1, the human homologue to SIR2, is expressed in human skin and in cultured keratinocytes fibroblasts and HaCaT cells; and its levels is closely related to stress and aging. *J Cosmet Sci*, **57**, 187-8.

147. Beausoleil, S.A., Jedrychowski, M., Schwartz, D., Elias, J.E., Villen, J., Li, J., Cohn, M.A., Cantley, L.C. and Gygi, S.P. (2004) Large-scale characterization of HeLa cell nuclear phosphoproteins. *Proc Natl Acad Sci U S A*, **101**, 12130-5.

148. Qin, J.Z., Chaturvedi, V., Denning, M.F., Choubey, D., Diaz, M.O. and Nickoloff, B.J. (1999) Role of NF-kappaB in the apoptotic-resistant phenotype of keratinocytes. *J Biol Chem*, **274**, 37957-64.

149. Chaturvedi, V., Qin, J.Z., Denning, M.F., Choubey, D., Diaz, M.O. and Nickoloff, B.J. (2001) Abnormal NF-kappaB signaling pathway with enhanced susceptibility to apoptosis in immortalized keratinocytes. *J Dermatol Sci*, **26**, 67-78.

150. Qin, J.Z., Bacon, P.E., Chaturvedi, V., Bonish, B. and Nickoloff, B.J. (2002) Pathways involved in proliferating, senescent and immortalized keratinocyte cell death mediated by two different TRAIL preparations. *Exp Dermatol*, **11**, 573-83.

151. Lewis, D.A., Zweig, B., Hurwitz, S.A. and Spandau, D.F. (2003) Inhibition of erbB receptor family members protects HaCaT keratinocytes from ultraviolet-B-induced apoptosis. *J Invest Dermatol*, **120**, 483-8.

152. Saunders, L.R. and Verdin, E. (2007) Sirtuins: critical regulators at the crossroads between cancer and aging. *Oncogene*, **26**, 5489-504.

153. Yeung, F., Hoberg, J.E., Ramsey, C.S., Keller, M.D., Jones, D.R., Frye, R.A. and Mayo, M.W. (2004) Modulation of NF-kappaB-dependent transcription and cell survival by the SIRT1 deacetylase. *Embo J*, **23**, 2369-80.

154. Jeong, J., Juhn, K., Lee, H., Kim, S.H., Min, B.H., Lee, K.M., Cho, M.H., Park, G.H. and Lee, K.H. (2007) SIRT1 promotes DNA repair activity and deacetylation of Ku70. *Exp Mol Med*, **39**, 8-13.

155. Scharffetter-Kochanek, K., Wlaschek, M., Brenneisen, P., Schauen, M., Blaudschun, R. and Wenk, J. (1997) UV-induced reactive oxygen species in photocarcinogenesis and photoaging. *Biol Chem*, **378**, 1247-57.

156. Kvam, E. and Tyrrell, R.M. (1997) Induction of oxidative DNA base damage in human skin cells by UV and near visible radiation. *Carcinogenesis*, **18**, 2379-84.

157. Agar, N.S., Halliday, G.M., Barnetson, R.S., Ananthaswamy, H.N., Wheeler, M. and Jones, A.M. (2004) The basal layer in human squamous tumors harbors more UVA than UVB fingerprint mutations: a role for UVA in human skin carcinogenesis. *Proc Natl Acad Sci U S A*, **101**, 4954-9.

158. Wondrak, G.T., Roberts, M.J., Cervantes-Laurean, D., Jacobson, M.K. and Jacobson, E.L. (2003) Proteins of the extracellular matrix are sensitizers of photo-oxidative stress in human skin cells. *J Invest Dermatol*, **121**, 578-86.

159. Wondrak, G.T., Roberts, M.J., Jacobson, M.K. and Jacobson, E.L. (2004) 3-hydroxypyridine chromophores are endogenous sensitizers of photooxidative stress in human skin cells. *J Biol Chem*, **279**, 30009-20.

160. Wondrak, G.T., Jacobson, M.K. and Jacobson, E.L. (2005) Identification of quenchers of photoexcited States as novel agents for skin photoprotection. *J Pharmacol Exp Ther*, **312**, 482-91.

161. Cheng, K.C. and Loeb, L.A. (1997) Genomic stability and instability: a working paradigm. *Curr Top Microbiol Immunol*, **221**, 5-18.

162. Shah, G.M., Le Rhun Y., Sutarjone I., and Kirkland J.B. (2002) Niacin deficient SKH-1 mice are more susceptible to ultraviolet B radiation-induced skin carcinogenesis. *Cancer Res*, **131**, 3150S.

163. Szabo, C., Zingarelli, B., O'Connor, M. and Salzman, A.L. (1996) DNA strand breakage, activation of poly (ADP-ribose) synthetase, and cellular energy depletion are involved in the cytotoxicity of macrophages and smooth muscle cells exposed to peroxynitrite. *Proc Natl Acad Sci U S A*, **93**, 1753-8.

164. Shall, S. and de Murcia, G. (2000) Poly(ADP-ribose) polymerase-1: what have we learned from the deficient mouse model? *Mutat Res*, **460**, 1-15.

165. Alvarez-Gonzalez, R. and Althaus, F.R. (1989) Poly(ADP-ribose) catabolism in mammalian cells exposed to DNA-damaging agents. *Mutat Res*, **218**, 67-74.

166. Berger, N.A., Sikorski, G.W., Petzold, S.J. and Kurohara, K.K. (1980) Defective poly(adenosine diphosphoribose) synthesis in xeroderma pigmentosum. *Biochemistry*, **19**, 289-93.

167. Chang, H., Sander, C.S., Muller, C.S., Elsner, P. and Thiele, J.J. (2002) Detection of poly(ADP-ribose) by immunocytochemistry: a sensitive new method for the early identification of UVB- and H2O2-induced apoptosis in keratinocytes. *Biol Chem*, **383**, 703-8.

168. Jacobson, E.L., Antol, K.M., Juarez-Salinas, H. and Jacobson, M.K. (1983) Poly(ADP-ribose) metabolism in ultraviolet irradiated human fibroblasts. *J Biol Chem*, **258**, 103-7.

169. Vodenicharov, M.D., Ghodgaonkar, M.M., Halappanavar, S.S., Shah, R.G. and Shah, G.M. (2005) Mechanism of early biphasic activation of poly(ADP-ribose) polymerase-1 in response to ultraviolet B radiation. *J Cell Sci*, **118**, 589-99.

170. Epstein, J.H. and Cleaver, J.E. (1992) 3-Aminobenzamide can act as a cocarcinogen for ultraviolet light-induced carcinogenesis in mouse skin. *Cancer Res*, **52**, 4053-4.

171. Farkas, B., Magyarlaki, M., Csete, B., Nemeth, J., Rabloczky, G., Bernath, S., Literati Nagy, P. and Sumegi, B. (2002) Reduction of acute photodamage in skin by topical application of a novel PARP inhibitor. *Biochem Pharmacol*, **63**, 921-32.

172. Stevnsner, T., Ding, R., Smulson, M. and Bohr, V.A. (1994) Inhibition of gene-specific repair of alkylation damage in cells depleted of poly(ADP-ribose) polymerase. *Nucleic Acids Res*, **22**, 4620-4.

173. Halappanavar, S.S., Rhun, Y.L., Mounir, S., Martins, L.M., Huot, J., Earnshaw, W.C. and Shah, G.M. (1999) Survival and proliferation of cells expressing caspase-uncleavable Poly(ADP-ribose) polymerase in response to death-inducing DNA damage by an alkylating agent. *J Biol Chem*, **274**, 37097-104.

174. Ha, H.C. and Snyder, S.H. (1999) Poly(ADP-ribose) polymerase is a mediator of necrotic cell death by ATP depletion. *Proc Natl Acad Sci U S A*, **96**, 13978-82.

175. Kostecki, L.M., Thomas, M., Linford, G., Lizotte, M., Toxopeus, L., Bartleman, A.P. and Kirkland, J.B. (2007) Niacin deficiency delays DNA

excision repair and increases spontaneous and nitrosourea-induced chromosomal instability in rat bone marrow. *Mutat Res*.

176. Landry, J., Slama, J.T. and Sternglanz, R. (2000) Role of NAD(+) in the deacetylase activity of the SIR2-like proteins. *Biochem Biophys Res Commun*, **278**, 685-90.

177. Li, J.H. and Zhang, J. (2001) PARP inhibitors. *IDrugs*, **4**, 804-12.

178. Altschul, R., Hoffer, A. and Stephen, J.D. (1955) Influence of nicotinic acid on serum cholesterol in man. *Arch Biochem*, **54**, 558-9.

179. Wise, A., Foord, S.M., Fraser, N.J., Barnes, A.A., Elshourbagy, N., Eilert, M., Ignar, D.M., Murdock, P.R., Steplewski, K., Green, A., Brown, A.J., Dowell, S.J., Szekeres, P.G., Hassall, D.G., Marshall, F.H., Wilson, S. and Pike, N.B. (2003) Molecular identification of high and low affinity receptors for nicotinic acid. *J Biol Chem*, **278**, 9869-74.

180. Schaub, A., Futterer, A. and Pfeffer, K. (2001) PUMA-G, an IFN-gamma-inducible gene in macrophages is a novel member of the seven transmembrane spanning receptor superfamily. *Eur J Immunol*, **31**, 3714-25.

181. Tunaru, S., Kero, J., Schaub, A., Wufka, C., Blaukat, A., Pfeffer, K. and Offermanns, S. (2003) PUMA-G and HM74 are receptors for nicotinic acid and mediate its anti-lipolytic effect. *Nat Med*, **9**, 352-5.

182. Soga, T., Kamohara, M., Takasaki, J., Matsumoto, S., Saito, T., Ohishi, T., Hiyama, H., Matsuo, A., Matsushime, H. and Furuichi, K. (2003) Molecular identification of nicotinic acid receptor. *Biochem Biophys Res Commun*, **303**, 364-9.

183. Pike, N.B. and Wise, A. (2004) Identification of a nicotinic acid receptor: is this the molecular target for the oldest lipid-lowering drug? *Curr Opin Investig Drugs*, **5**, 271-5.

184. Zhang, Y., Schmidt, R.J., Foxworthy, P., Emkey, R., Oler, J.K., Large, T.H., Wang, H., Su, E.W., Mosior, M.K., Eacho, P.I. and Cao, G. (2005) Niacin mediates lipolysis in adipose tissue through its G-protein coupled receptor HM74A. *Biochem Biophys Res Commun*, **334**, 729-32.

185. Carlson, L.A. (2005) Nicotinic acid: the broad-spectrum lipid drug. A 50th anniversary review. *J Intern Med*, **258**, 94-114.

186. Benyo, Z., Gille, A., Kero, J., Csiky, M., Suchankova, M.C., Nusing, R.M., Moers, A., Pfeffer, K. and Offermanns, S. (2005) GPR109A (PUMA-G/HM74A) mediates nicotinic acid-induced flushing. *J Clin Invest*, **115**, 3634-40.

187. Draelos, Z.D., Jacobson, E.L., Kim, H., Kim, M. and Jacobson, M.K. (2005) A pilot study evaluating the efficacy of topically applied niacin derivatives for treatment of female pattern alopecia. *J Cosmet Dermatol*, **4**, 258-61.

188. Meyers, C.D., Liu, P., Kamanna, V.S. and Kashyap, M.L. (2007) Nicotinic acid induces secretion of prostaglandin D2 in human macrophages: an in vitro model of the niacin flush. *Atherosclerosis*, **192**, 253-8.

189. Kim, H., Jacobson, M.K., Kim, M., Jacobson, E.L., Qasem, J.G. (2002) A Topical Niacin Prodrug Enhances Wound Healing by Stimulation of Leptin Secretion. *Journal of Investigative Dermatology*, **119**, A840.